BERKELEY LAB
Bringing Science Solutions to the World

U.S. DEPARTMENT OF ENERGY
Office of Science

Module-0

First operation of the *modular*
DUNE LAr Near Detector prototype LArTPC

Brooke Russell

Los Alamos National Laboratory P3 Seminar

June 30, 2021

Outline

1 DUNE ν oscillation physics

2 LAr Near Detector (ND-LAr) design

3 Module-0: first ND-LAr prototype detector

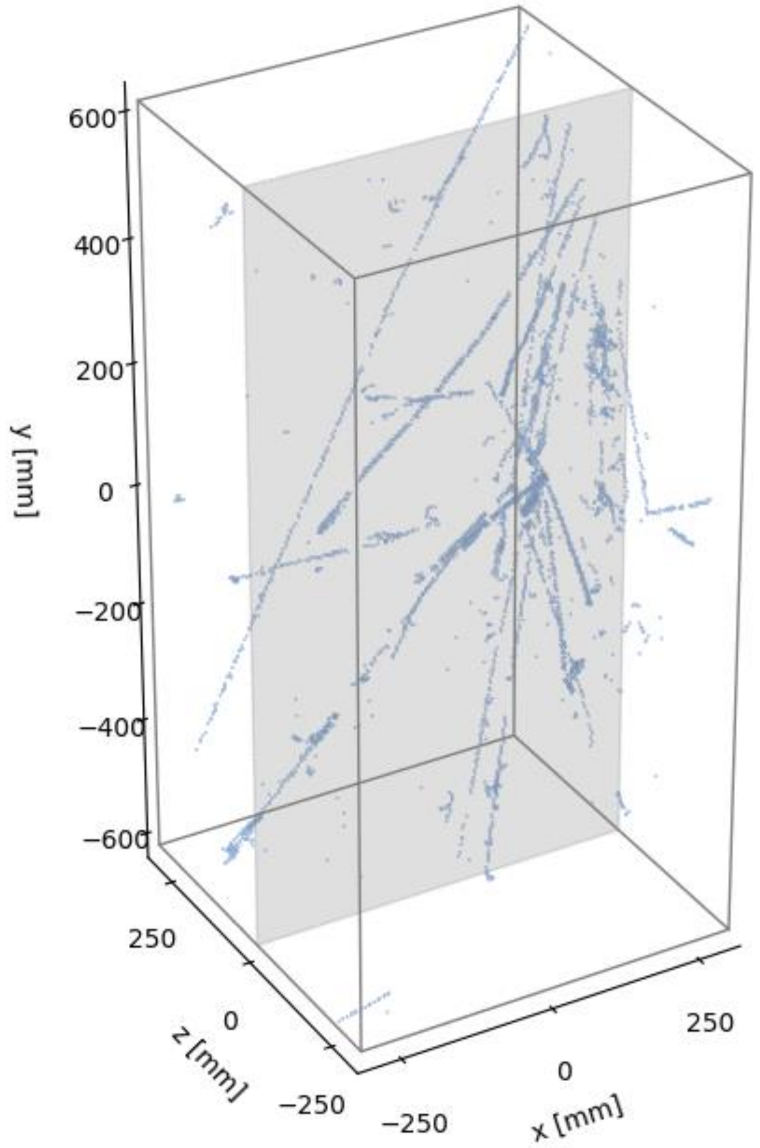

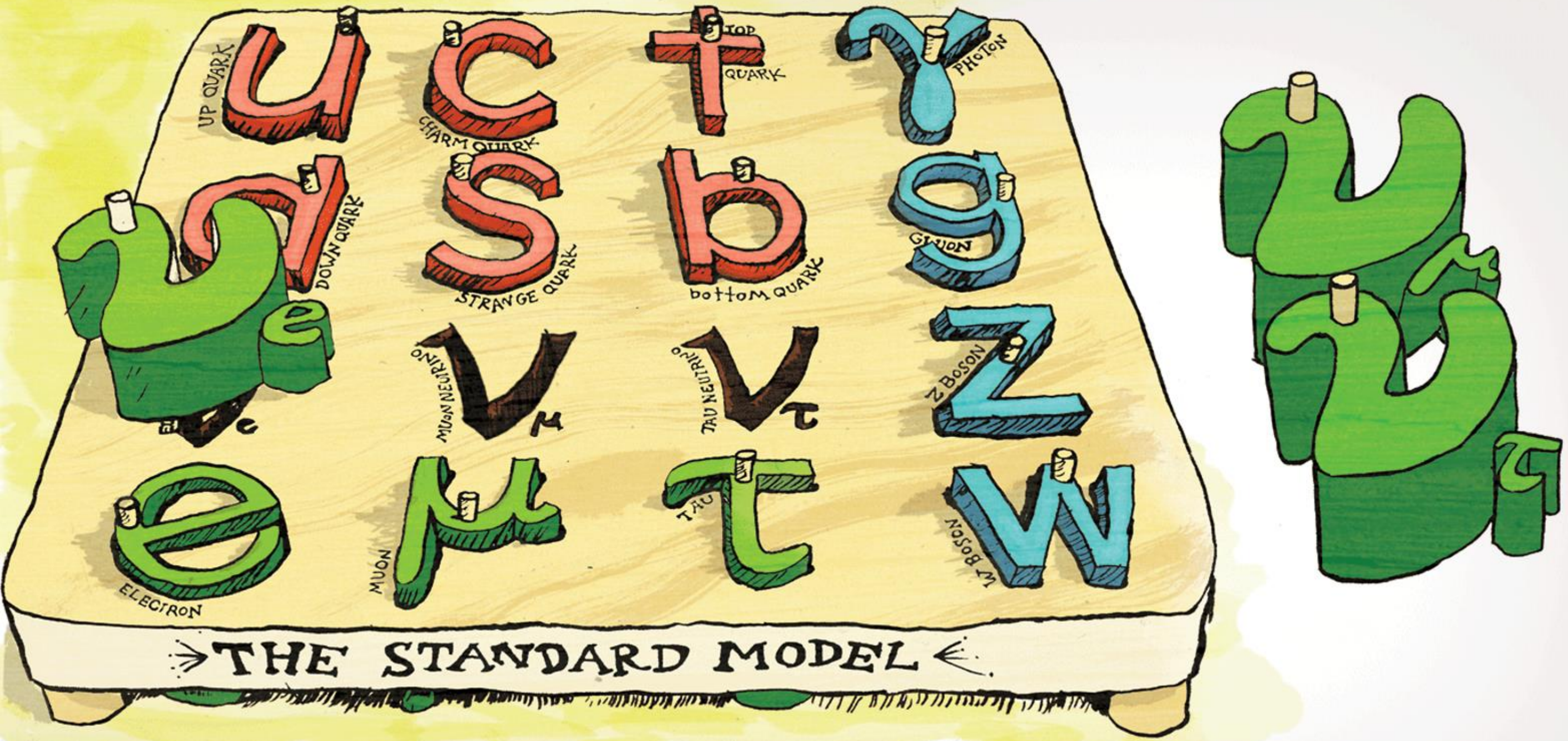

Figure credit: Symmetry magazine / Sandbox studio, Chicago

ν oscillation

In-flight transition between different neutrino flavors, caused by nonzero neutrino masses and neutrino mixing

Vogel, P. *et al*. Neutrino oscillation studies with reactors. *Nat. Commun.* 6:6935 (2015).

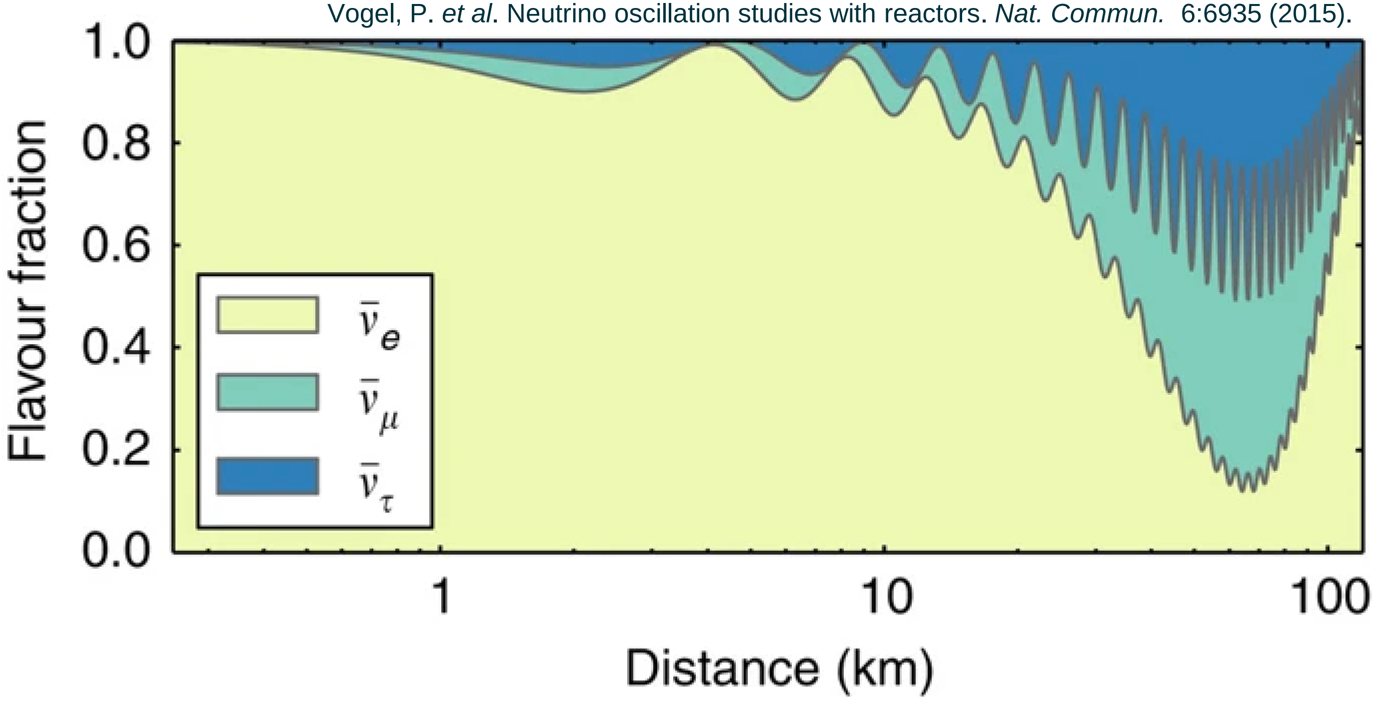

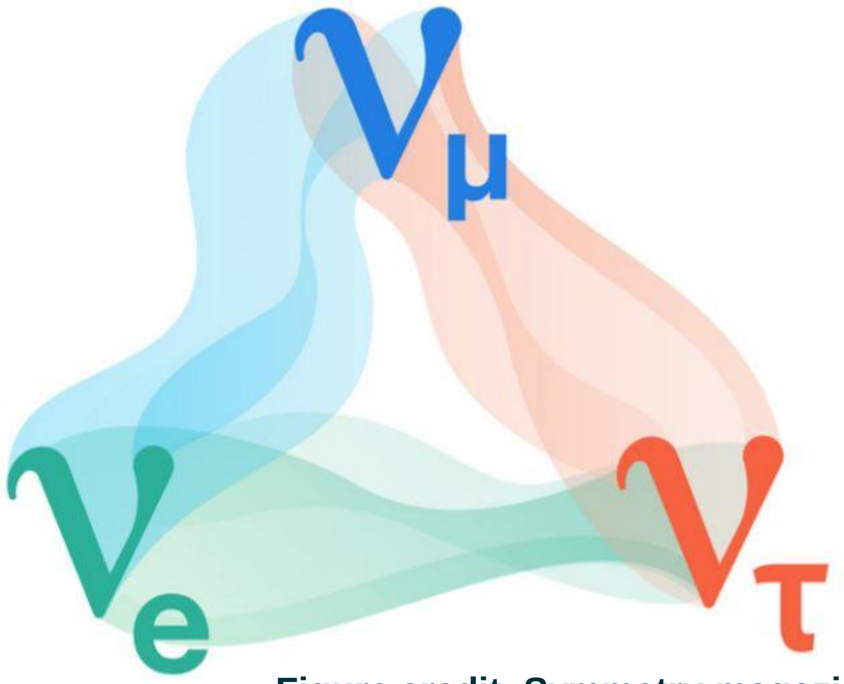

Figure credit: Symmetry magazine

ν sources to study oscillation

ν_e from nuclear fusion in the sun

$\bar{\nu}_e$ from beta decay
$n \rightarrow p + e^- + \bar{\nu}_e$

J.A. Formaggio and G.P. Zeller, Rev. Mod. Phys. **84**, 1307 (2012)

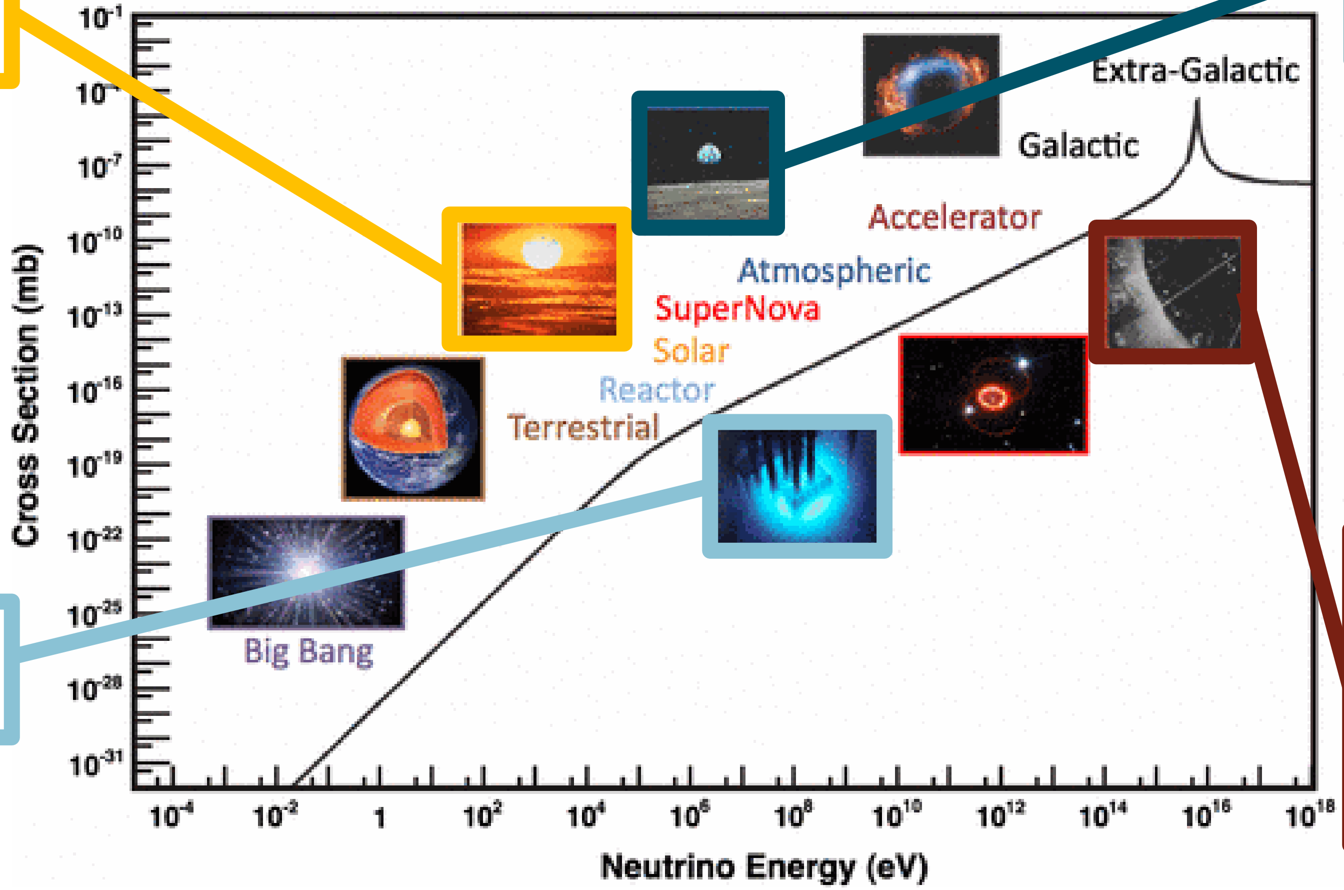

Primarily ν_μ (or $\bar{\nu}_\mu$) from in-flight meson decay

Primarily ν_μ (or $\bar{\nu}_\mu$) from in-flight meson decay – *can tune neutrino energy and baseline distance*

Neutrino Oscillation

M.V. Diwan, V. Galymov, X. Qian, A. Rubbia, Annu. Rev. Nucl. Part. Sci. 2016, 66:47-71

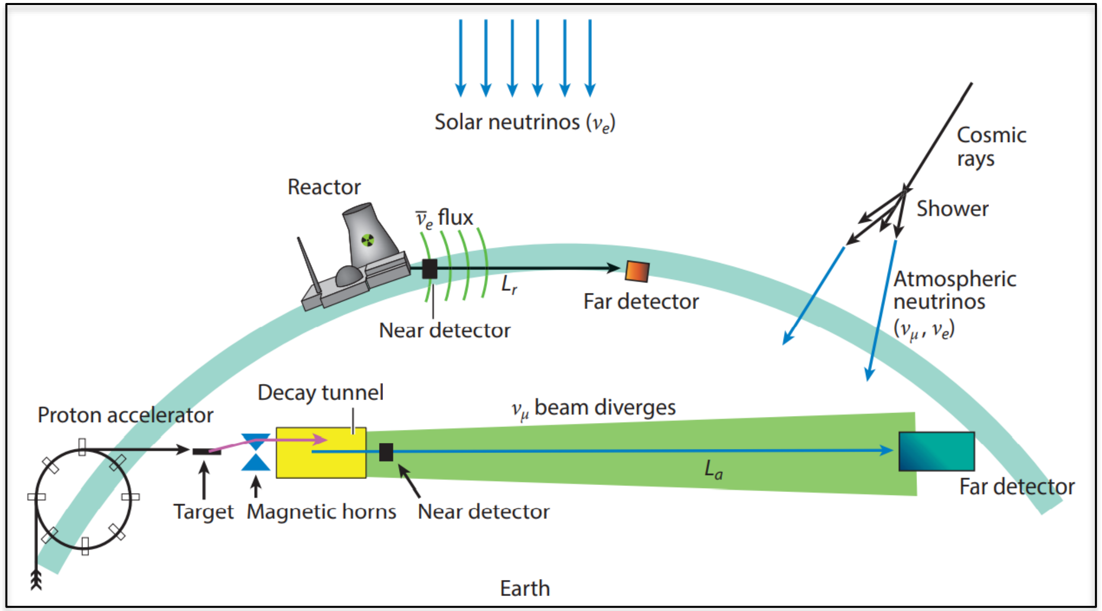

Neutrinos change flavor $(\nu_e, \nu_\mu, \nu_\tau)$ with time

- Governing principle: interaction (flavor) eigenstates ≠ mass eigenstates

$$\begin{pmatrix} \nu_e \\ \nu_\mu \\ \nu_\tau \end{pmatrix} = U \times \begin{pmatrix} \nu_1 \\ \nu_2 \\ \nu_3 \end{pmatrix}$$

- Physical parameters
  - Three angles between mass/flavor eigenstates set **oscillation amplitude** $\theta_{12}, \theta_{23}, \theta_{13}$
  - Differences in three neutrino masses determine **oscillation frequency** $\Delta m^2_{21}, \Delta m^2_{31}$
  - Off-diagonal phase δ_{CP}

Open questions:

Mass hierarchy: $\Delta m^2_{32} > 0$?

CP violation: $\delta_{CP} = ?$

ν oscillation probability

Probability to measure a particular flavor of neutrino as it propagates through space

$$\left|\begin{matrix}\nu_e\\ \nu_\mu\\ \nu_\tau\end{matrix}\right\rangle = \begin{pmatrix}1 & & \\ & c_{23} & s_{23}\\ & -s_{23} & c_{23}\end{pmatrix}\begin{pmatrix}c_{13} & & s_{13}e^{-i\delta}\\ & 1 & \\ -s_{13}e^{i\delta} & & c_{13}\end{pmatrix}\begin{pmatrix}c_{12} & s_{12} & \\ -s_{12} & c_{12} & \\ & & 1\end{pmatrix}\left|\begin{matrix}\nu_1\\ \nu_2\\ \nu_3\end{matrix}\right\rangle$$

$$P_{\alpha\beta} = \sin^2(2\theta)\sin^2\left(1.27\Delta m^2\ [\mathrm{eV}^2]\frac{L\ [\mathrm{km}]}{E\ [\mathrm{GeV}]}\right)$$

Flavor states

Mass states

Neutrino energy

Distance traveled

Probablity of neutrino of flavor α to transition to neutrino of flavor β

Neutrino oscillation parameters:

$\theta_{13}, \theta_{12}, \theta_{23}$

$\Delta m^2_{21}, \Delta m^2_{31}$

δ_{CP}

Precision measurement of ν oscillation parameters

Complimentary ability to explore the nature of ν oscillation physics with solar, atmospheric, reactor, and accelerator oscillation experiments

Disappearance: $P(\nu_\mu \to \nu_\mu)$ or $P(\nu_e \to \nu_e)$

Appearance: $P(\nu_\mu \to \nu_e)$

$$\underbrace{}_{}\quad |\Delta m^2_{32}| \qquad \Delta m^2_{31} \simeq \Delta m^2_{32} \qquad \Delta m^2_{21}$$

$$\left|\begin{array}{c}\nu_e\\ \nu_\mu\\ \nu_\tau\end{array}\right\rangle = \begin{pmatrix} 1 & & \\ & c_{23} & s_{23} \\ & -s_{23} & c_{23}\end{pmatrix}\begin{pmatrix} c_{13} & & s_{13}e^{-i\delta} \\ & 1 & \\ -s_{13}e^{i\delta} & & c_{13}\end{pmatrix}\begin{pmatrix} c_{12} & s_{12} & \\ -s_{12} & c_{12} & \\ & & 1\end{pmatrix}\left|\begin{array}{c}\nu_1\\ \nu_2\\ \nu_3\end{array}\right\rangle$$

$$P_{\alpha\beta} = \sin^2(2\theta)\sin^2\left(1.27\Delta m^2\ [\mathrm{eV}^2]\frac{L\ [\mathrm{km}]}{E\ [\mathrm{GeV}]}\right)$$

Atmospheric and long-baseline accelerator experiments
$\nu_\mu \to \nu_\mu$
$\nu_\mu \to \nu_\tau$

Reactor and long-baseline accelerator experiments
$\nu_e \to \nu_e$
$\nu_\mu \to \nu_e$

Reactor and solar experiments
$\nu_e \to \nu_e$
$\nu_e \to \nu_\mu + \nu_\tau$

Precision measurement of ν oscillation parameters

Complimentary ability to explore the nature of ν oscillation physics with solar, atmospheric, reactor, and accelerator oscillation experiments

Disappearance: $P(\nu_\mu \to \nu_\mu)$ or $P(\nu_e \to \nu_e)$

Appearance: $P(\nu_\mu \to \nu_e)$

$|\Delta m^2_{32}|$ $\quad$ $\Delta m^2_{31} \simeq \Delta m^2_{32}$ $\quad$ Δm^2_{21}

$$\left|\begin{matrix}\nu_e\\ \nu_\mu\\ \nu_\tau\end{matrix}\right\rangle = \underbrace{\begin{pmatrix}1 & & \\ & c_{23} & s_{23}\\ & -s_{23} & c_{23}\end{pmatrix}}_{|\Delta m^2_{32}|}\underbrace{\begin{pmatrix}c_{13} & & s_{13}e^{-i\delta}\\ & 1 & \\ -s_{13}e^{i\delta} & & c_{13}\end{pmatrix}}_{\Delta m^2_{31} \simeq \Delta m^2_{32}}\underbrace{\begin{pmatrix}c_{12} & s_{12} & \\ -s_{12} & c_{12} & \\ & & 1\end{pmatrix}}_{\Delta m^2_{21}}\left|\begin{matrix}\nu_1\\ \nu_2\\ \nu_3\end{matrix}\right\rangle$$

$$P_{\alpha\beta} = \sin^2(2\theta)\sin^2\left(1.27\Delta m^2\ [\mathrm{eV}^2]\frac{L\ [\mathrm{km}]}{E\ [\mathrm{GeV}]}\right)$$

Atmospheric and long-baseline accelerator experiments

$\nu_\mu \to \nu_\mu$

$\nu_\mu \to \nu_\tau$

Reactor and long-baseline accelerator experiments

$\nu_e \to \nu_e$

$\nu_\mu \to \nu_e$

Reactor and solar experiments

$\nu_e \to \nu_e$

$\nu_e \to \nu_\mu + \nu_\tau$

Neutrino Oscillation

Neutrinos change flavor $(\nu_e, \nu_\mu, \nu_\tau)$ with time

- Governing principle: interaction (flavor) eigenstates $\neq$ mass eigenstates

$$\begin{pmatrix} \nu_e \\ \nu_\mu \\ \nu_\tau \end{pmatrix} = U \times \begin{pmatrix} \nu_1 \\ \nu_2 \\ \nu_3 \end{pmatrix}$$

- Physical parameters
  - Three angles between mass/flavor eigenstates set **oscillation amplitude** $\theta_{12}, \theta_{23}, \theta_{13}$
  - Differences in three neutrino masses determine **oscillation frequency** $\Delta \mathrm{m}^2_{21}, \Delta \mathrm{m}^2_{31}$
  - Off-diagonal phase δ_{CP}

Mass hierarchy: $\Delta m^2_{32} > 0$?

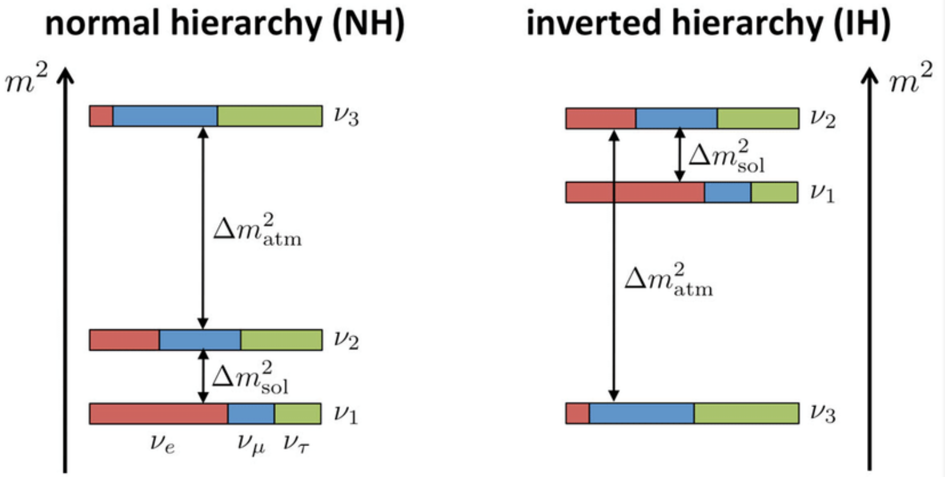

CP violation: $\delta_{CP} =$?

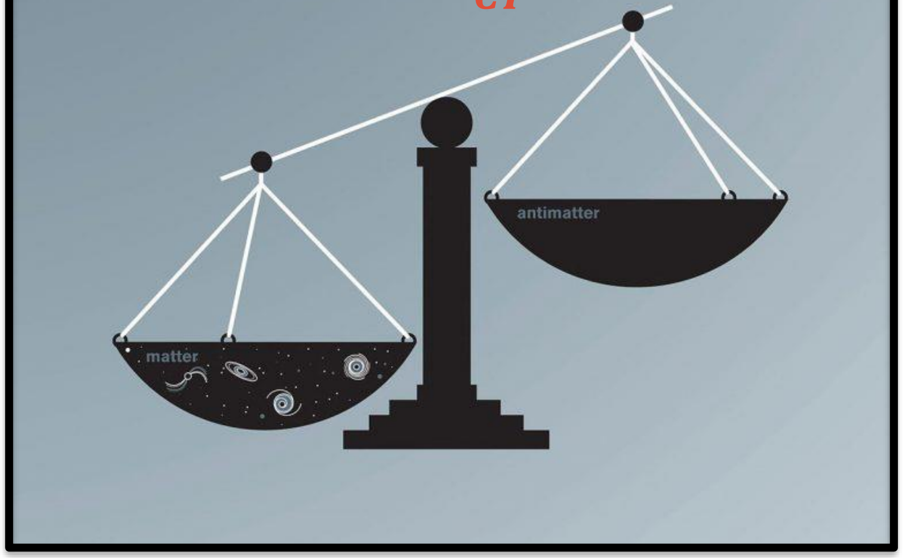

DUNE ν oscillation physics

DEEP UNDERGROUND NEUTRINO EXPERIMENT

Horn-focused broadband neutrino beam to maximize statistics and enhance dynamic range

Measure enhancement (normal ordering) or suppression (inverted ordering) in neutrino oscillation probability to determine sign of Δm^2_{32}

Measure δ_{CP} exploiting the distortion of the energy spectrum and neutrino-antineutrino oscillation probability asymmetry $A^{ll'}$

$$A^{ll'} \equiv \frac{P(\nu_l \rightarrow \nu_{l'}) - P(\overline{\nu_l} \rightarrow \overline{\nu_{l'}})}{P(\nu_l \rightarrow \nu_{l'}) + P(\overline{\nu_l} \rightarrow \overline{\nu_{l'}})}$$

Exploiting the matter effect which increases as a function of baseline like $\pm \frac{2N_e}{N_e^{res}}$

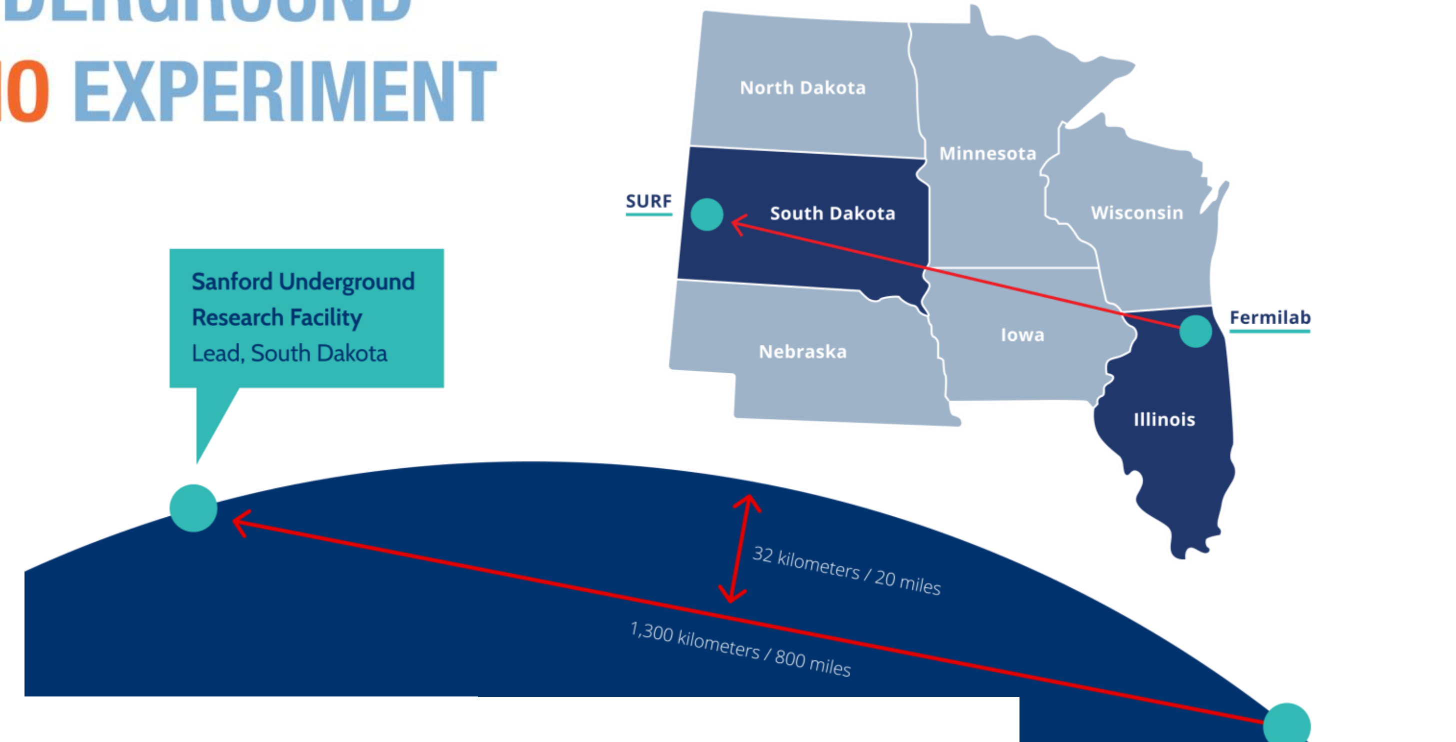

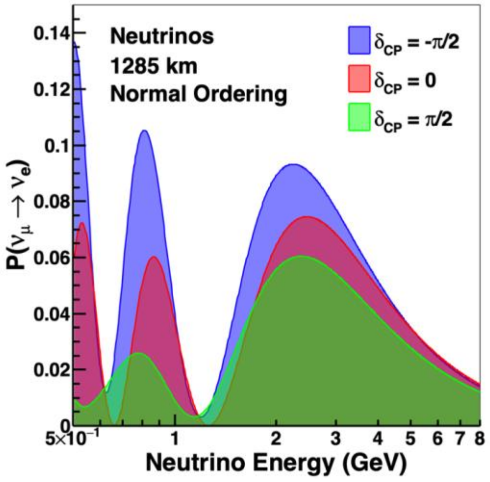

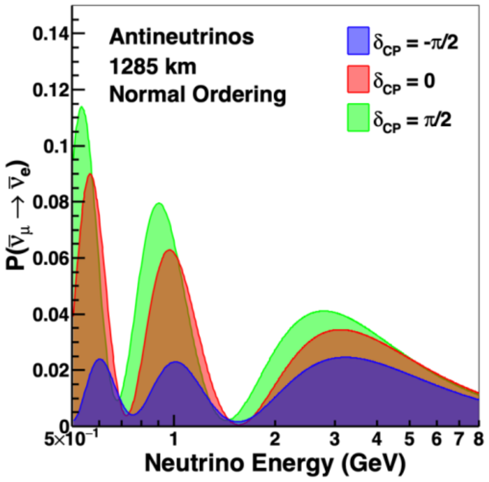

Physics Milestone	Exposure	
($\sin^2\theta_{23} = 0.580$)	Staged years	kt-MW-years
5σ Mass Ordering $\delta_{CP} = -\pi/2$	1	16
5σ Mass Ordering 100% of δ_{CP} values	2	66
3σ CP Violation $\delta_{CP} = -\pi/2$	3	100
3σ CP Violation 50% of δ_{CP} values	5	197
5σ CP Violation $\delta_{CP} = -\pi/2$	7	334
5σ CP Violation 50% of δ_{CP} values	10	646
3σ CP Violation 75% of δ_{CP} values	13	936
δ_{CP} Resolution of 10 degrees $\delta_{CP} = 0$	8	400
δ_{CP} Resolution of 20 degrees $\delta_{CP} = -\pi/2$	12	806
$\sin^2 2\theta_{13}$ Resolution of 0.004	15	1079

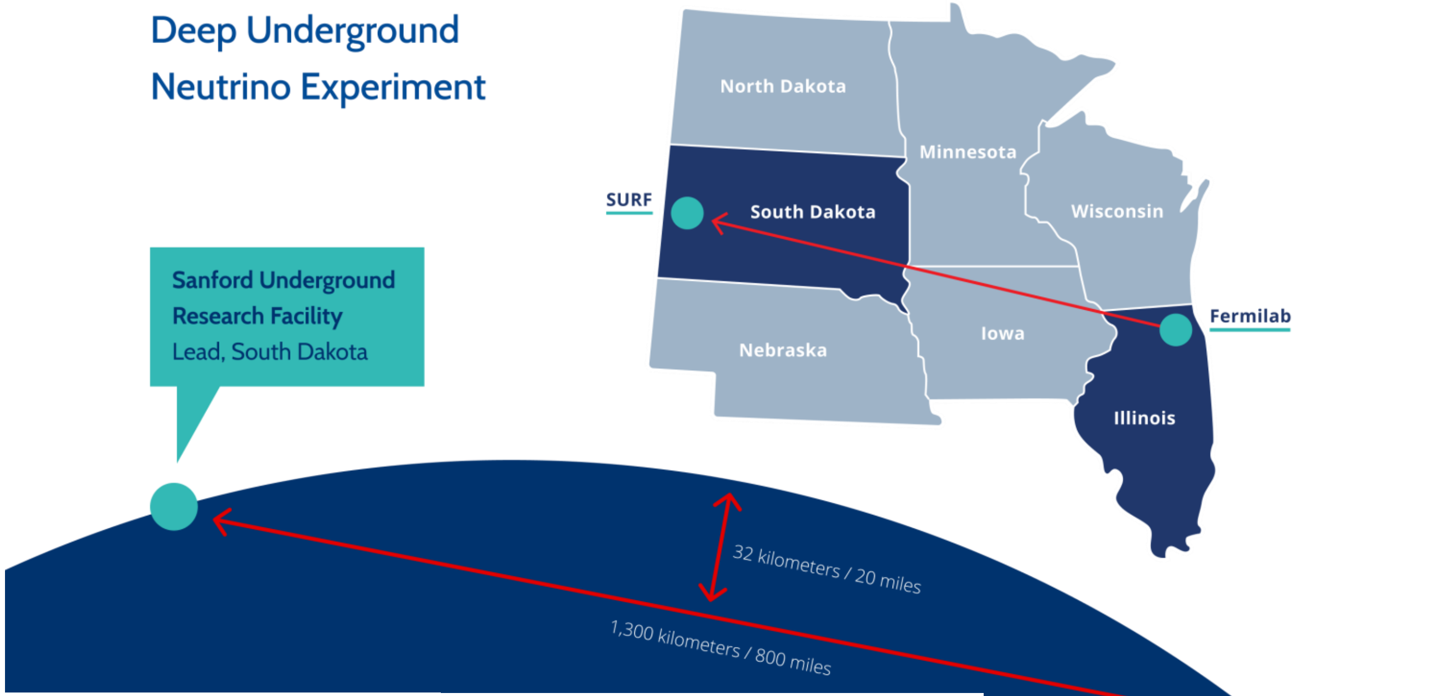

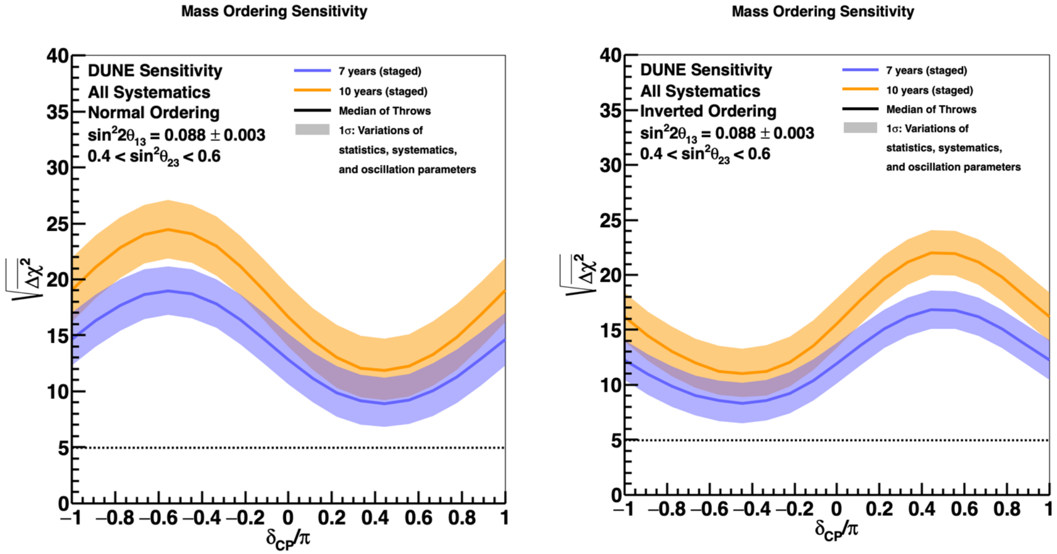

Physics Milestone	Exposure	
($\sin^2\theta_{23} = 0.580$)	Staged years	kt-MW-years
5σ Mass Ordering $\delta_{CP} = -\pi/2$	1	16
5σ Mass Ordering 100% of δ_{CP} values	2	66
3σ CP Violation $\delta_{CP} = -\pi/2$	3	100
3σ CP Violation 50% of δ_{CP} values	5	197
5σ CP Violation $\delta_{CP} = -\pi/2$	7	334
5σ CP Violation 50% of δ_{CP} values	10	646
3σ CP Violation 75% of δ_{CP} values	13	936
δ_{CP} Resolution of 10 degrees $\delta_{CP} = 0$	8	400
δ_{CP} Resolution of 20 degrees $\delta_{CP} = -\pi/2$	12	806
$\sin^2 2\theta_{13}$ Resolution of 0.004	15	1079

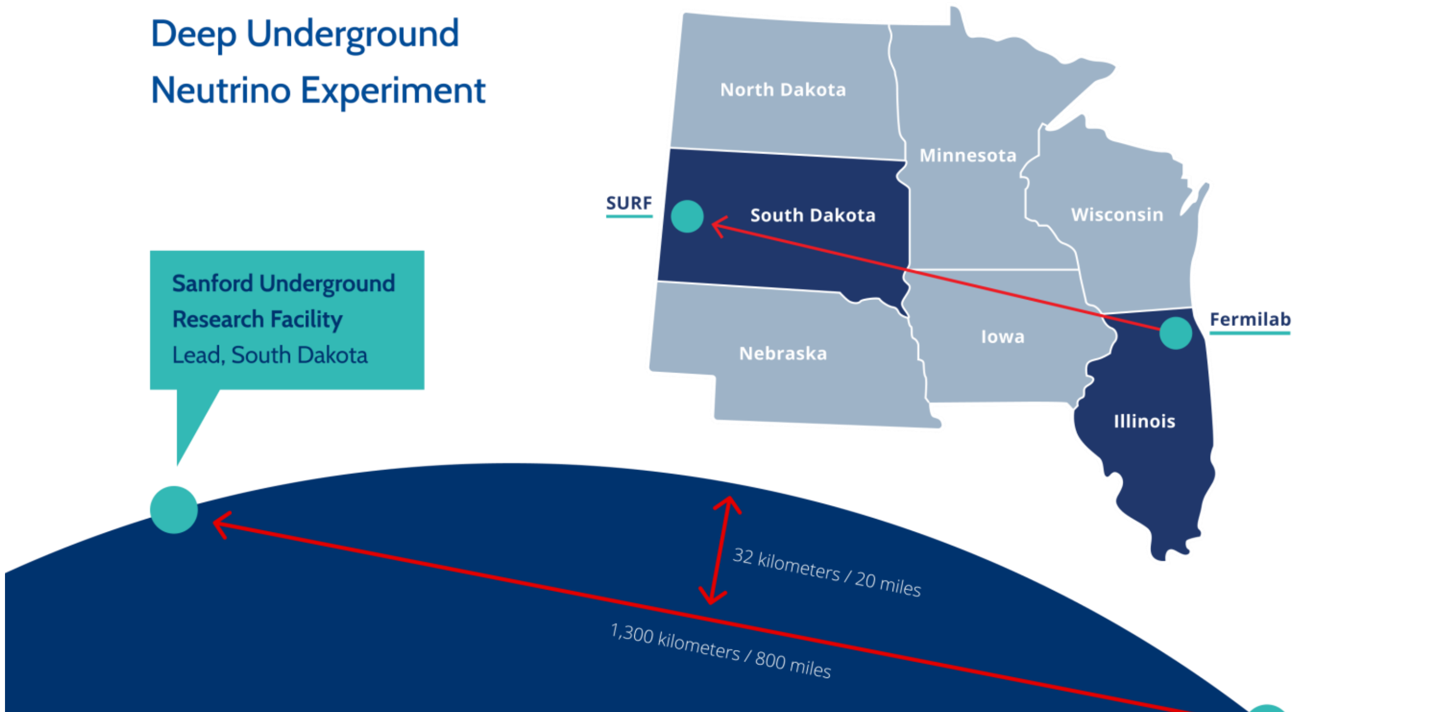

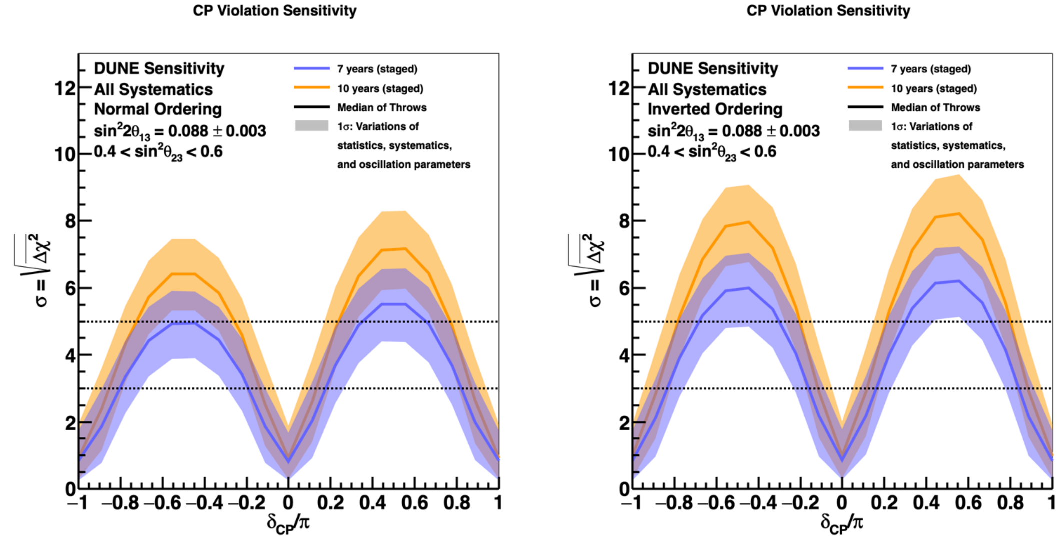

The near detector's role in long-baseline ν oscillation measurements

A performant near detector is required such that measurements can be extrapolated to the far detector to *predict far detector observed $\nu_{\mu,e}$CC event spectra*

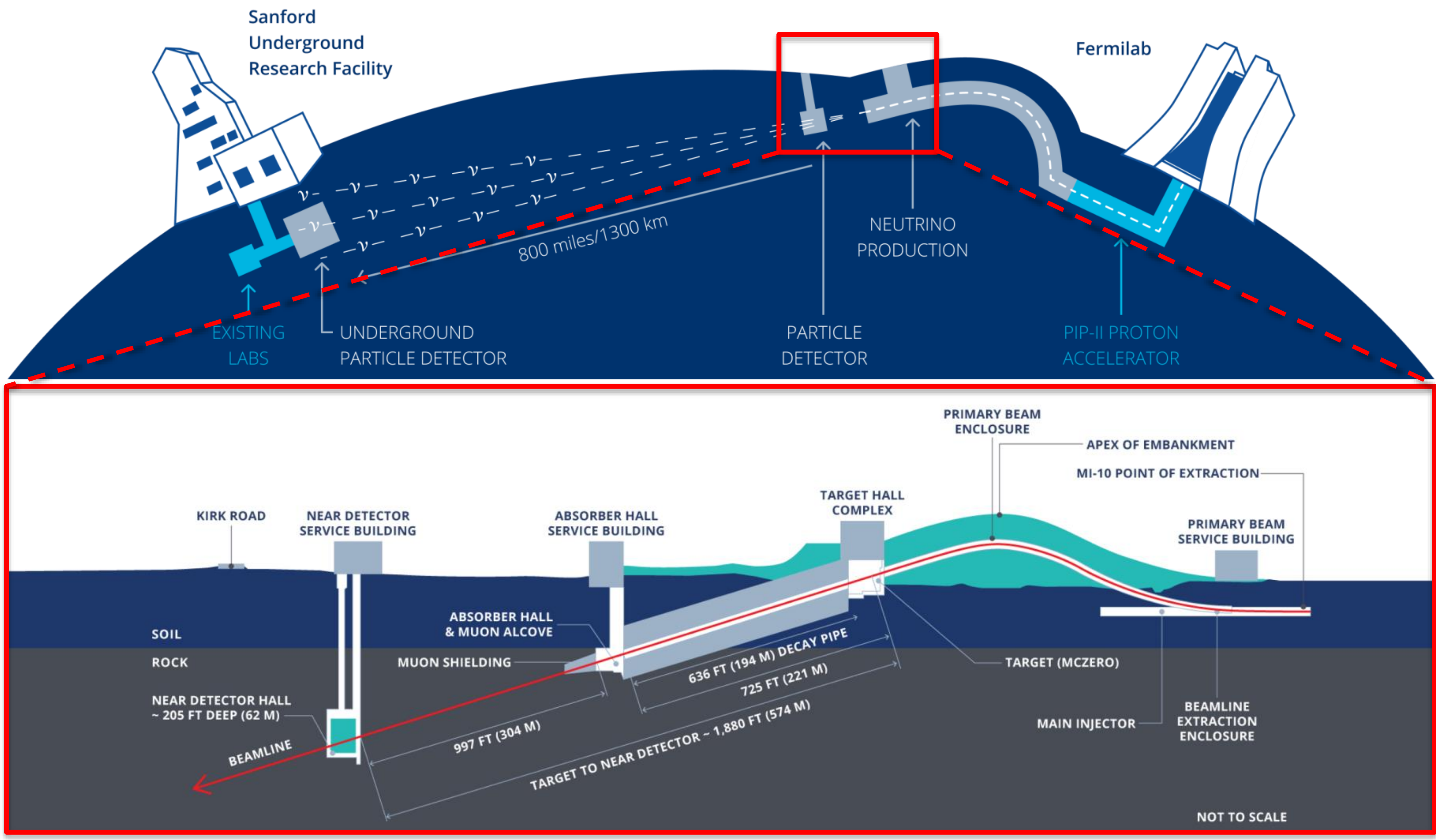

LAr Near Detector (ND-LAr) design

DUNE Near Detector Complex

Three complementary detector systems working in concert to <u>*constrain*</u>
(1) neutrino flux,
(2) interaction model,
(3) and detector response
to predict the observed neutrino spectrum at the far detector

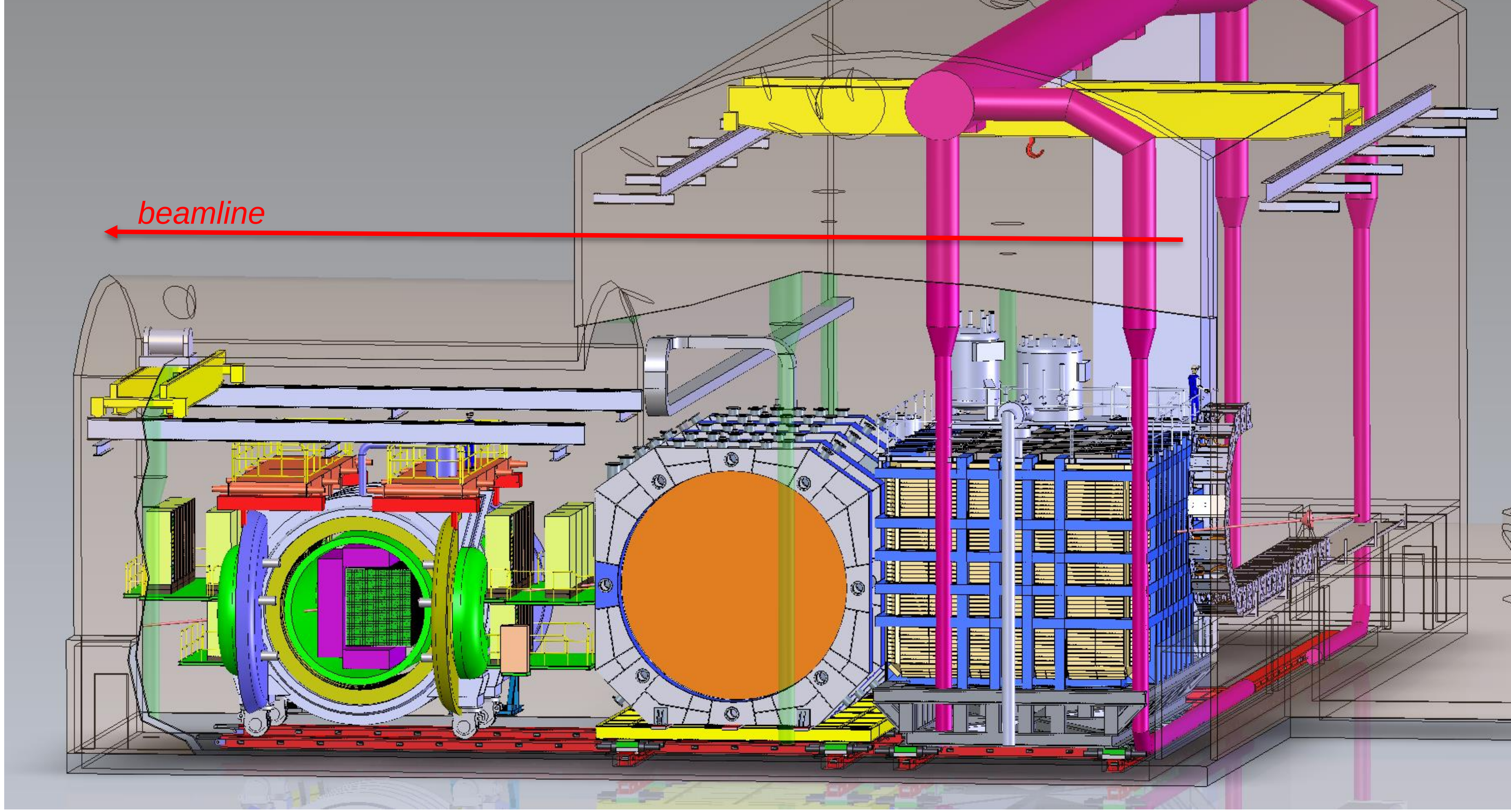

ND-LAr
- *Transfer measurements to FD*

DUNE Near Detector Complex

Three complementary detector systems working in concert to *constrain*
(1) neutrino flux,
(2) interaction model,
(3) and detector response
to predict the observed neutrino spectrum at the far detector

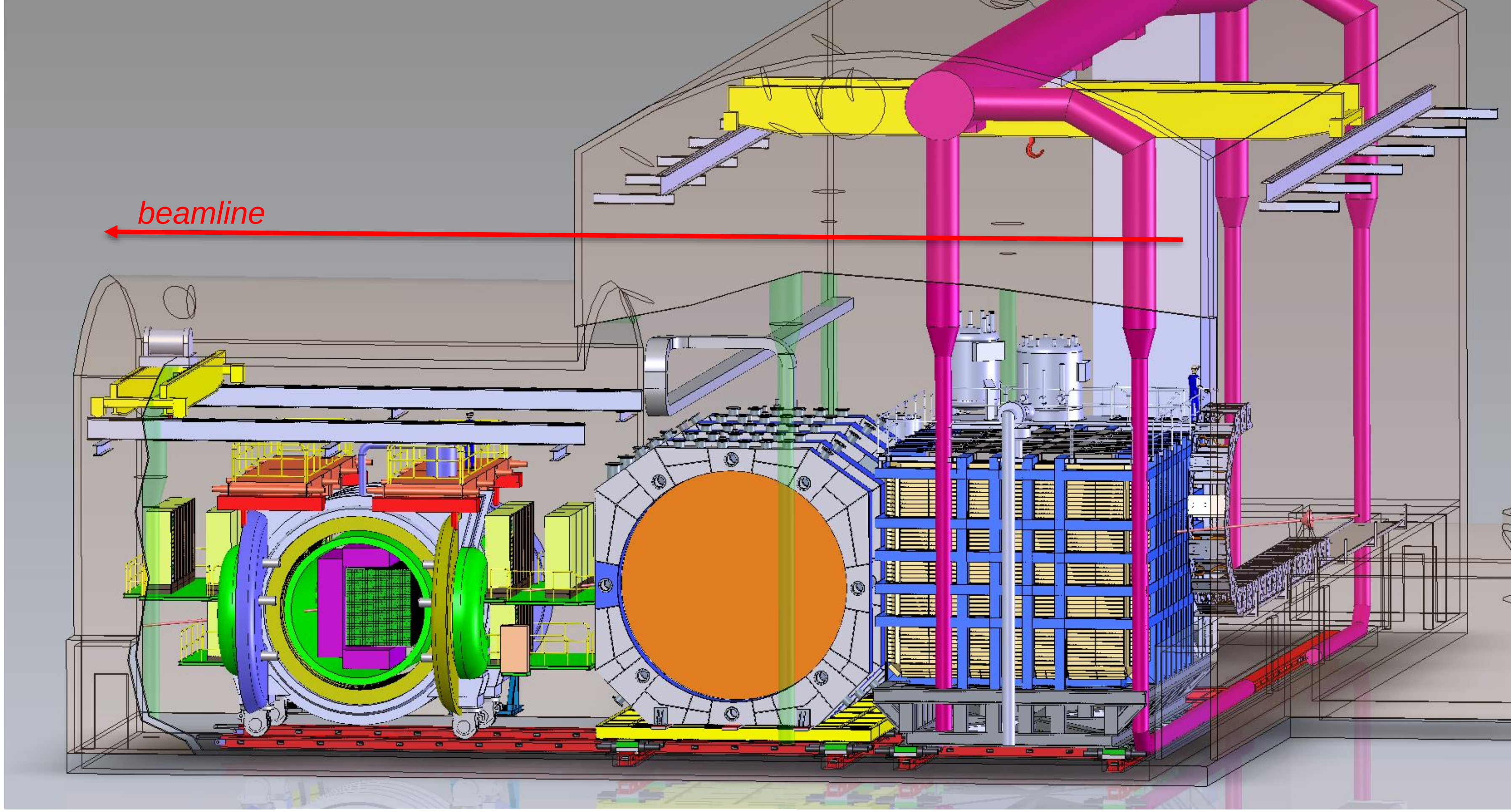

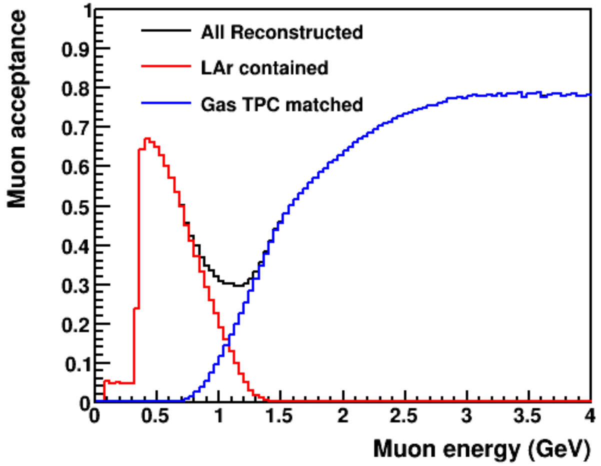

ND-LAr
- *Transfer measurements to FD*

DUNE Near Detector Complex

Three complementary detector systems working in concert to *constrain*
(1) neutrino flux,
(2) interaction model,
(3) and detector response
to predict the observed neutrino spectrum at the far detector

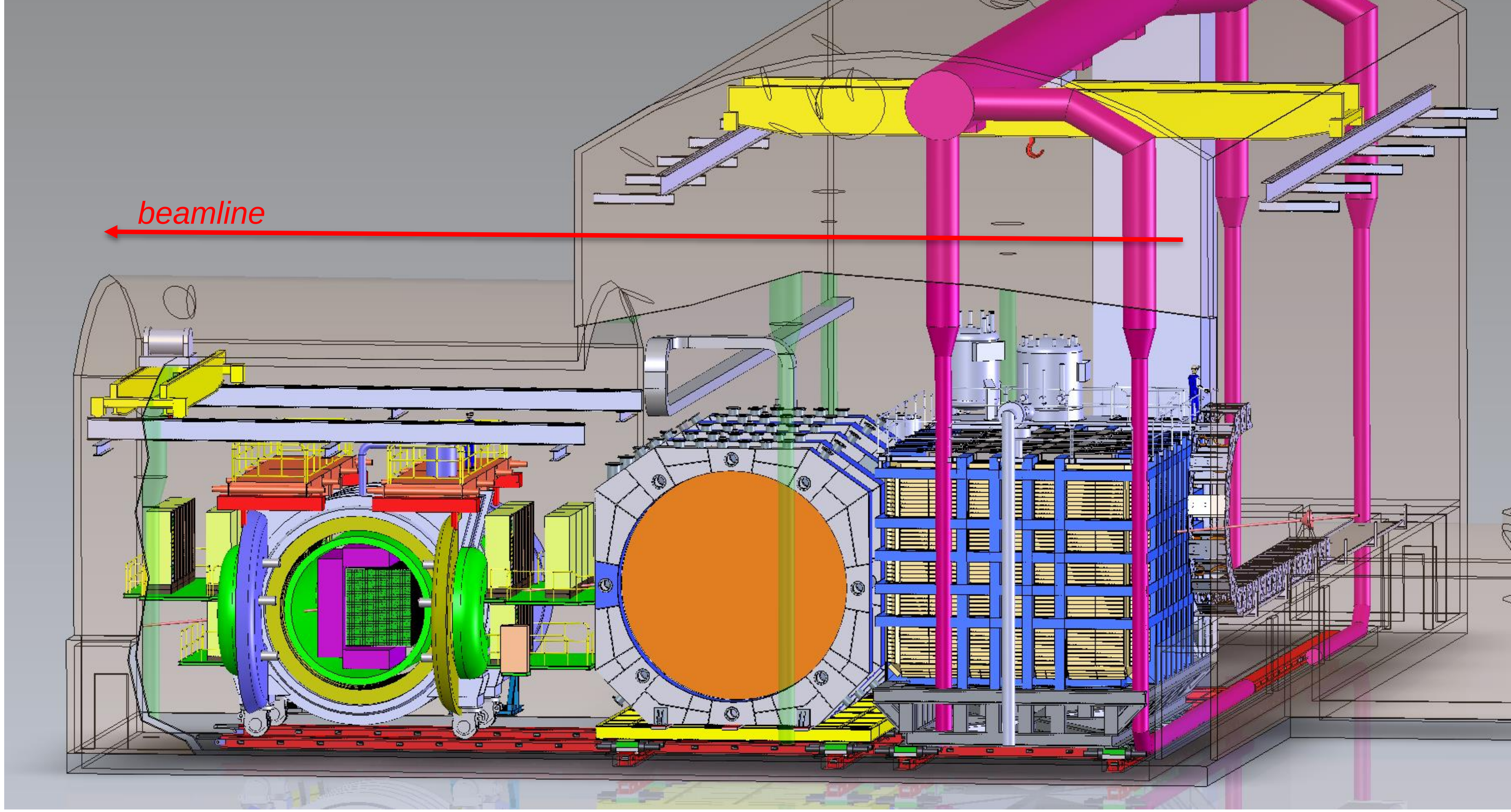

ND-GAr

ND-LAr

- *Transfer measurements to FD*

- *Constrain the ν-Ar cross section model*

DUNE Near Detector Complex

Three complementary detector systems working in concert to *constrain*

(1) neutrino flux,

(2) interaction model,

(3) and detector response

to predict the observed neutrino spectrum at the far detector

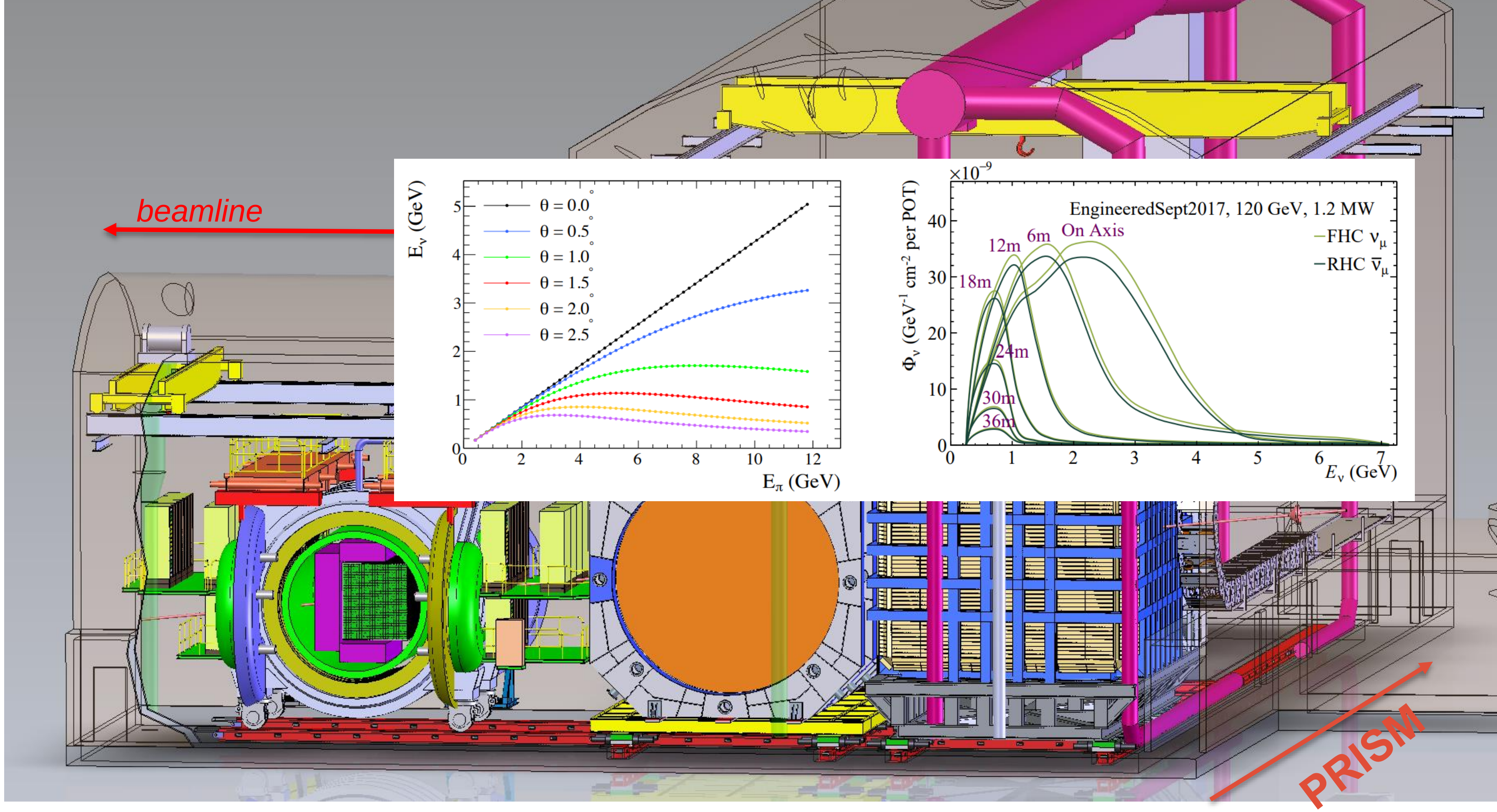

ND-GAr

ND-LAr

- *Transfer measurements to FD*

- *Constrain the ν-Ar cross section model*
- *Sample measurements with different ν fluxes*

DUNE Near Detector Complex

Three complementary detector systems working in concert to *constrain*

(1) neutrino flux,

(2) interaction model,

(3) and detector response

to predict the observed neutrino spectrum at the far detector

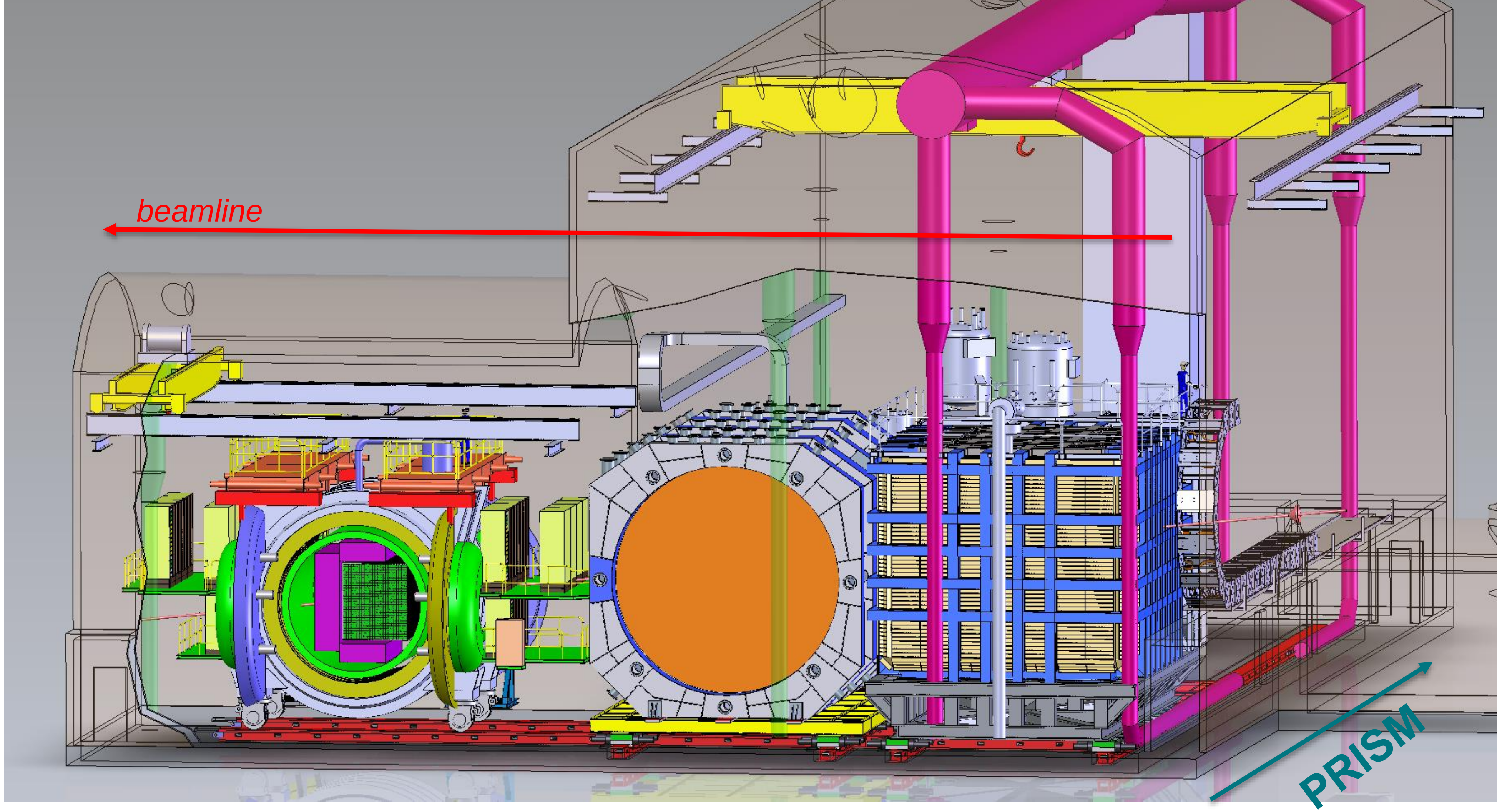

SAND

- *Monitor ν beam time variations*

ND-GAr

ND-LAr

- *Transfer measurements to FD*

- *Constrain the ν-Ar cross section model*
- *Sample measurements with different ν fluxes*

DUNE Near Detector Complex

Three complementary detector systems working in concert to *constrain*

(1) neutrino flux,

(2) interaction model,

(3) and detector response

to predict the observed neutrino spectrum at the far detector

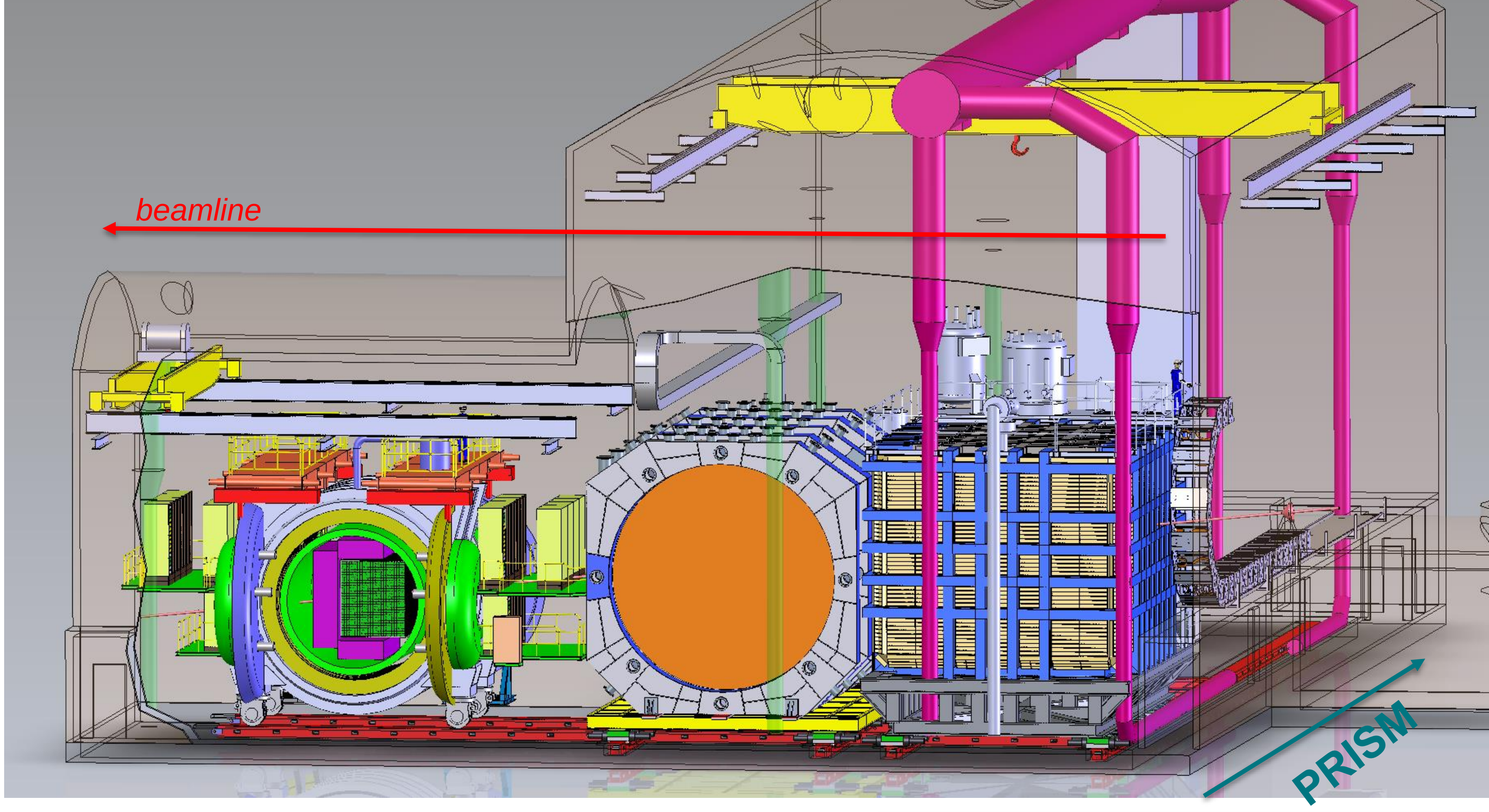

SAND
- *Monitor ν beam time variations*

ND-GAr

ND-LAr
- *Transfer measurements to FD*

- *Constrain the ν-Ar cross section model*
- *Sample measurements with different ν fluxes*

Operate in ***high rate*** environment

→ challenging for LArTPCs due to slow charge signals

Liquid Argon Time Projection Chamber (LArTPC)

- Charge signal is slow – microsecond to millisecond timescales
- Light signal is fast – nanosecond timescales

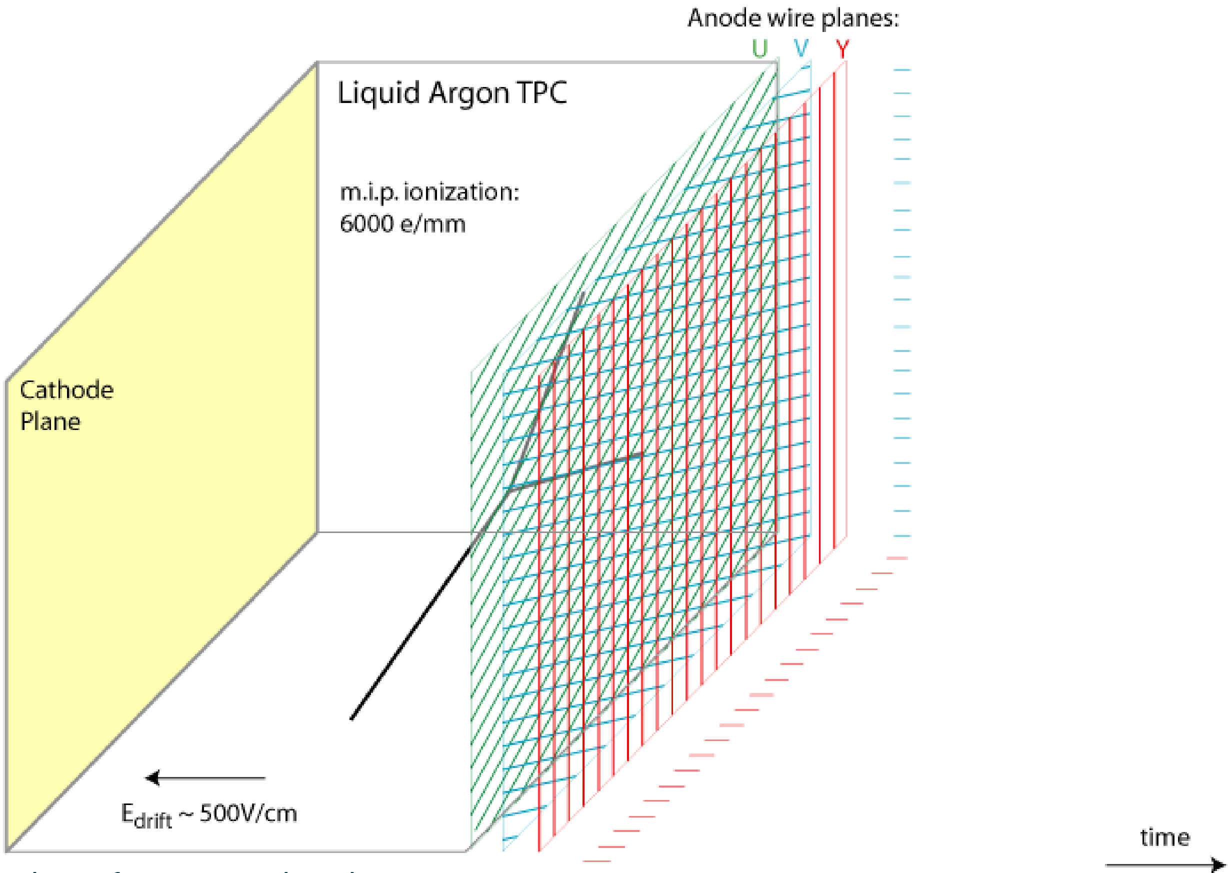

Figure from Bo Yu (BNL)

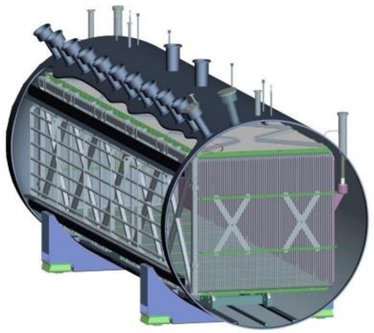
MicroBooNE
85t

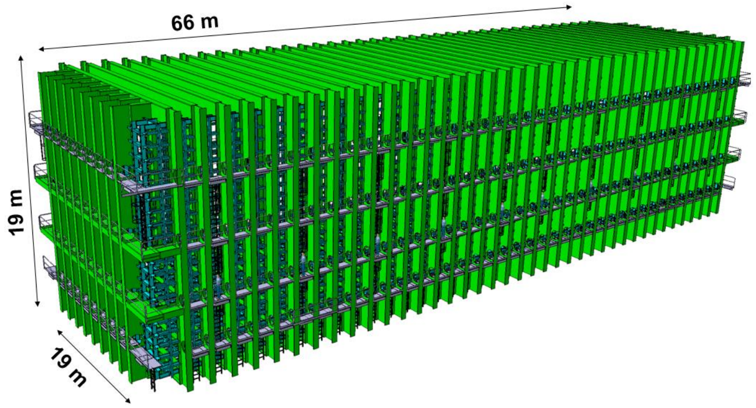

DUNE far detector
four 17kt modules

ND-LAr Event Rates

Ample statistics for FD constraint & rich physics program

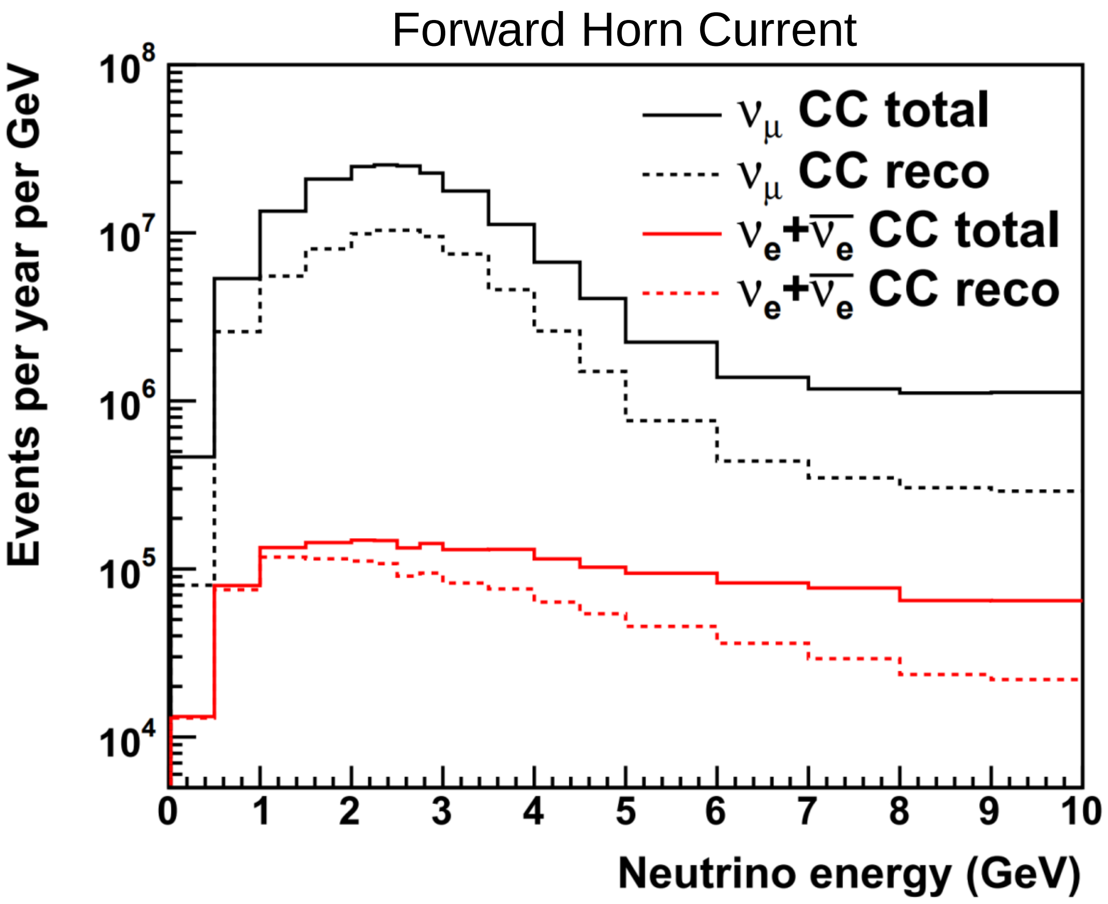

*On-axis

FHC mode	total	accepted	0.5 GeV to 4.0 GeV	accepted
CC ν_μ	8.21e+07	3.01e+07	5.88e+07	2.41e+07
CC $\bar{\nu}_\mu$	3.56e+06	1.47e+06	1.09e+06	5.29e+05
neutral current (NC) total	2.76e+07	1.66e+07	1.9e+07	1.36e+07
CC $\nu_\mu + 0\,\pi$	2.93e+07	1.57e+07	2.57e+07	1.34e+07
CC $\nu_\mu + 1\,\pi^\pm$	2.04e+07	7.48e+06	1.66e+07	6.04e+06
CC $\nu_\mu + 1\,\pi^0$	8.05e+06	2.85e+06	6.45e+06	2.23e+06
CC $\nu_\mu + 2\,\pi$	1.05e+07	2.59e+06	6.86e+06	1.77e+06
CC $\nu_\mu + 3\,\pi$	4.62e+06	7.2e+05	1.73e+06	3.78e+05
CC $\nu_\mu +$ other	9.22e+06	7.44e+05	1.46e+06	3.09e+05
CC $\nu_e + \bar{\nu}_e$	1.43e+06	6.56e+05	4.47e+05	3.34e+05
$\nu + e^-$	8.39e+03	7.16e+03	5.31e+03	4.24e+03

Key measurements:

- Charged-current ν_μ as a function of off-axis angle
- Direct flux constraints ($\nu - e$ elastic scattering and low-ν CC ν_μ)
- Exclusive, multidimensional ν-Ar cross section measurements

Beam ν Pileup Mitigation with Modularity at ND-LAr

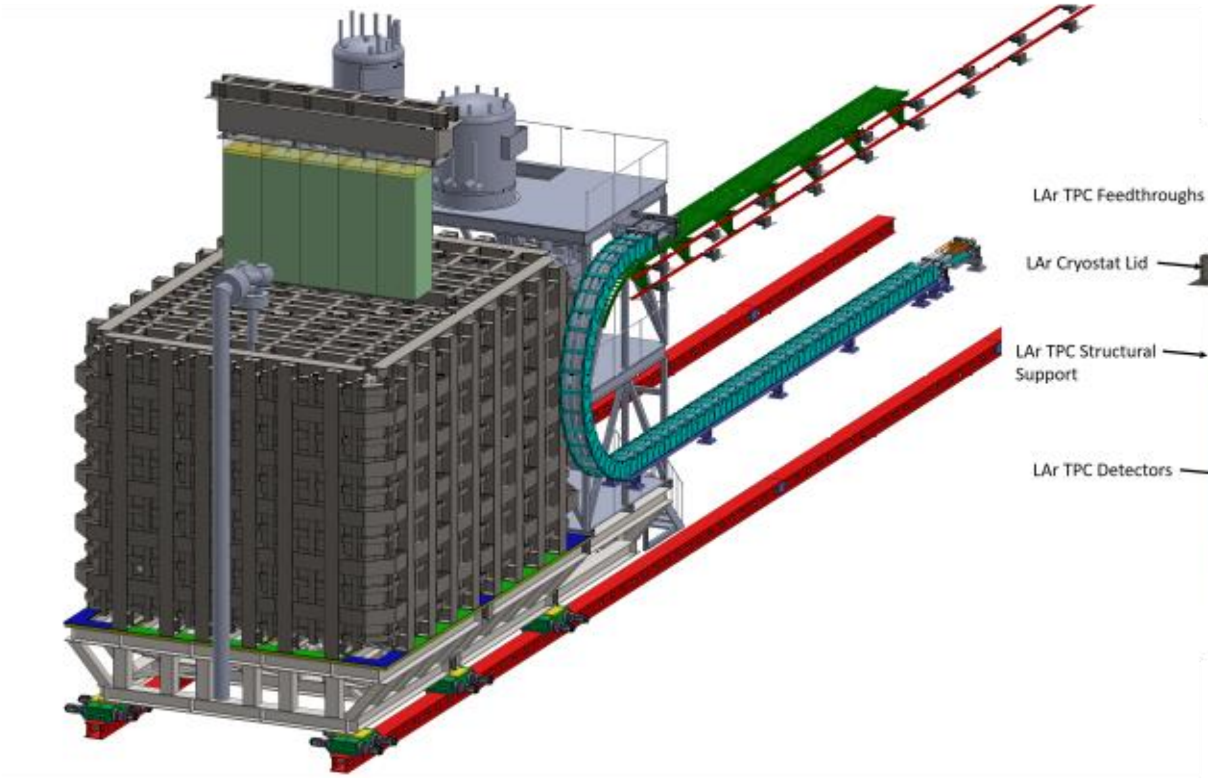

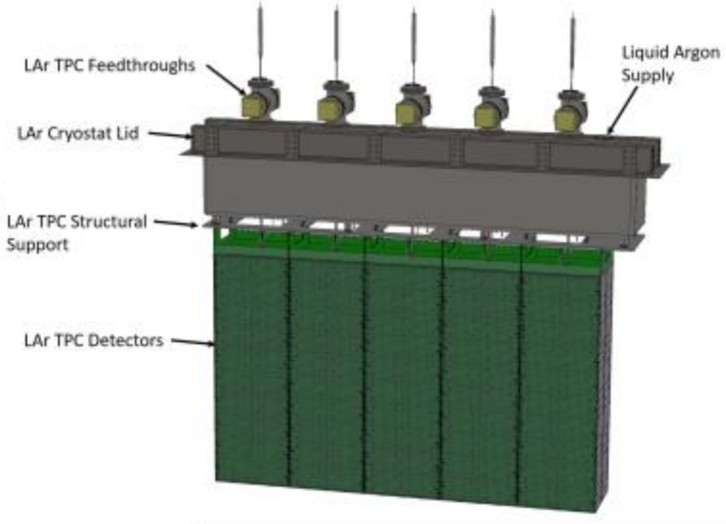

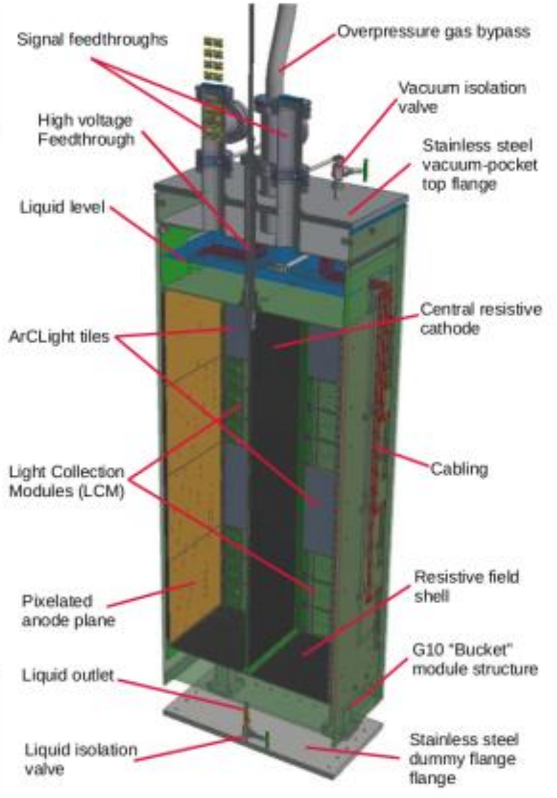

- *Optical segmentation* – ArgonCube modular LArTPC technology to enhance charge-light signal association
- *High photodetector coverage with minimal mass* – ~40% photocoverage coupled with low-profile field structures
- *Unambiguous 3D charge* – low-power pixelated readout eliminates the ambiguities common to projective readout

3D charge reconstruction ambiguity

3 GeV ν_e

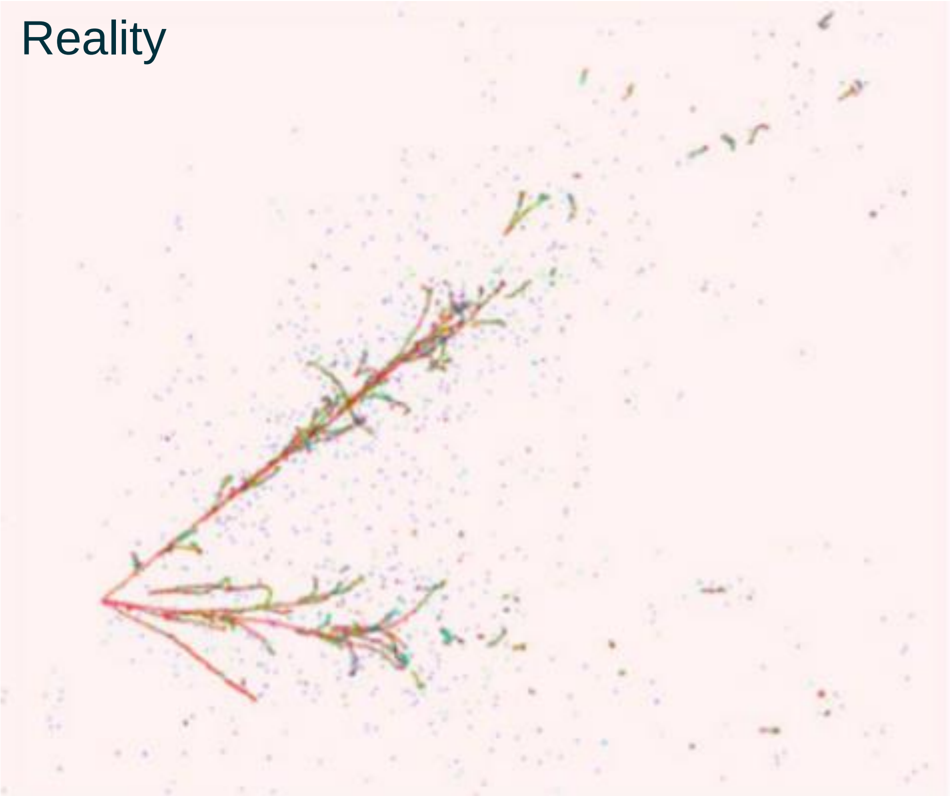

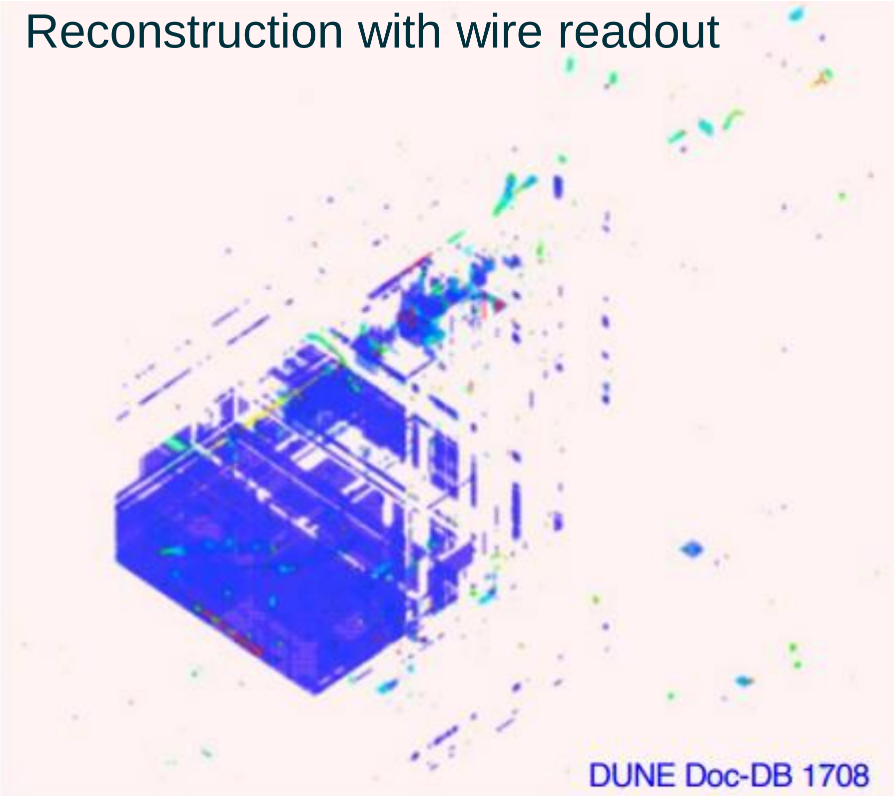

- Natural consequence of projective readout with wire geometry

Neutrino Pile-up at ND-LAr

- Within a given 10 μs beam spill, on average **55 ν interactions** produce signals within the ND-LAr active volume
- Scintillation signals can resolve each neutrino interaction within a spill, assuming that the scintillation and ionization signals are **accurately associated**
- Use ***optical segmentation*** to enhance fidelity of ionization-scintillation signal association

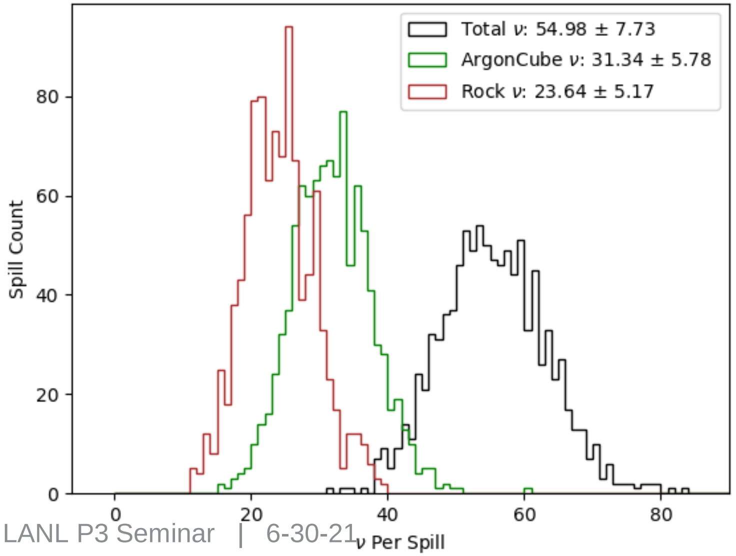

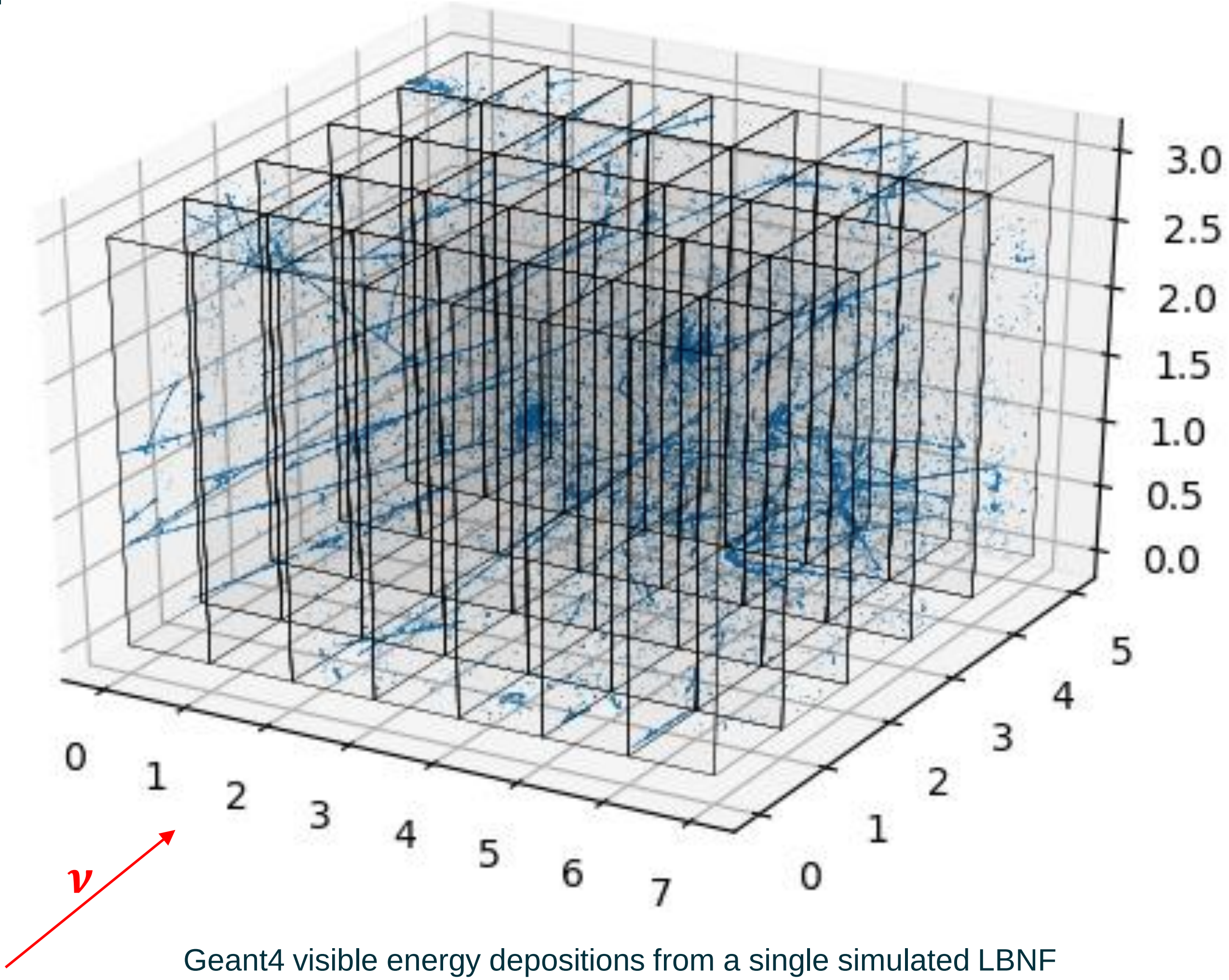

Geant4 visible energy depositions from a single simulated LBNF neutrino beam spill at forward horn current and 1.2 MW beam power. Neutrino interactions on material both internal and external to ND-LAr are shown.

Light-assisted charge clustering

Charge before (A) and after (B) association to light signals, where (C) provides the corresponding scintillation light signals with the charge-light signal association provided between (B) and (D).

The light-tight meter-scale modular design should afford **few-to-few charge-light signal association combinatorics**, a tractable situation for software solutions.

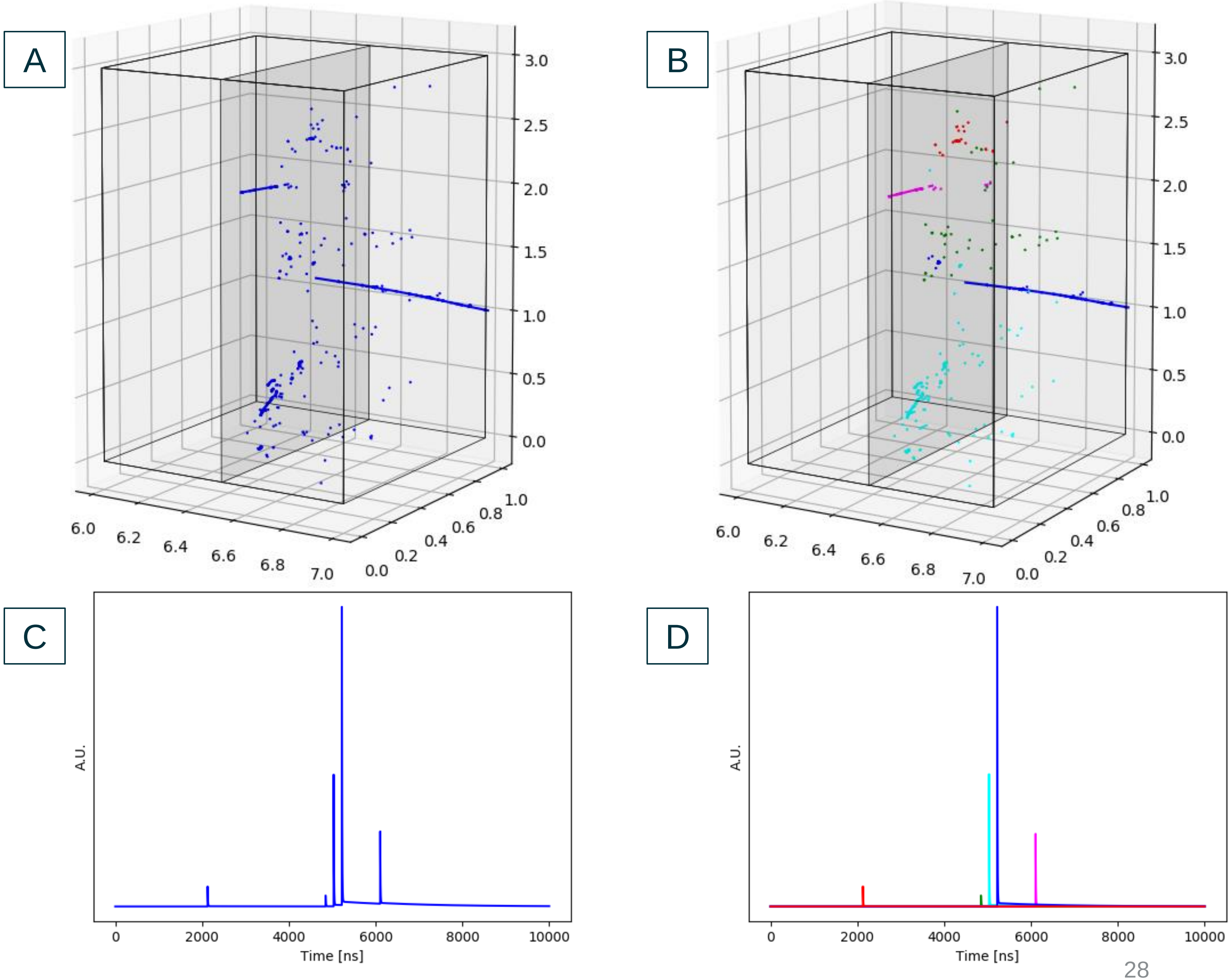

ND-LAr prototyping program

ND LArTPC Module Design

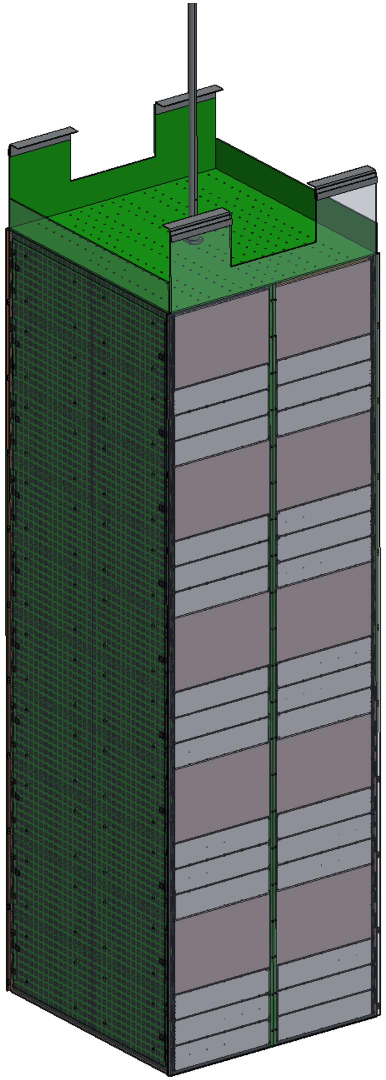

Module size

Each 1m x 1m x 3m module has signals from multiple neutrinos (~5) per 10us beam spill at 1.2 MW.

Pixelated charge readout

Provides true 3D imaging of ionization

Low-profile field cage

Maximizes instrumented region

Provides optical segmentation

High-performance light readout

Enables accurate charge-light signal matching within each module to overcome pile-up.

Enables accurate signal reconstruction in high pile-up ND environment

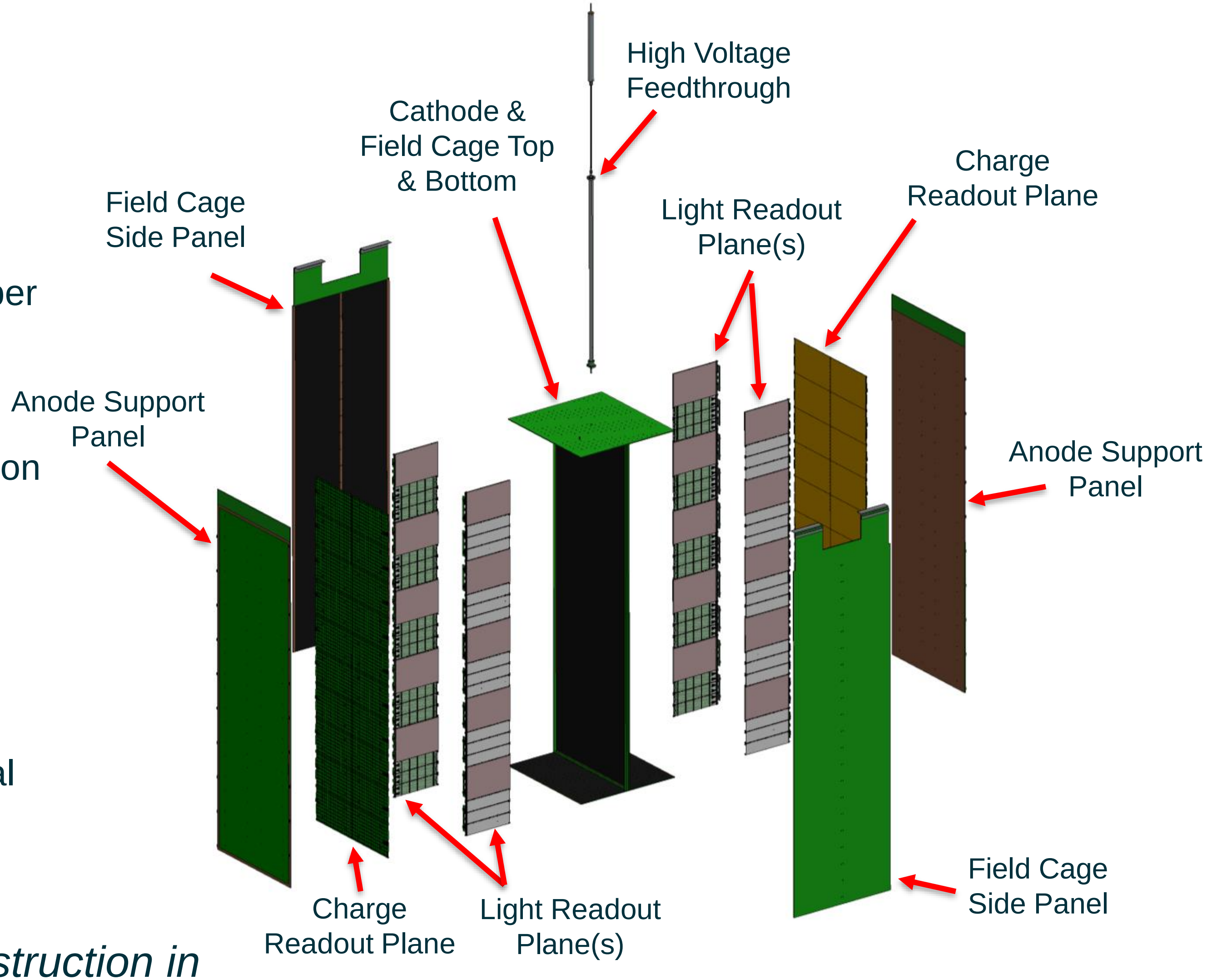

ND LArTPC Module Design

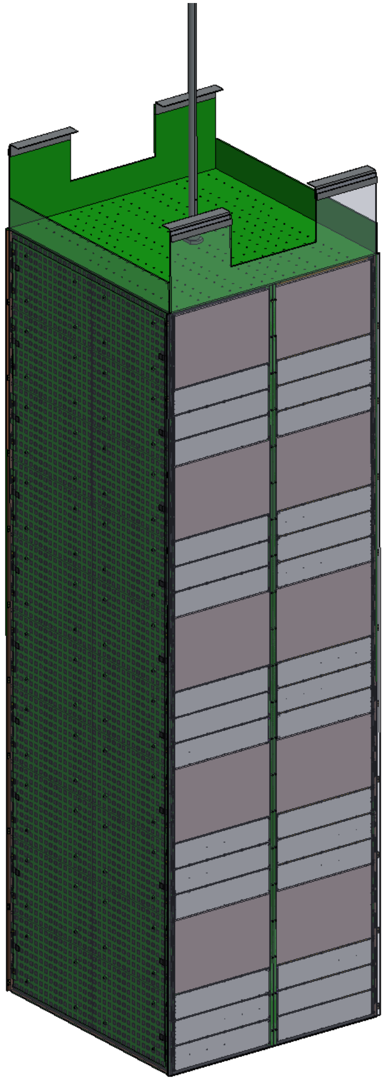

Module size
Each 1m x 1m x 3m module has signals from multiple neutrinos (~5) per 10us beam spill at 1.2 MW.

Pixelated charge readout
Provides true 3D imaging of ionization

Low-profile field cage
Maximizes instrumented region
Provides optical segmentation

High-performance light readout
Enables accurate charge-light signal matching within each module to overcome pile-up.

Enables accurate signal reconstruction in high pile-up ND environment

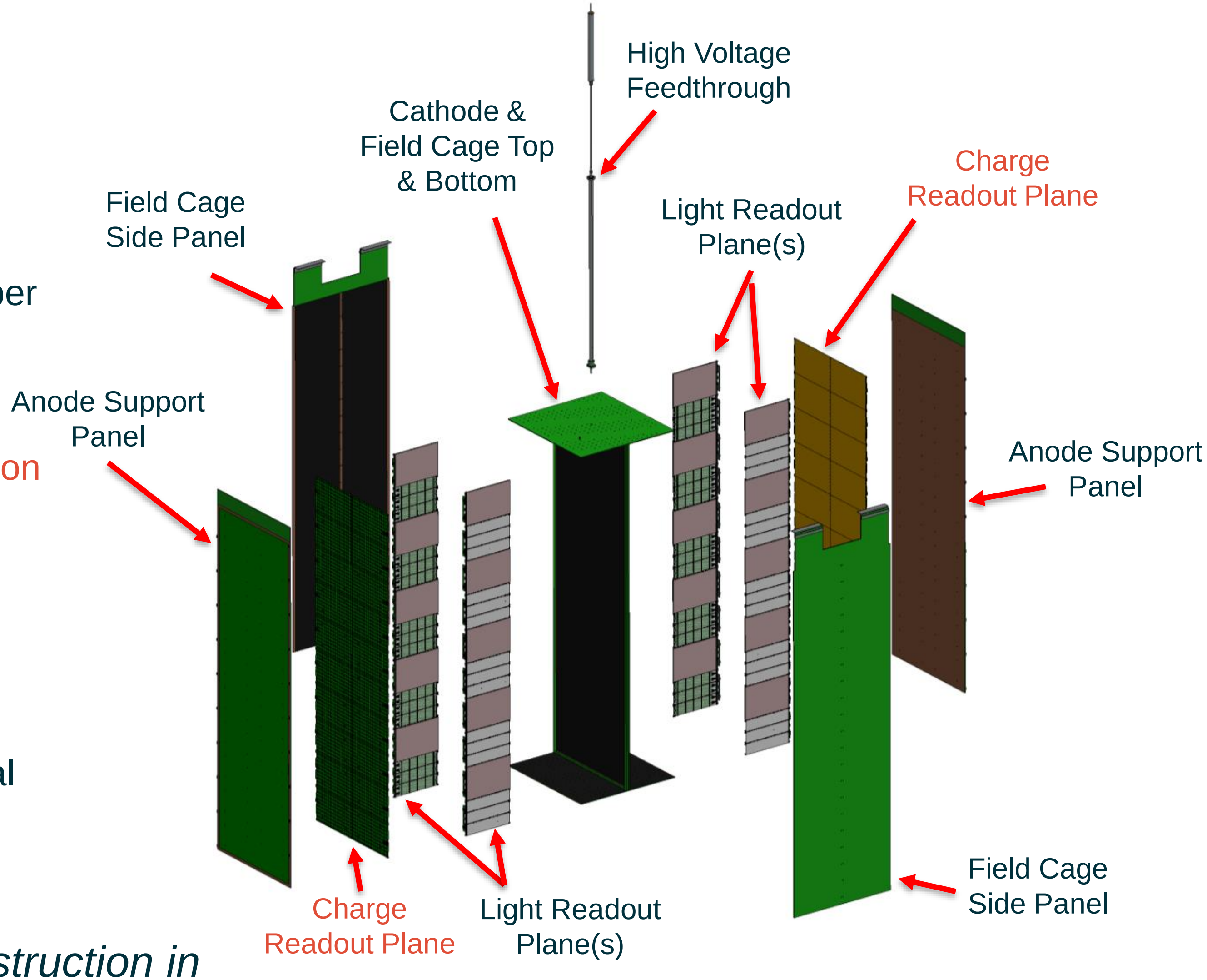

Pixel Readout R&D for LArTPCs

Key challenges:

- Power
- Channel density
- Cost

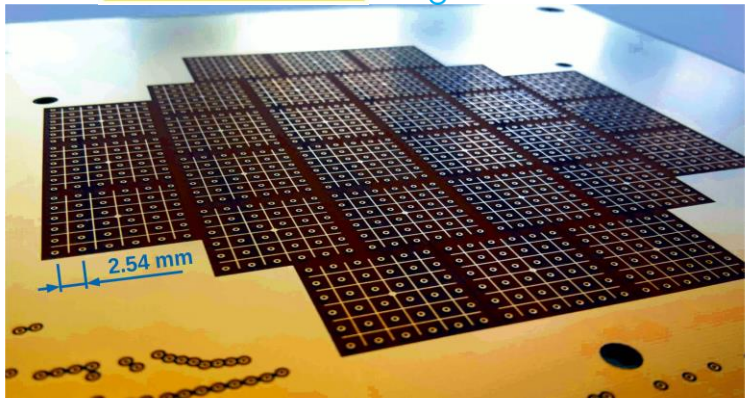

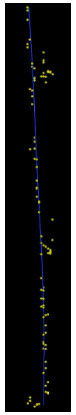

Demonstrated pixel readout in LAr (Summer '16)

Combined pixel signals to dramatically reduce channel count

J. Asaadi *et al.* Instruments 4 (2020) 1,9

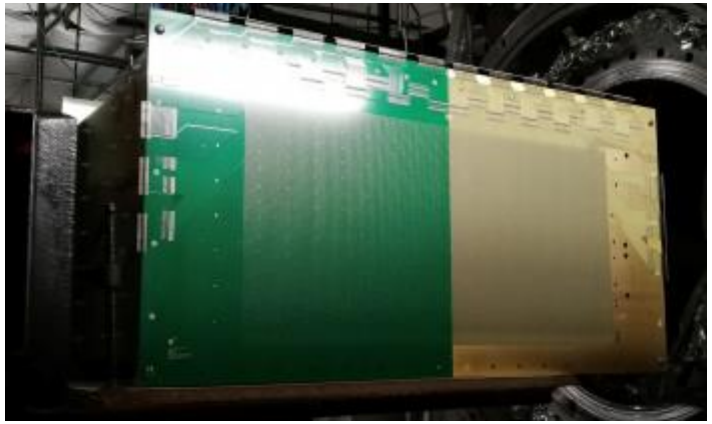

Large-area pixel sensor in LArIAT (Dec. '17 – Jan. '18)

28,800 pixels merged into 480 channels

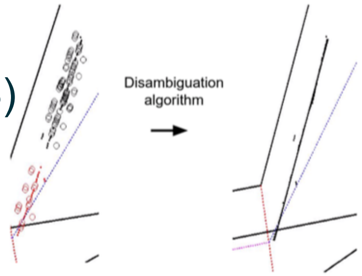

Q-Pix

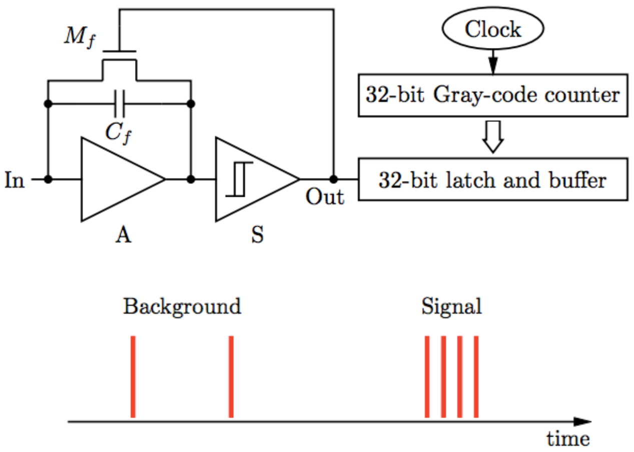

Each pixel produces a series of digital trigger pulses

Given a Scmitt threshold *dQ*, current arriving at pixel in interval *dt* between triggers is *dQ/dt*

D. Nygren & Y. Mei arXiv: 1809.10213

Low-power, integrating amplifier with self-triggered digitization and readout

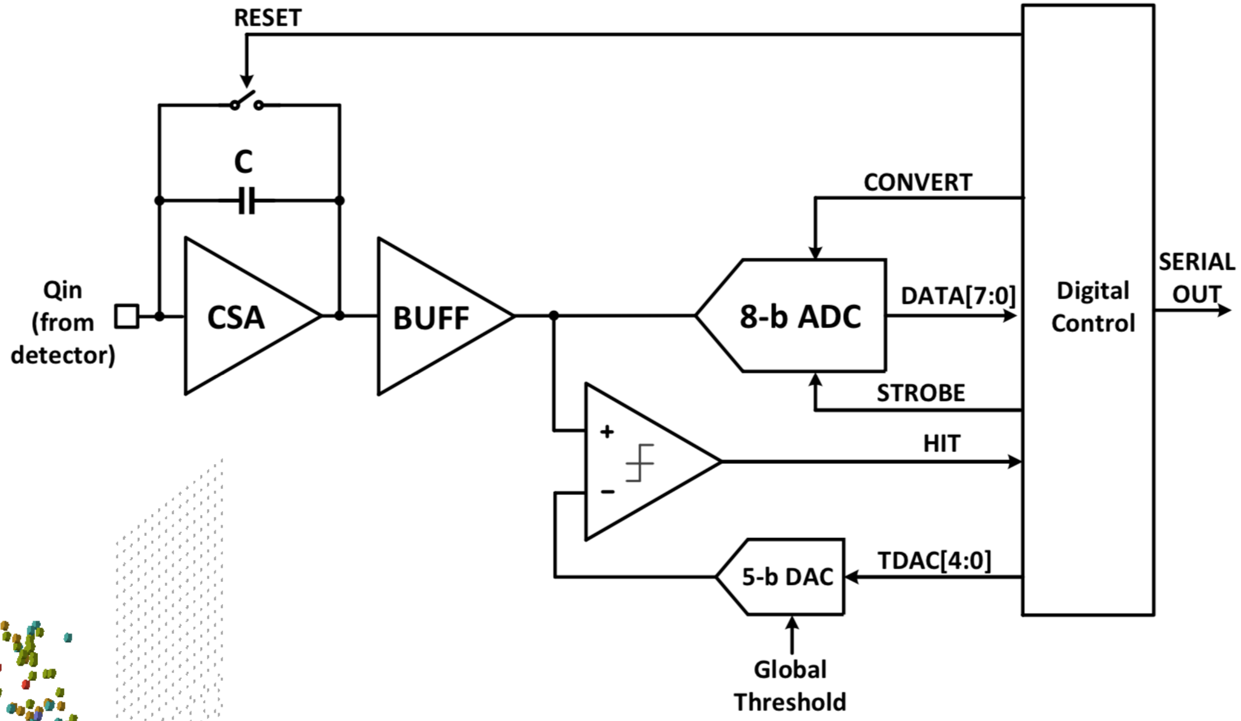

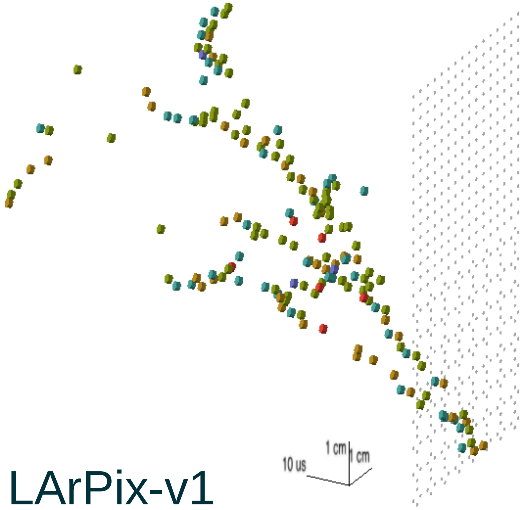

LArPix-v1

First proof of principle demonstration by Dan Dwyer *et al. JINST 13 (2018) P10007*

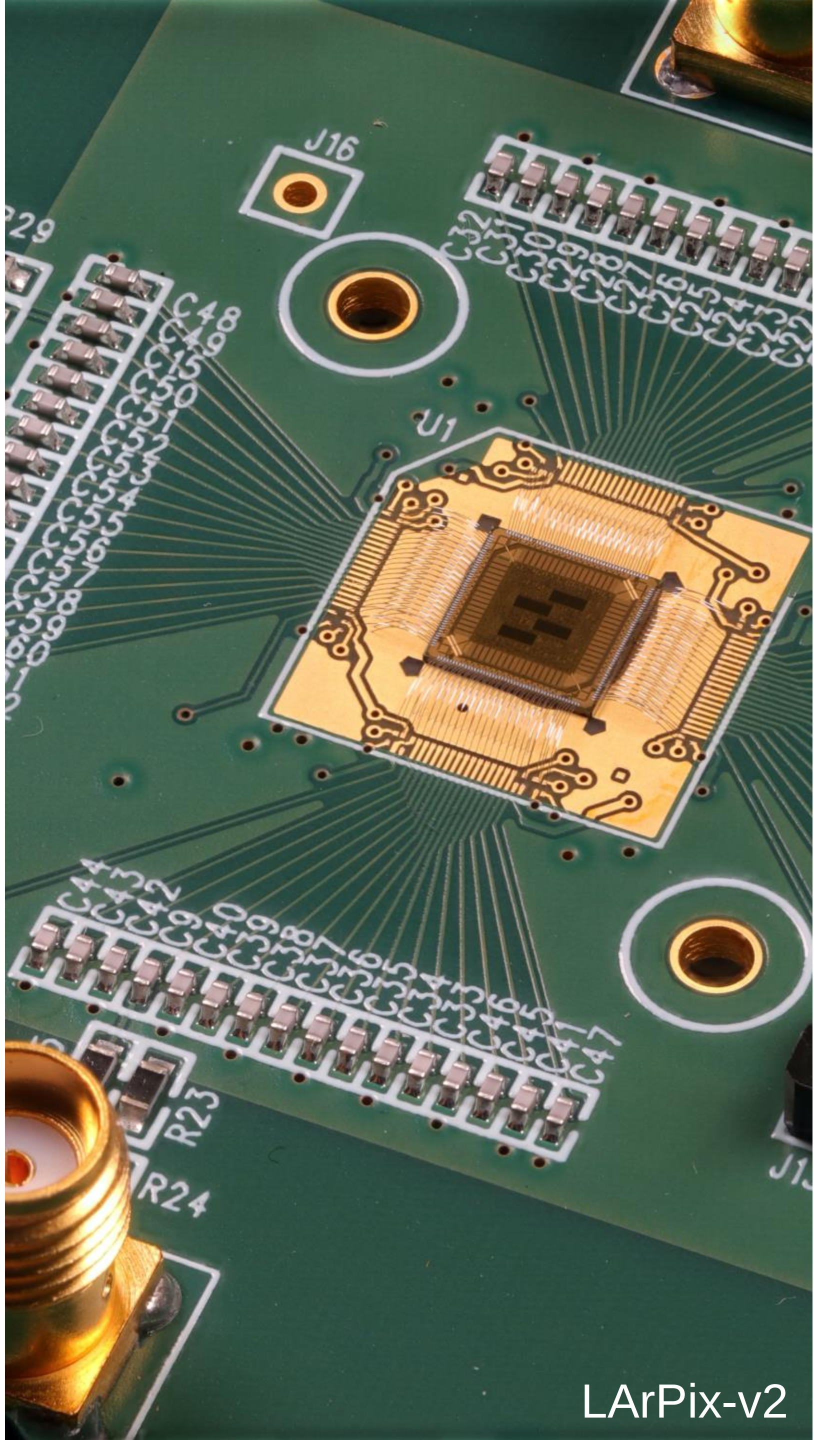

LArPix-v2

LArPix-v2 ASIC

64 channels
on 25 mm^2 die

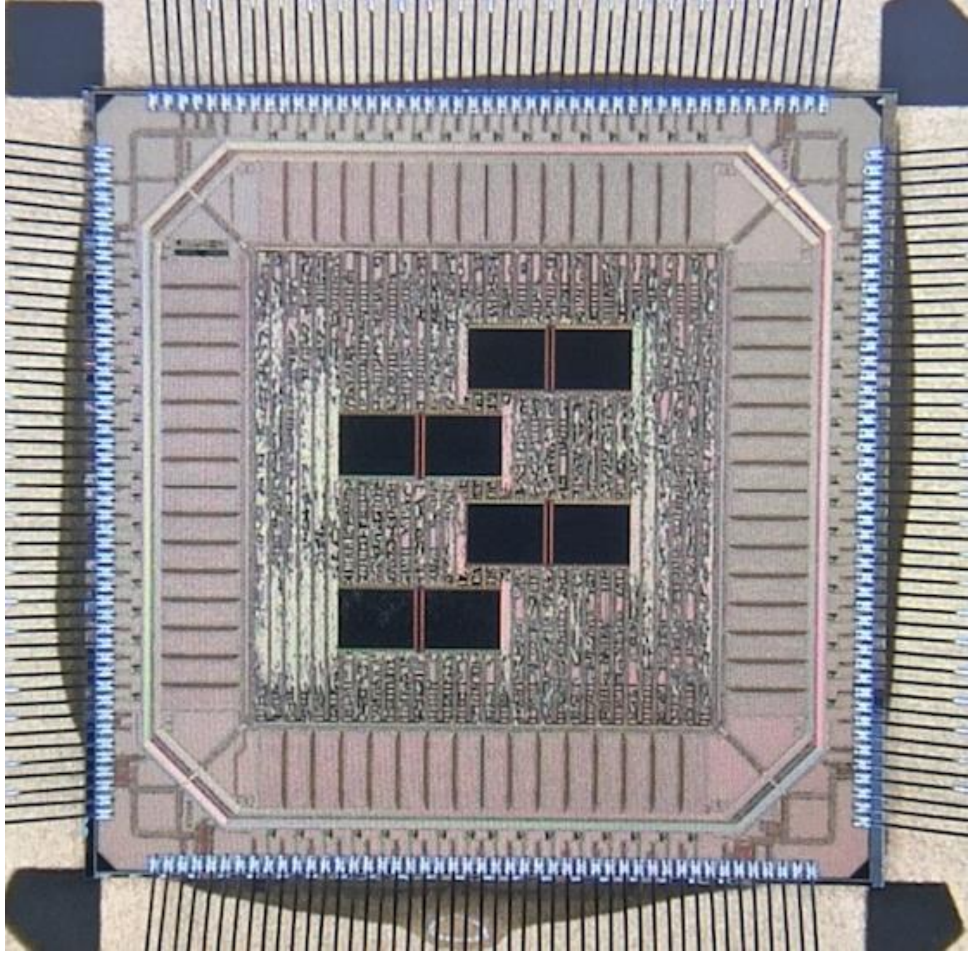

Custom ASIC with amplifier, digitizer, multiplexer

- Low-power, low-noise cryogenic-compatible ASIC
  - S/N ratio of ~30:1 for MIP tracks
- No resistive feedback or shaping
  - Charge stays on pixel until you do something with it
  - Self-, external-, cross-, and periodic-trigger reset modes
    - Optional “burst” modes to process N hit cycles
- Pixels are continuously active
  - Serial data packets stream out of system as channels self-trigger
  - Serial I/O data rate is slow (~ 5Mb/s per channel) to limit digital power in cryogenic environment
  - Modest data volumes: ~1 MB/s per square meter of anode in surface cosmic flux

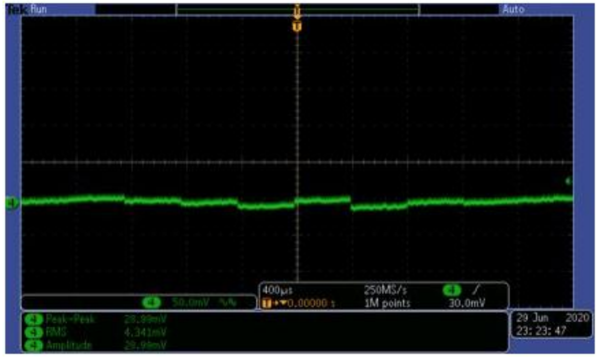

Unexpected substantial reset-correlated noise

LArPix-v2 Anode Tile

A commercially scalable large-format 3D charge-readout scheme

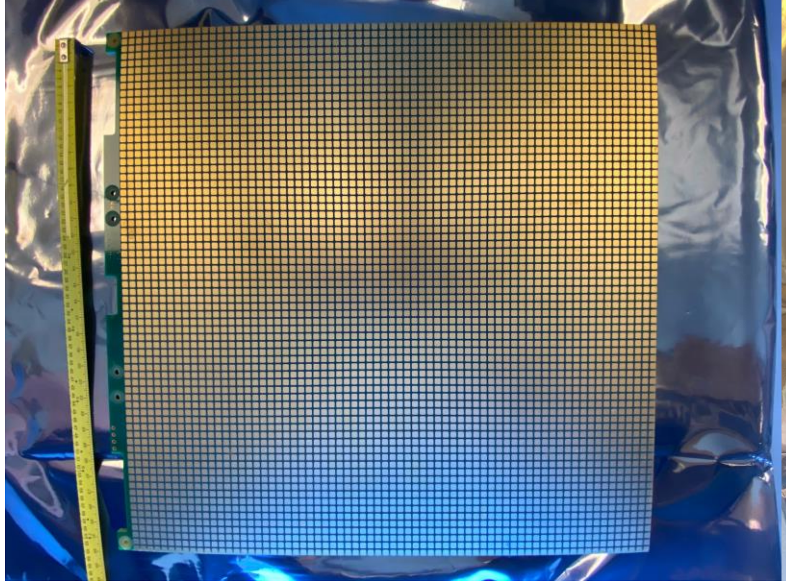

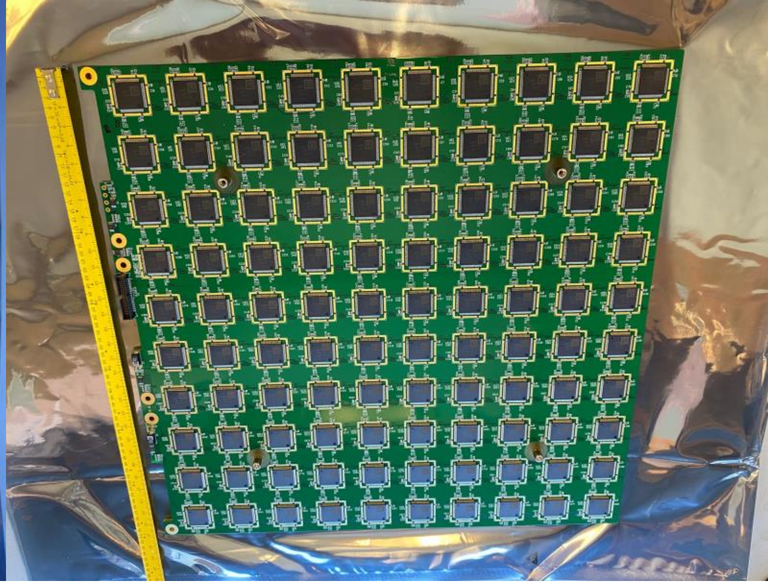

- Digital multiplexing for viable cable plant & cryostat feedthroughs
  - 10x10 array of ASICs instrument a 4.9k pixel PCB-based anode (32 cm by 32 cm)

- Scalabe design compatible with standard large-scale commercial electronics mass production techniques
  - >200 m^2 anode at <\$10k/m^2
  - ‘Tileable’ design to cover anodes of arbitrary scale
  - Quick-turn (~few weeks) fully-commercial production/assembly

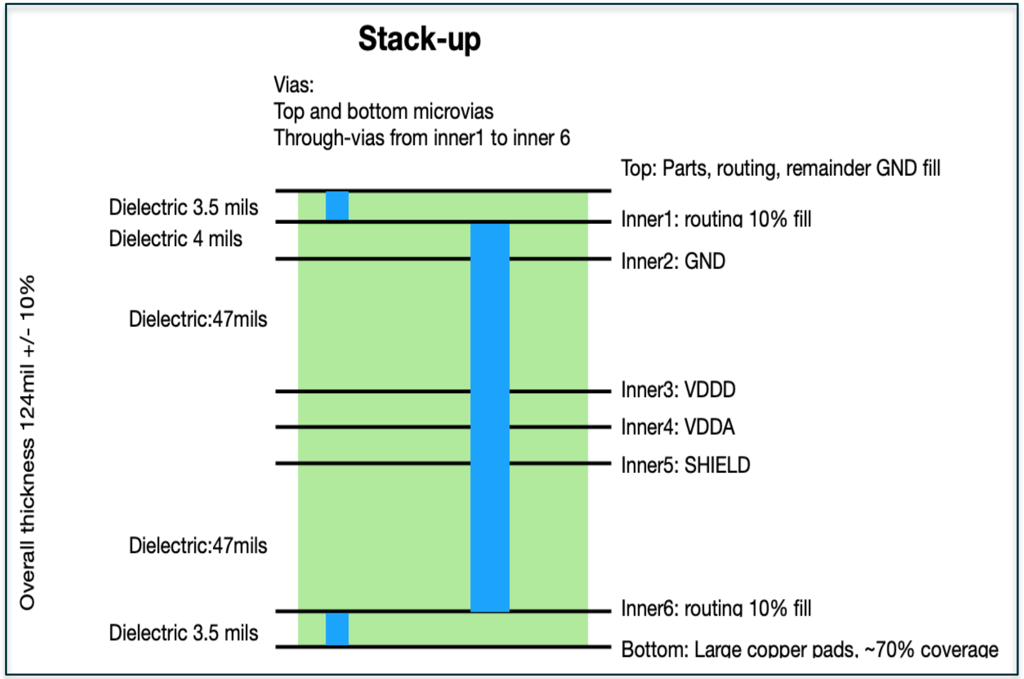

Micro-vias to enhance shielding between digital/analog traces and vias

LArPix-v2 Robustness

Four chips have direct off-tile I/O channels

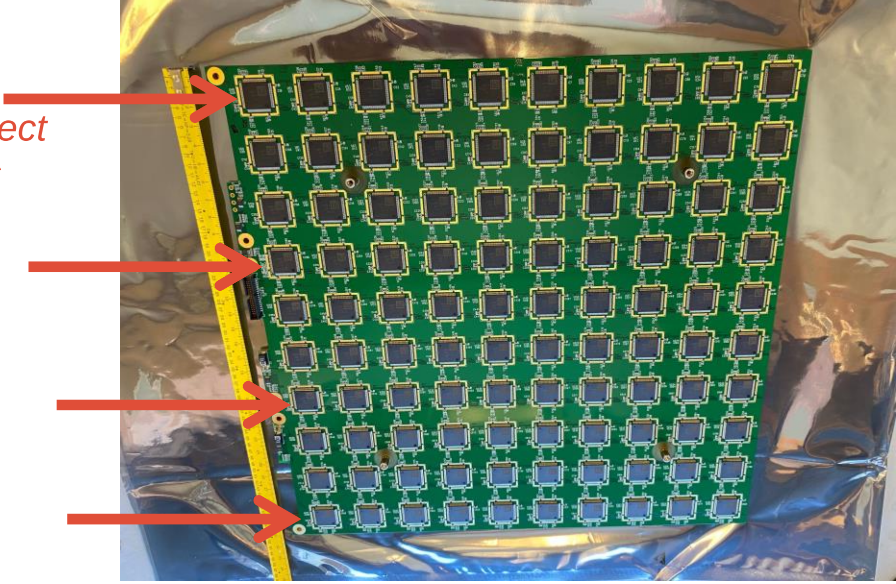

- Minimize single-point failures in cryogenic environment
  - Tile robust to failed ASICs
- Robust to repeated cryogenic cycling

Example: 5 x 5 Pixel Tile

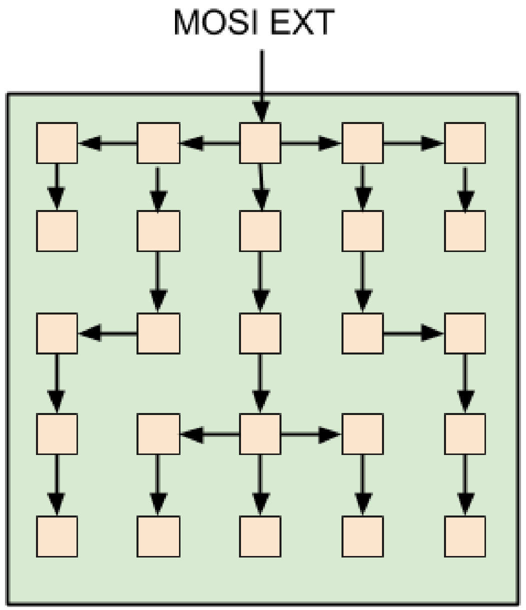

Upstream configuration commands

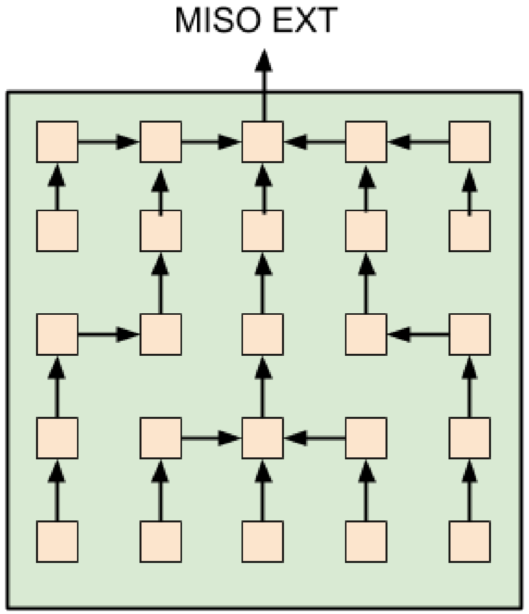

Downstream data flow

I/O can occur between any neighboring ASICs on pixel tile

LArPix-v2 Robustness

- Minimize single-point failures in cryogenic environment
  - Tile robust to failed ASICs
- Robust to repeated cryogenic cycling

Four chips have direct off-tile I/O channels

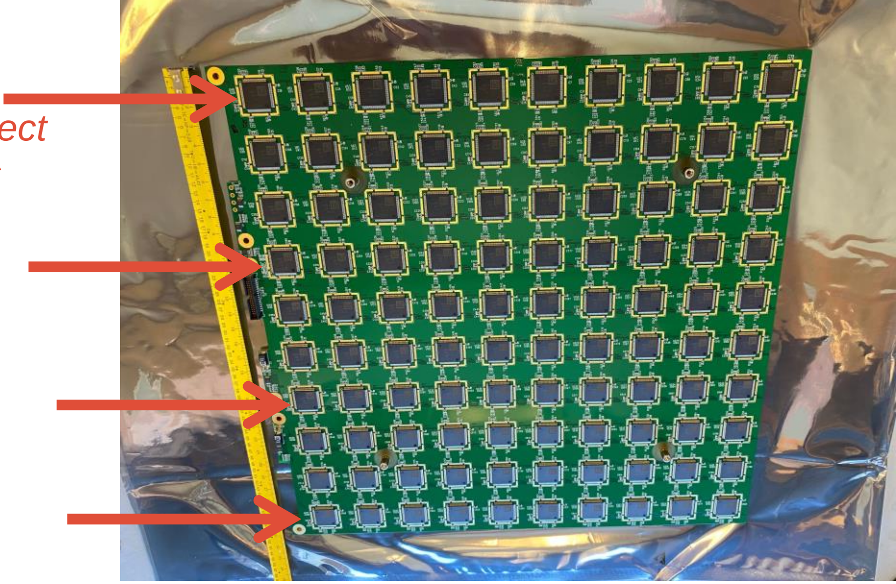

Example: 5 x 5 Pixel Tile

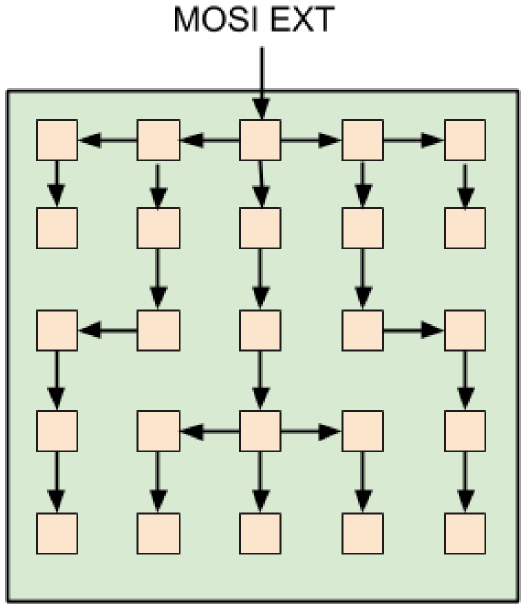

Upstream configuration commands

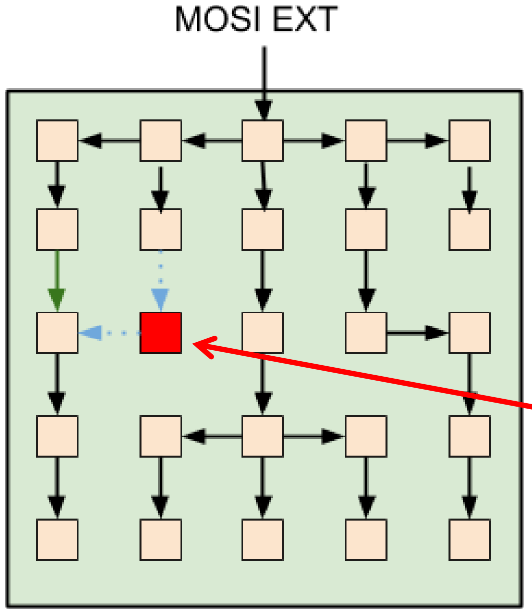

Example failed chip.

Network reconfigured to avoid failed ASIC

LArPix-v2 System

ASIC integration with feedthrough, cold cables, and controller

LArPix Team

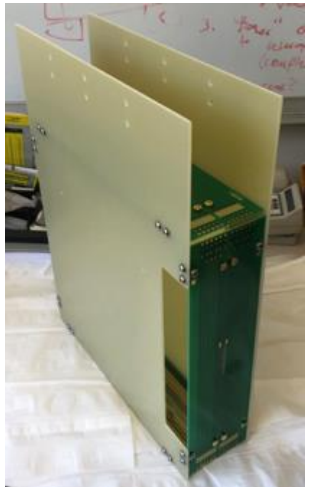

QC LArTPC 3-cm drift
Successful 1st tile run
Oct. 12 ‘20

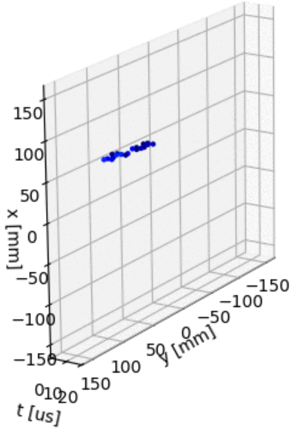

3D images of cosmic rays
25 events overlayed

PACMAN multi-tile controller

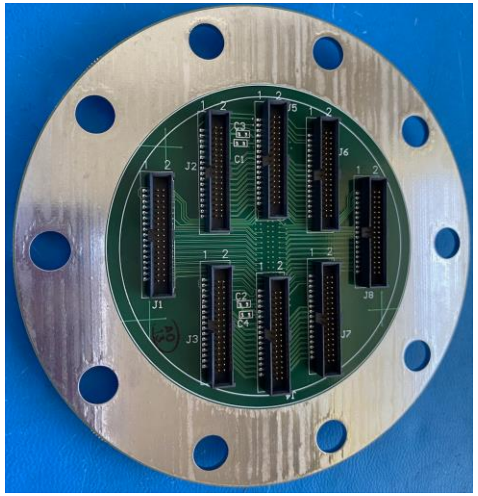

8-tile feedthrough

System Integration Demonstrators

SingleCube @ Bern
October 2020

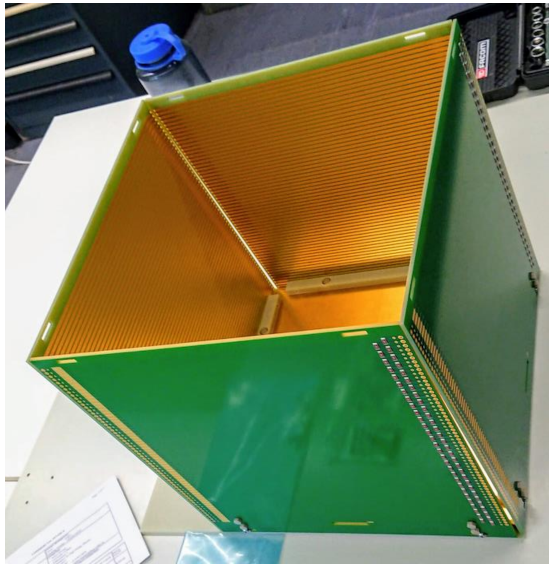

Single charge/light detector element

(Covid19 risk mitigation step)

Module0-HV @ Bern
November 2020

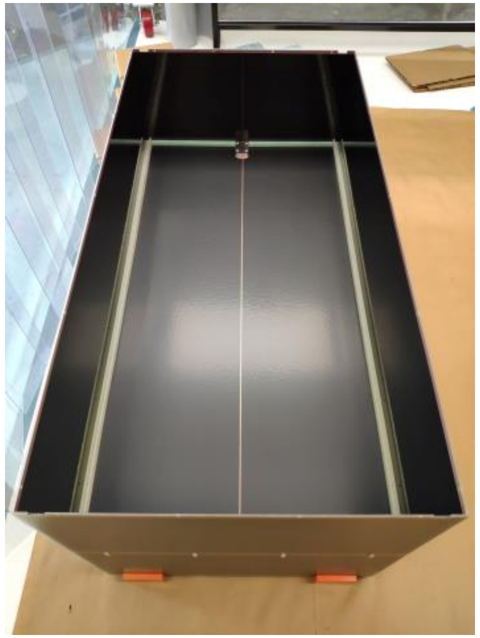

+ Resistive field cage & cathode

+ Additional light detector element

Module0 @ Bern
April, June 2021

+ Fully-instrumented single module

ProtoDUNE-ND @ FNAL in NuMI
Summer/Fall 2022

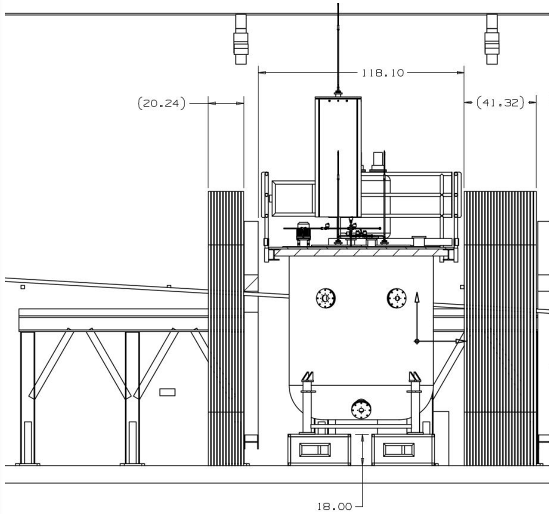

+ Four fully-instrumented modules

SingleCube: single charge/light detector elements

Successful first demonstration of charge & light readout integration

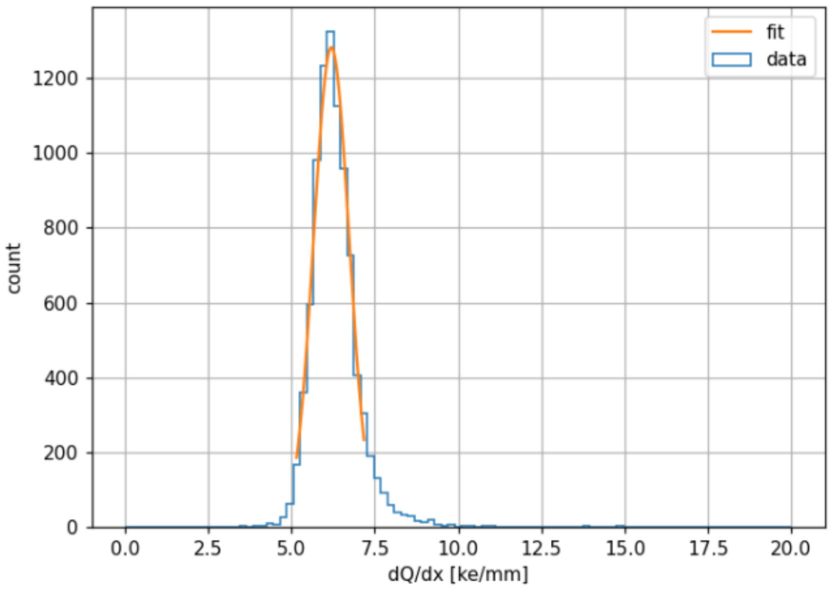

Observed charge consistent with expectation

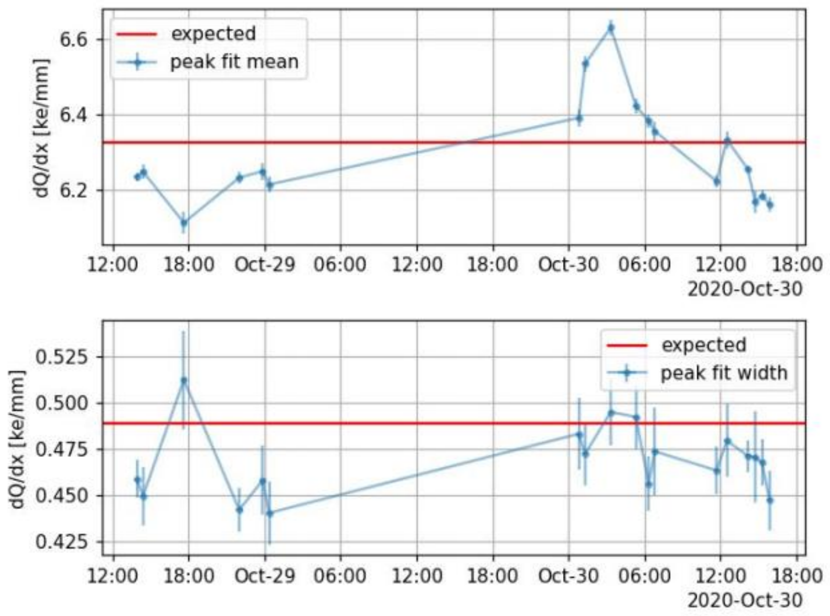

Charge measurement stable the duration of TPC operations

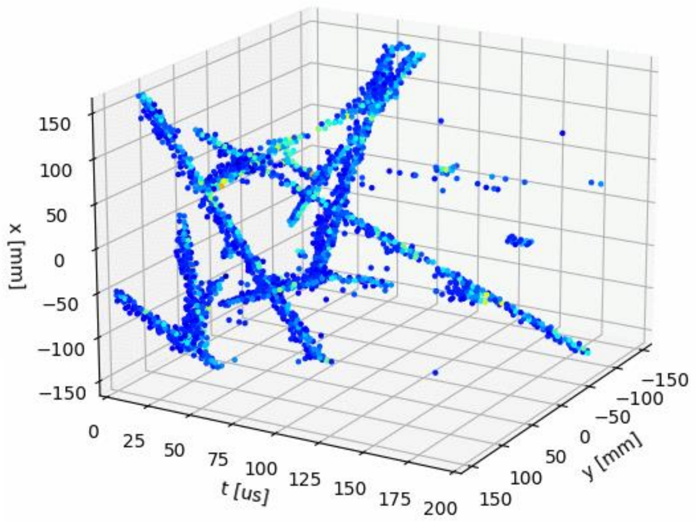

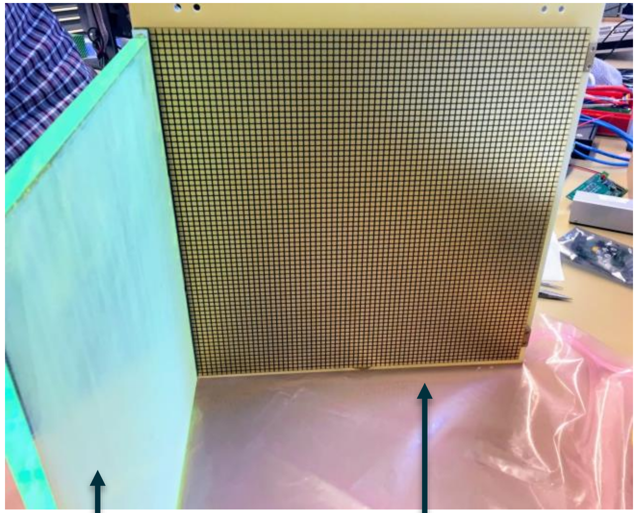

ArCLight scintillation trap

LArPix-v2 pixel tile

SingleCube: single charge/light detector elements

Successful first demonstration of charge & light readout integration

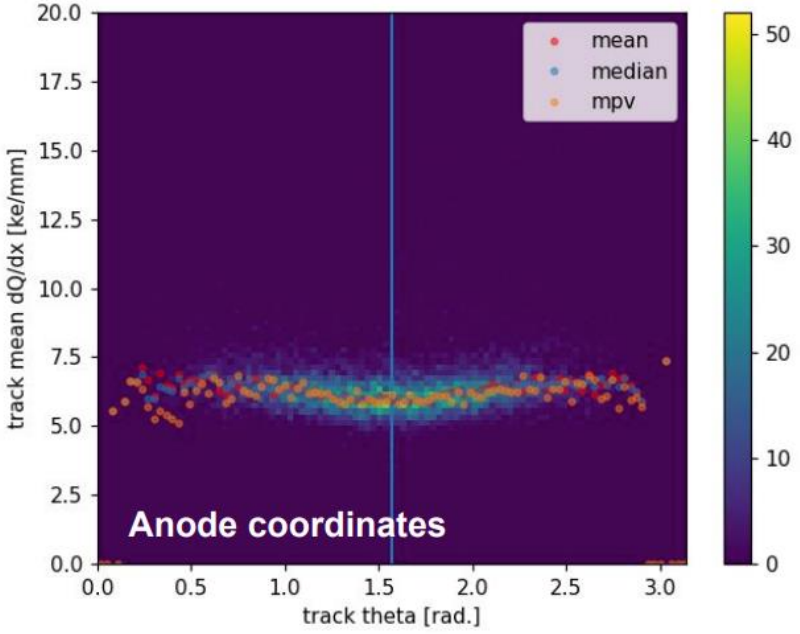

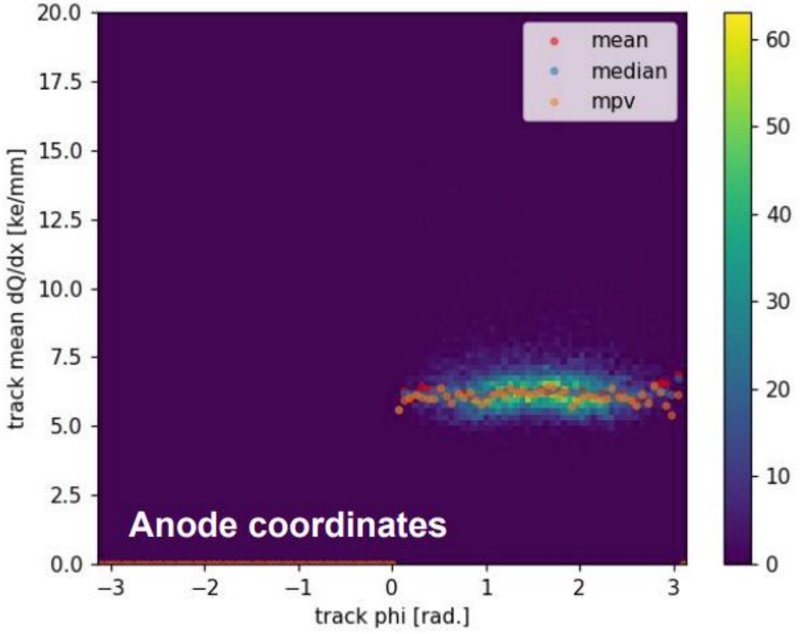

Small variation in dQ/dx based on muon track orientation to anode

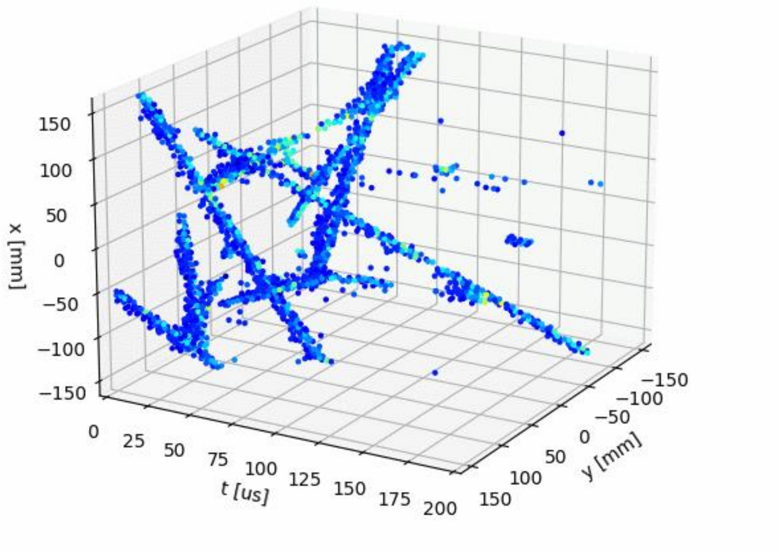

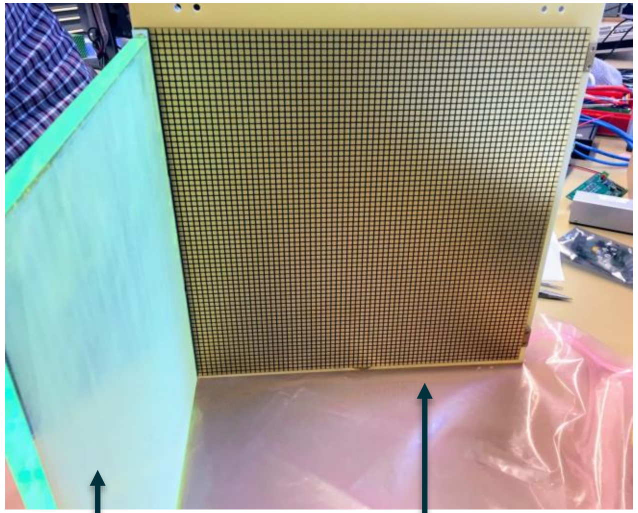

ArCLight scintillation trap

LArPix-v2 pixel tile

Module0-HV

First large-scale test of resistive sheet field cage & LAr purity/flow over run period

- High voltage stable entirety of run up to 1 kV/cm
- Validated LAr flow though field cage provides sufficient, stable purity (>2 ms electron lifetime)
- Successful integration of light triggers into LArPix datastream
- **Emerging issue:**
  Intermittent noise on subset of pixels

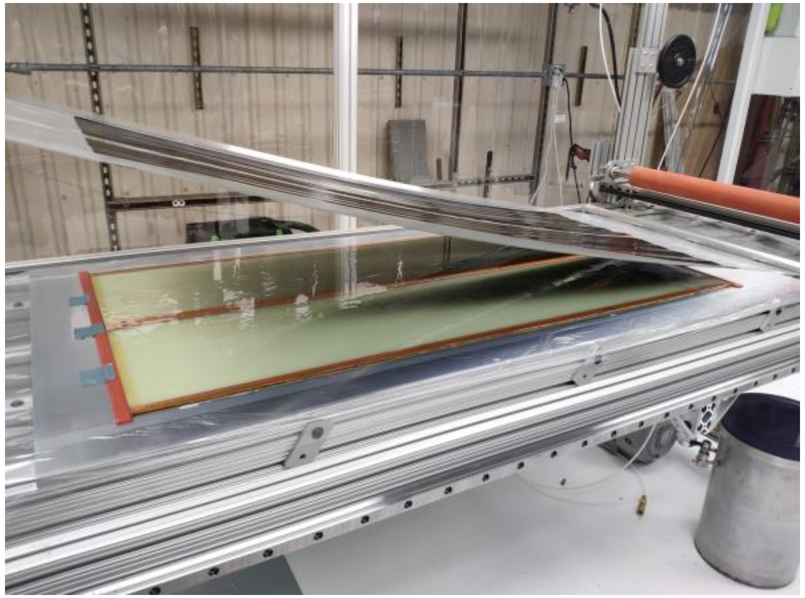
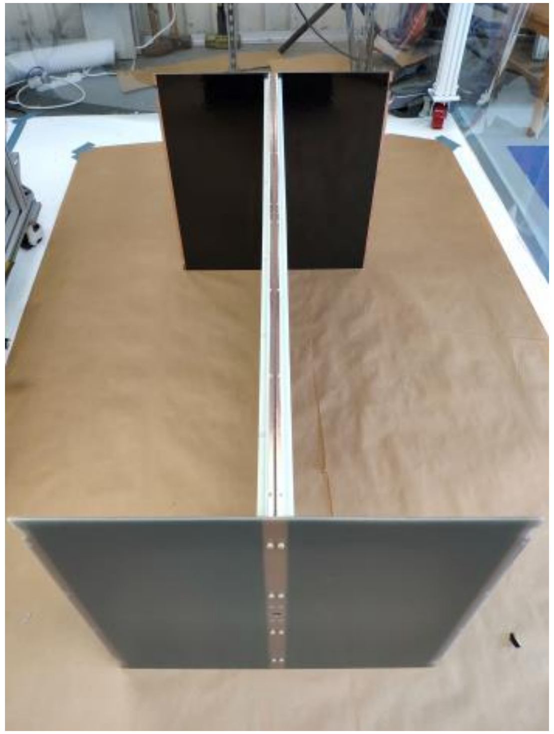

Low-profile field structures
laminated high-resistivity polyamide film on G10 panels

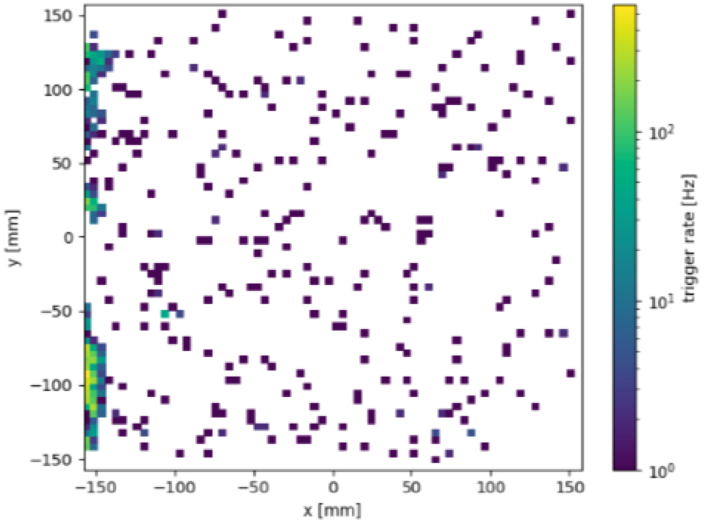

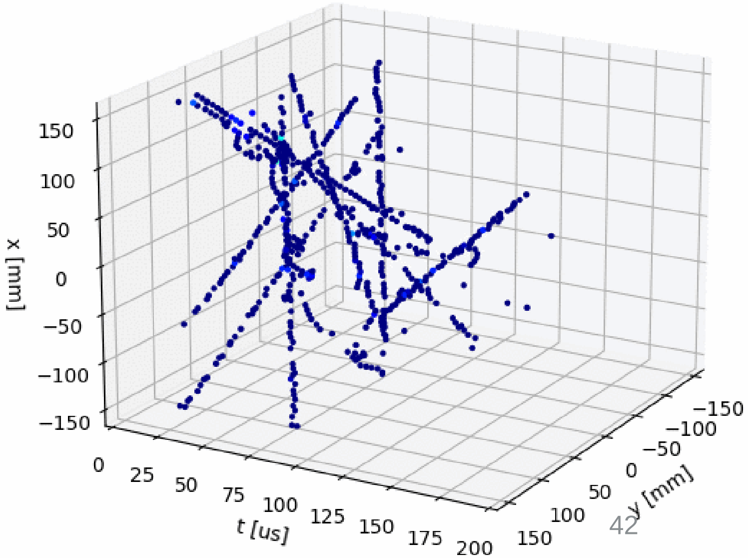

M. Mooney (CSU)

Module 0

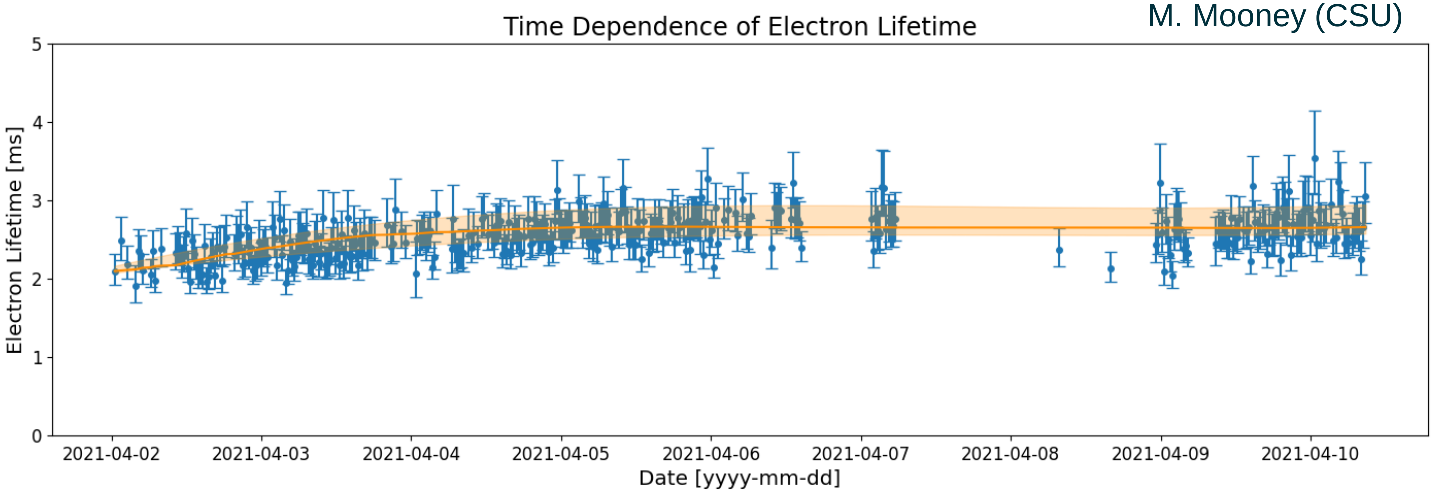

- 70 cm x 70 cm x 140 cm fully instrumented ND-LAr module prototype
  - ~1.6 m^2 charge sensitive area
- Successful cosmic ray imaging with ~80k channel readout
  - 92.2% of 78,400 total channels active
  - No ASIC failures at cold
- Emerging issues
  - far-field induction
  - whole-tile triggering

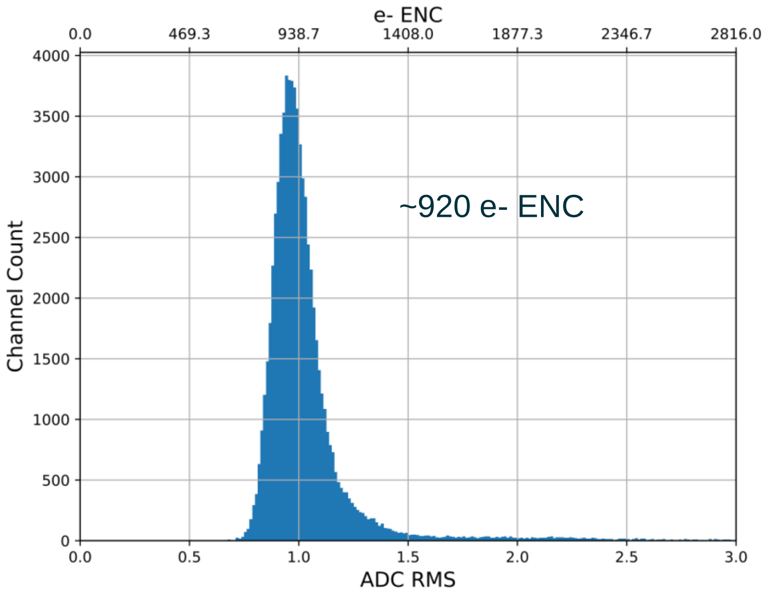

Expect ~1800 e- intrinsic fluctuation from 4 GeV MIP ➔ **current charge resolution smaller than intrinsic physical fluctuations**

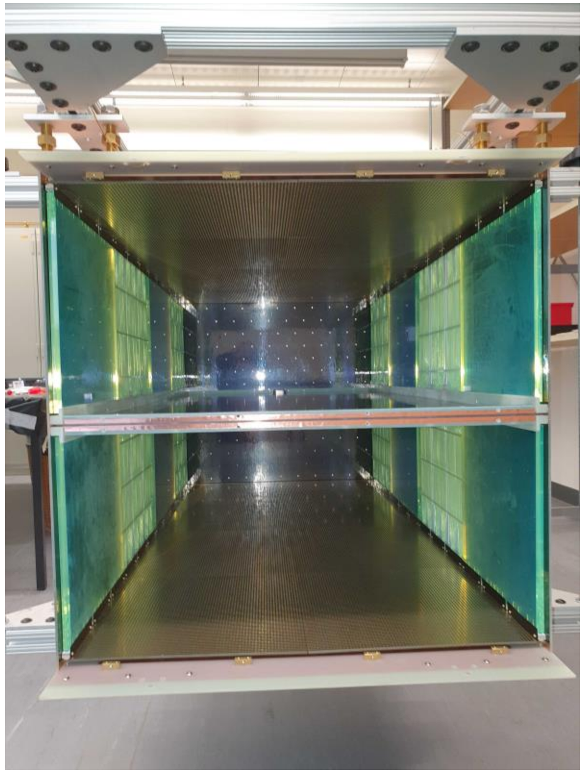

Cosmic Ray Reconstruction

Evaluation on standard candle cosmic-ray samples (through-going MIPs, stopping muons, Michel electrons) suggests high fidelity charge reconstruction

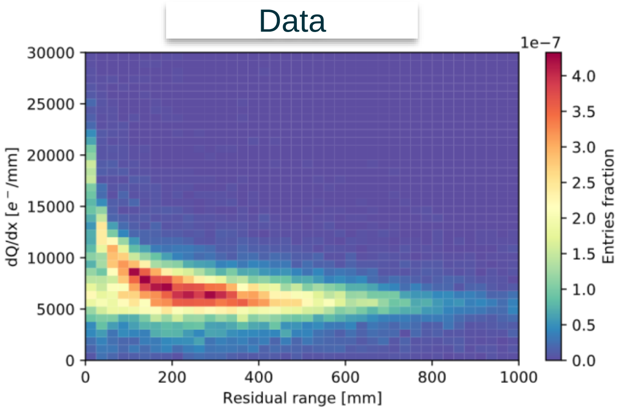

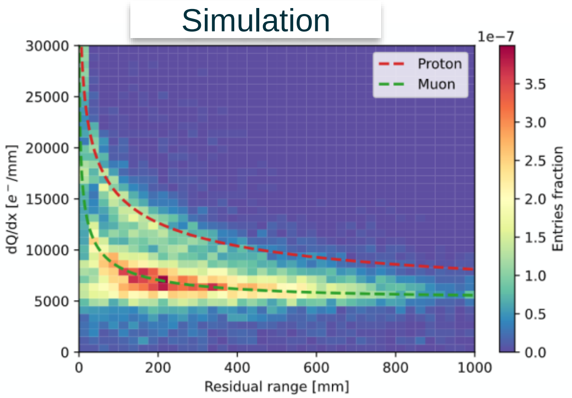

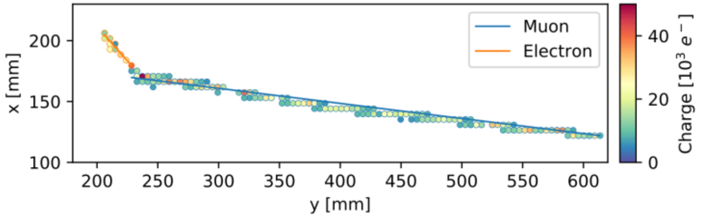

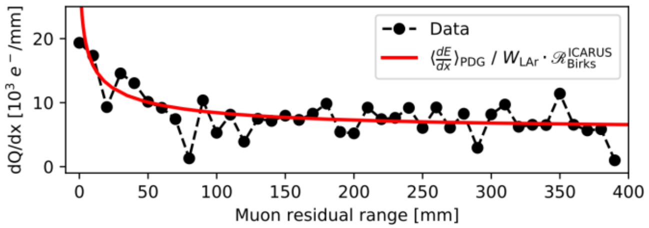

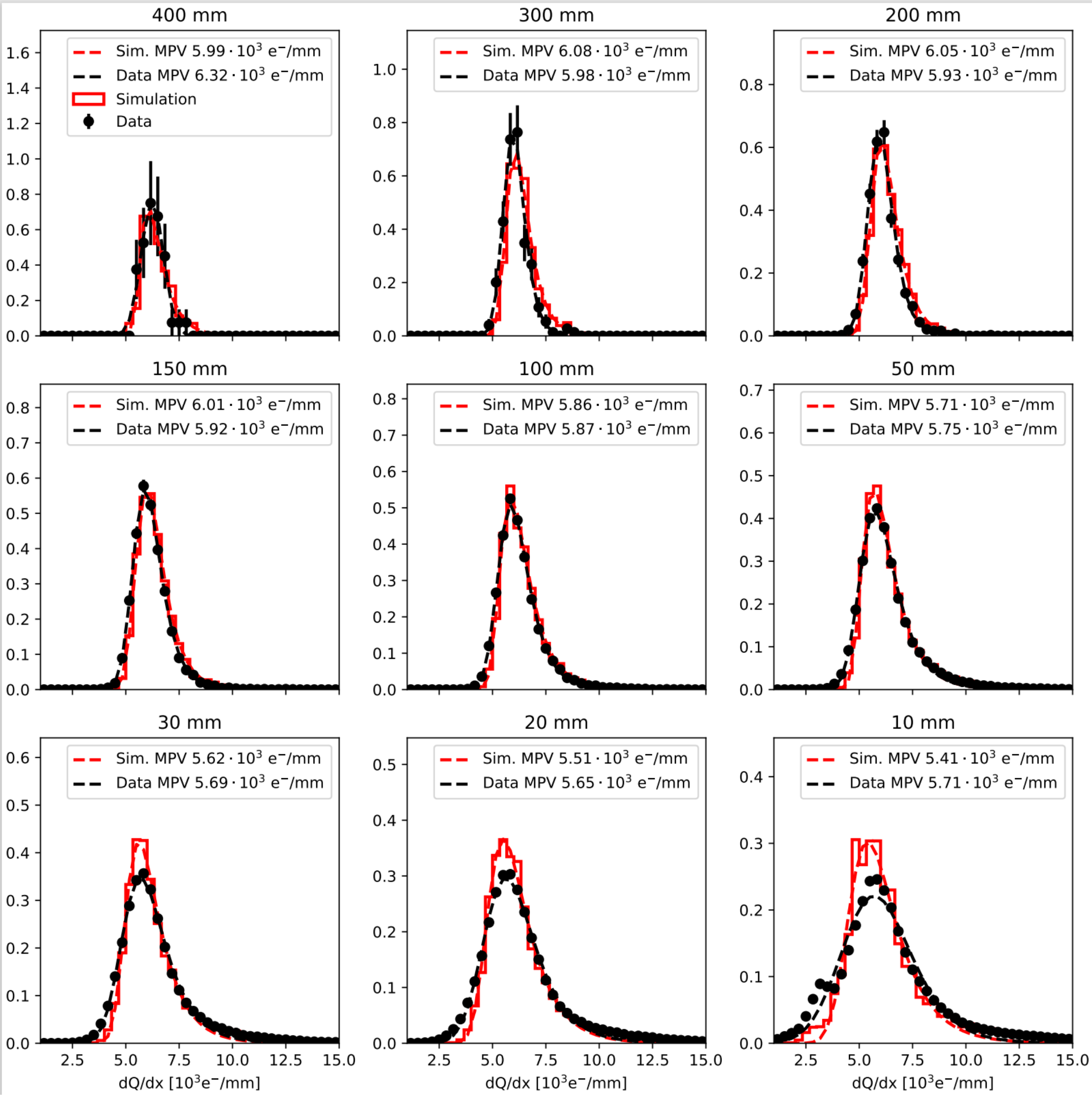

Cosmic Ray Reconstruction

Evaluation on standard candle cosmic-ray samples (through-going MIPs, stopping muons, Michel electrons) suggests high fidelity charge reconstruction

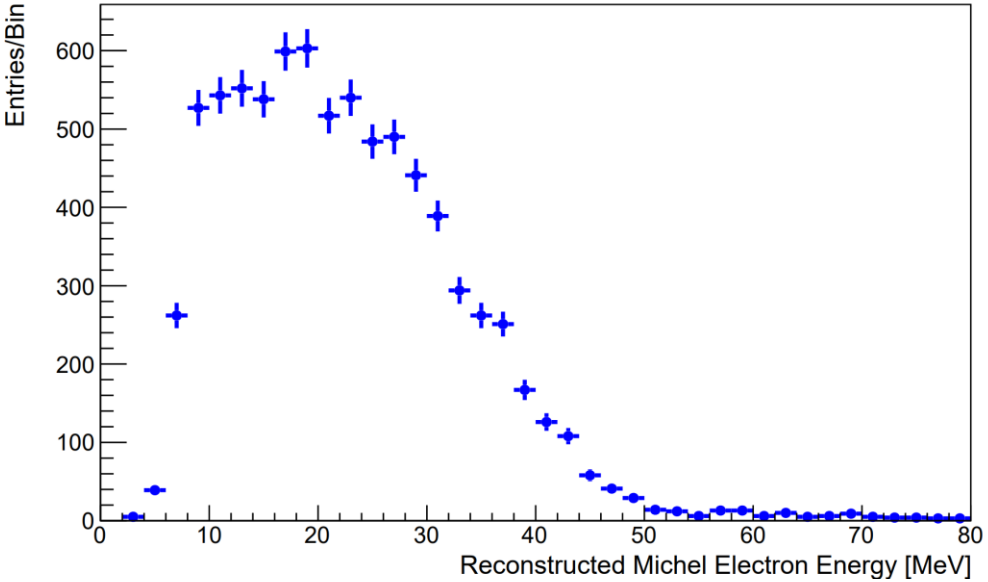

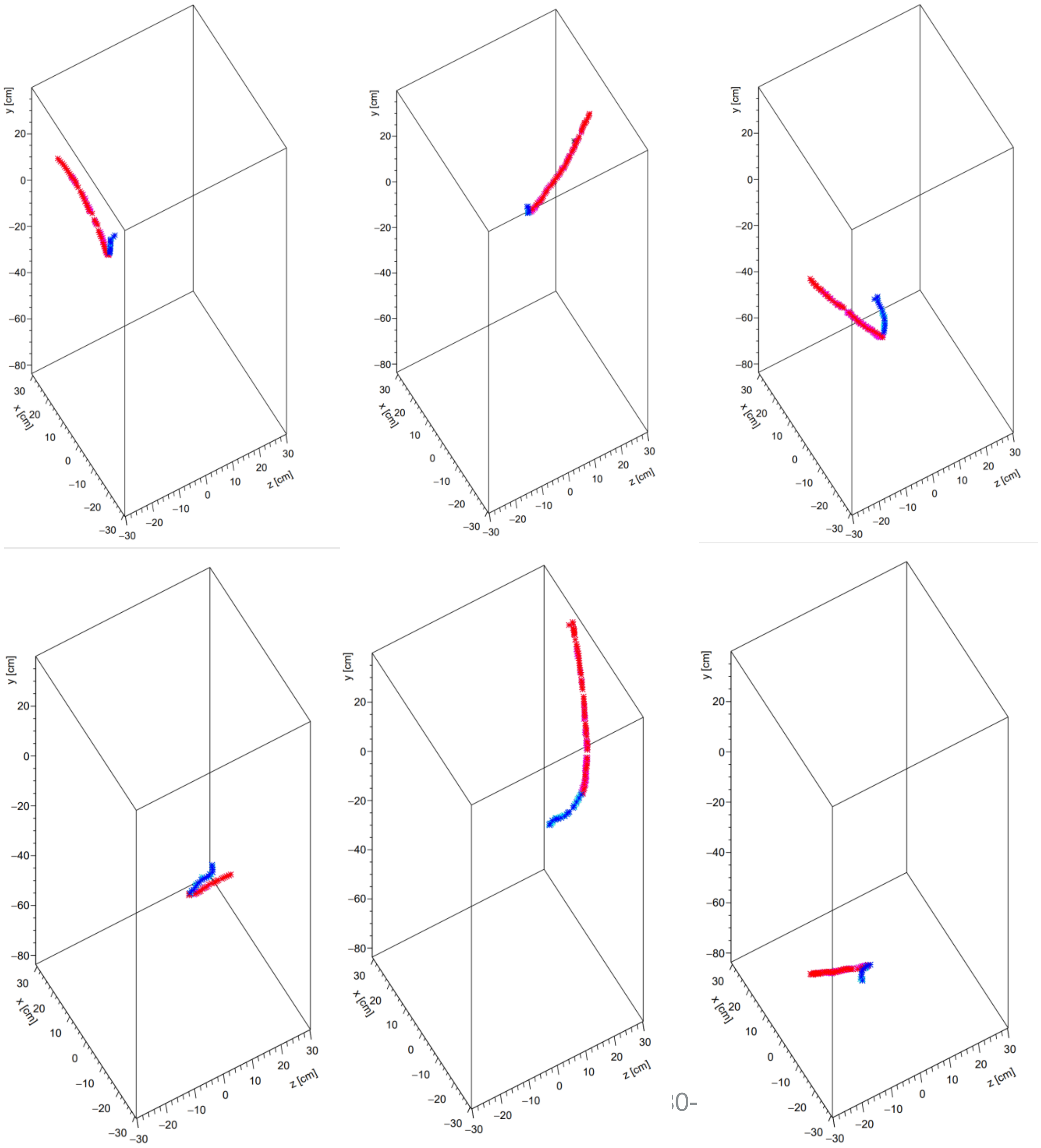

ProtoDUNE-ND

Infrastructure testbed for DUNE oscillation measurements

- Develop neutrino signal analysis and reconstruction techniques
- Gauge tolerance to beam ν pileup: charge-light signal correlations
- Track matching with external trackers

Containment limitations

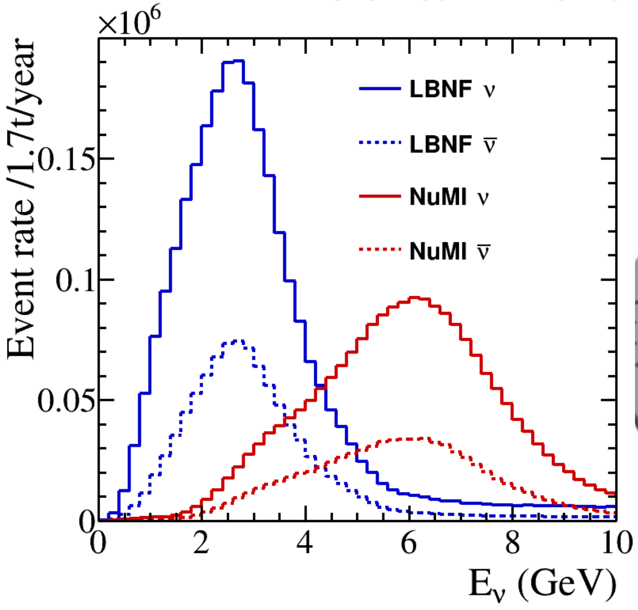

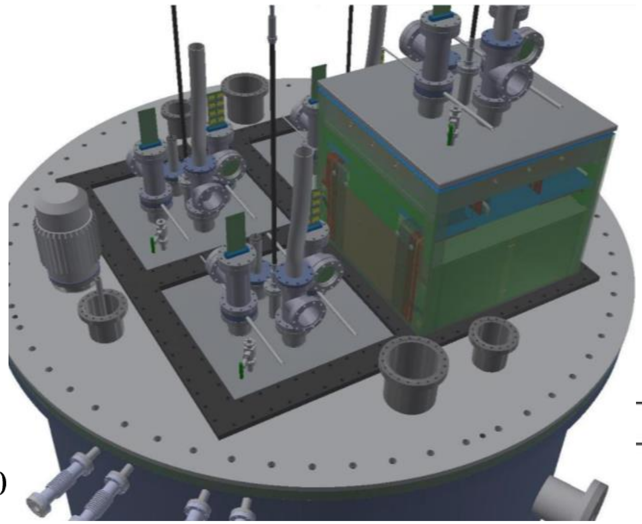

MINOS Hall @ FNAL

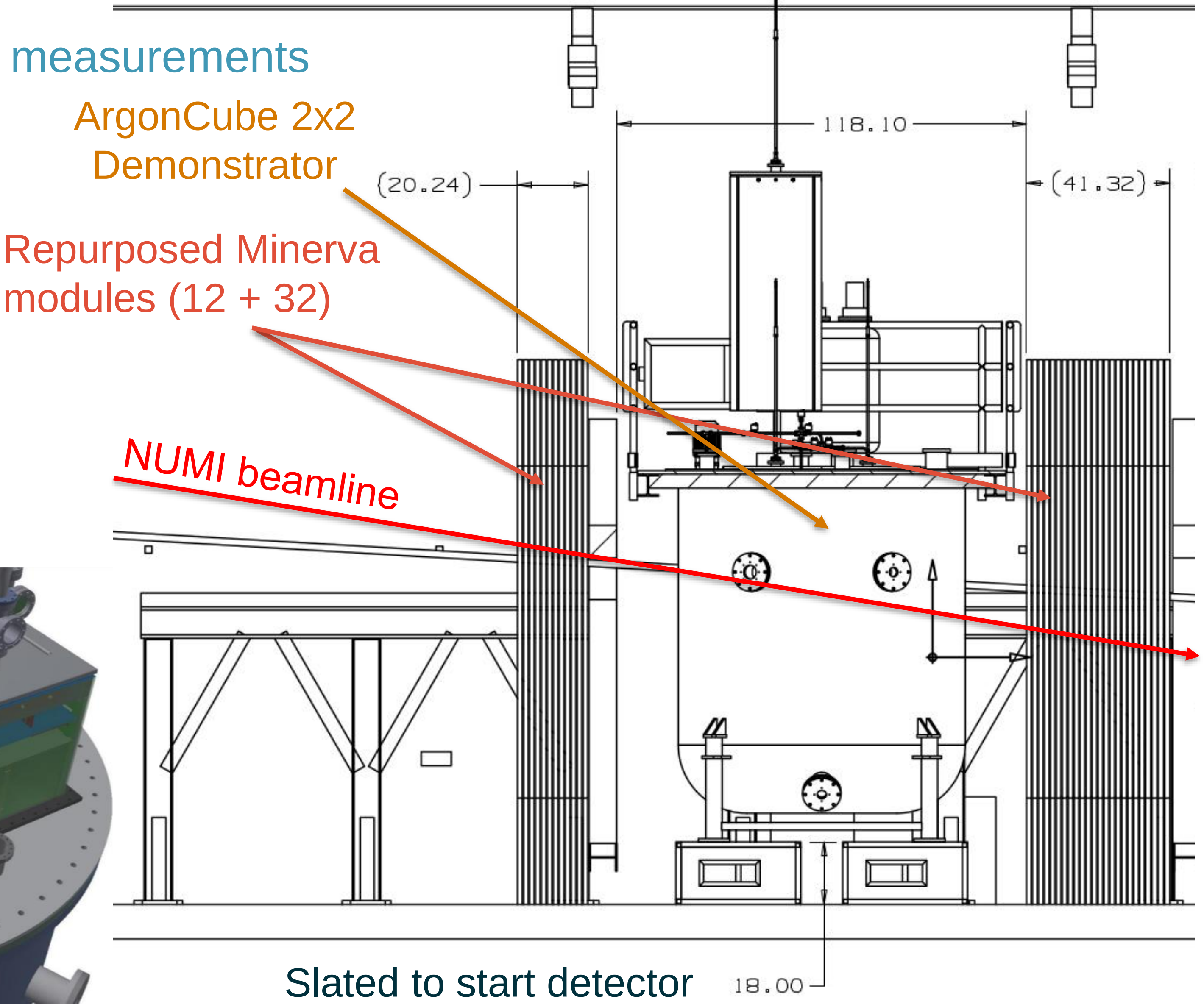

Slated to start detector commissioning June 2022

ND-LAr program to installation

System Integration Demonstrators
2019-2022

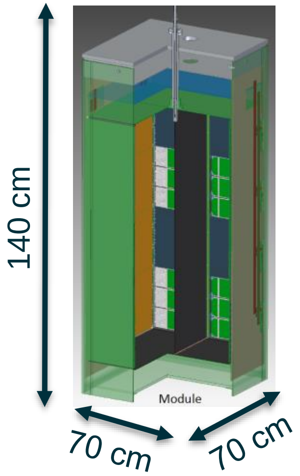

SingleCube, Module0–HV, Module0 cosmics operation @ Bern

2x2 demonstrator NuMI beam operation @ FNAL

Full-scale ND Demonstrator
2022-2023

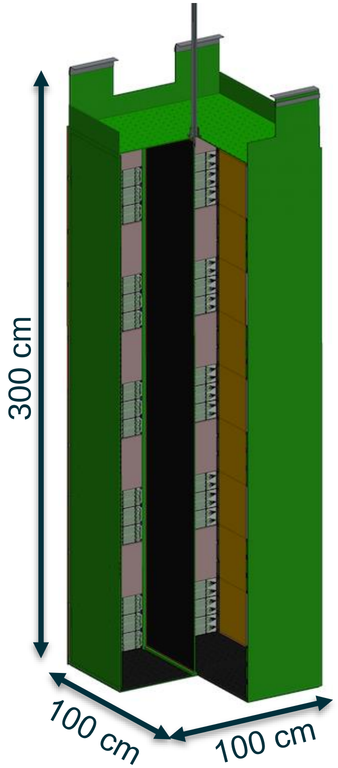

Full-scale module operated in single-module cryostat

Module Production
2024-2026

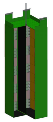

‘first article’ production

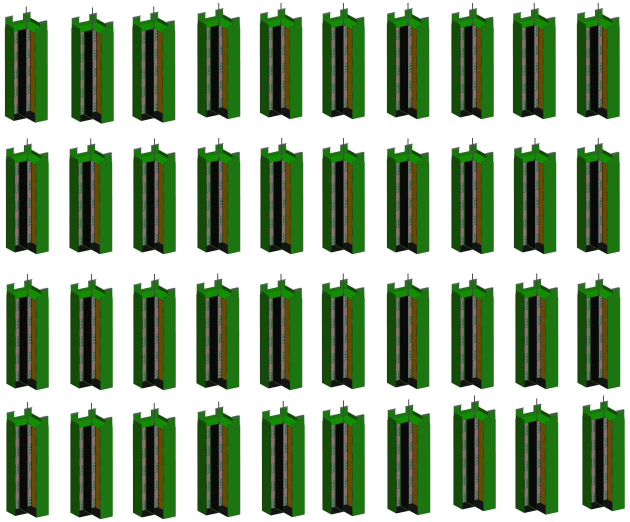

35 (+5 spare) fully cyro-tested production modules

Installation
2027-2029

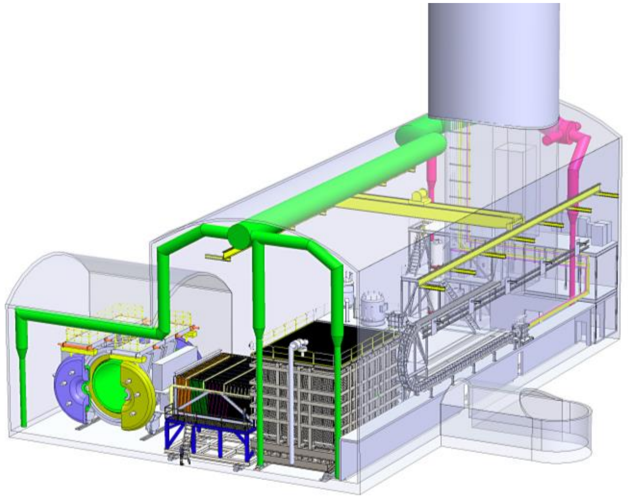

Module installation in Near Detector Complex

Summary

- DUNE is designed to resolve the neutrino mass hierarchy and observe charge-parity violation in the neutrino sector
  - *Significant technological advancements are needed to deliver the DUNE neutrino oscillation physics program*

- For the LAr component of the Near Detector, beam neutrino pileup is particularly challenging
  - *An optically segmented modular design and 3D charge readout are central to delivering the DUNE physics program*

- Physics studies and detector prototyping are on-going to realize the ND-LAr design
  - ***With Module-0 we've shown that pixelated charge readout for LArTPCs is becoming a reality!!***

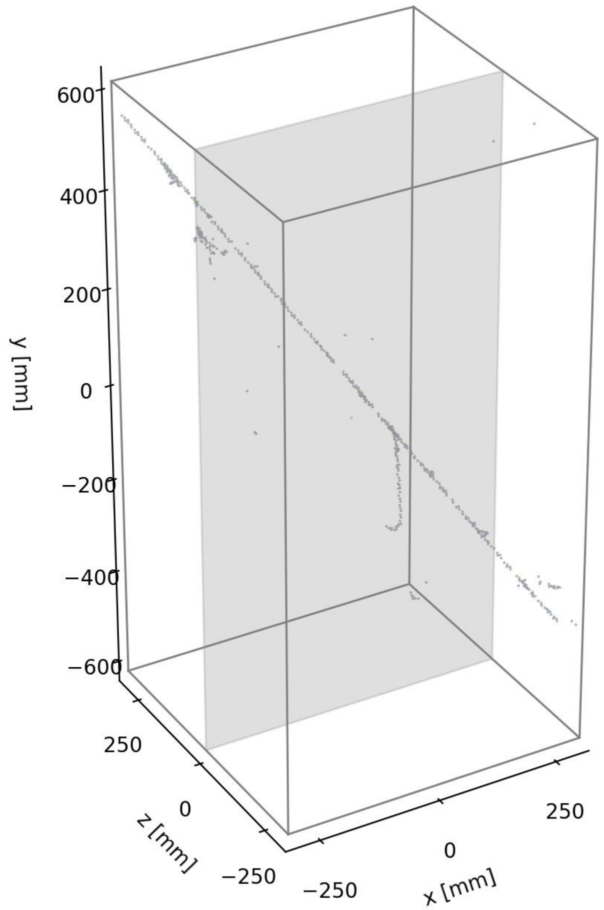

Backup Slides

DUNE TDR θ_{23} sensitivity

With $\sin^2 2\theta_{13}$ constrained by NuFIT 4.0

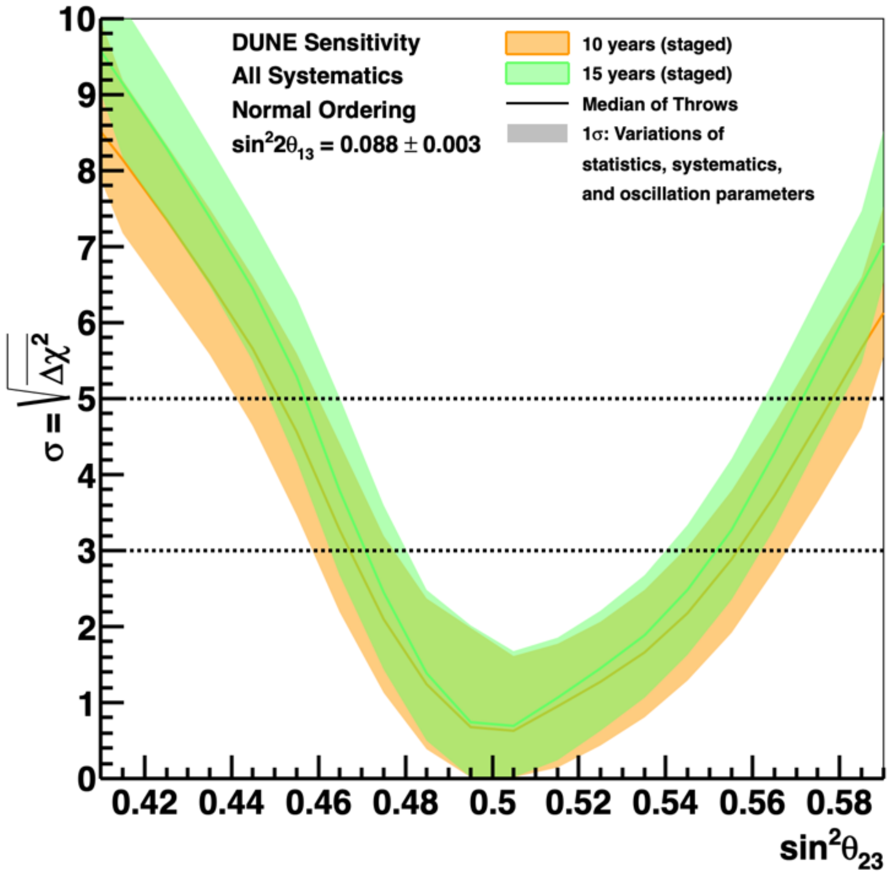

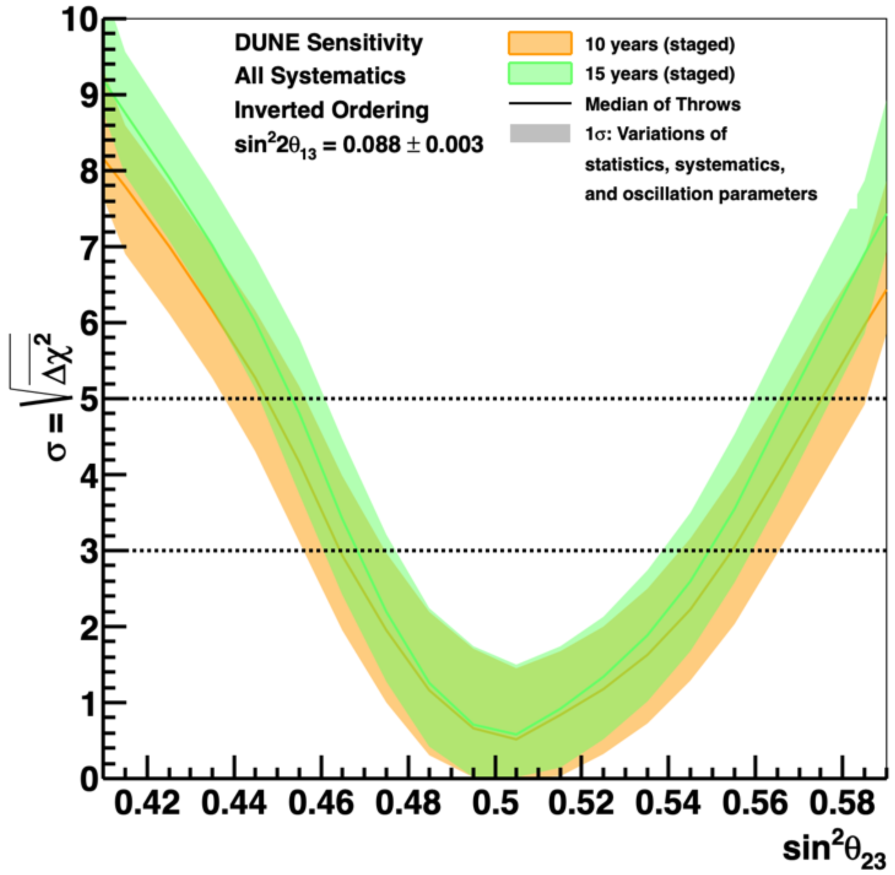

DUNE TDR reconstructed energy distributions

3.5 year exposure

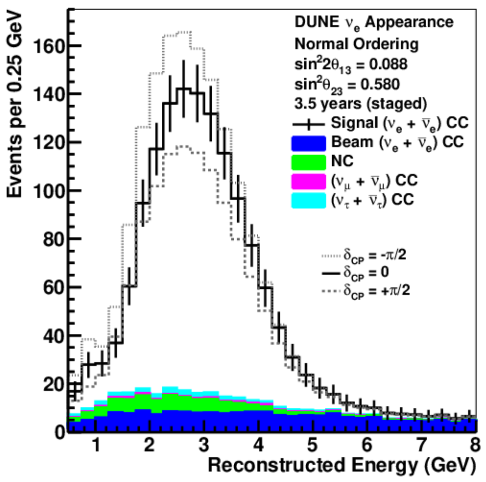

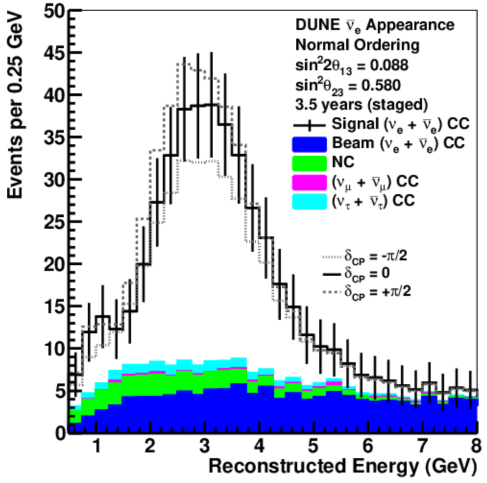

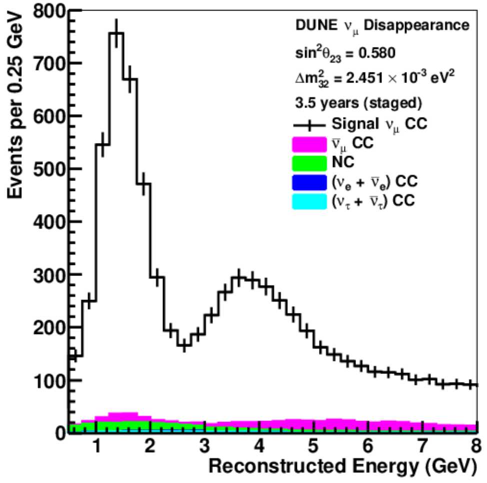

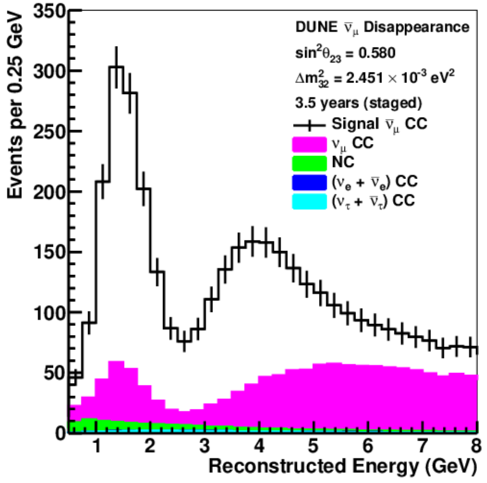

Extracting physics from the data

- Ultimately, near and far detectors measure a flavor dependent interaction rate N

- $N(E_{reco}) = \left(F(E_{true}) \times P(E_{true})\right) \otimes R(E_{true}, E_{reco})$
- where F is the neutrino flux, P is the neutrino oscillation probability, and R is the "response".

- The key to interpreting our measurements in order to extract neutrino oscillation parameters is to have a solid understanding in $\boldsymbol{F}$ and $\boldsymbol{R}$.

- *****The near detector plays an essential role in developing this understanding*****

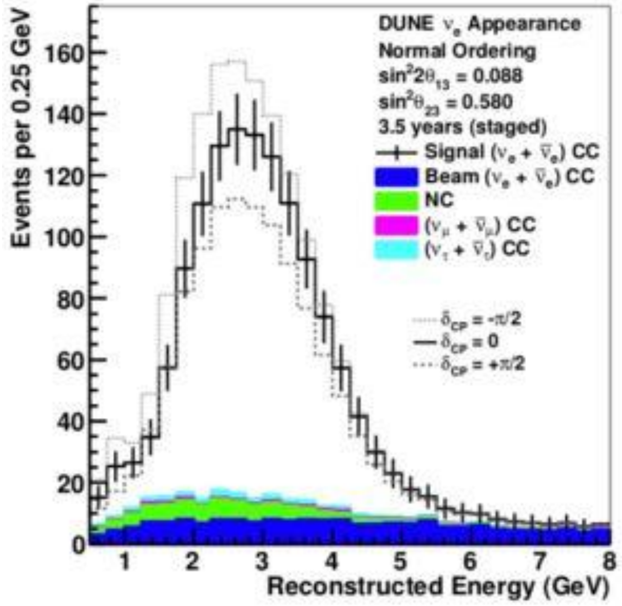

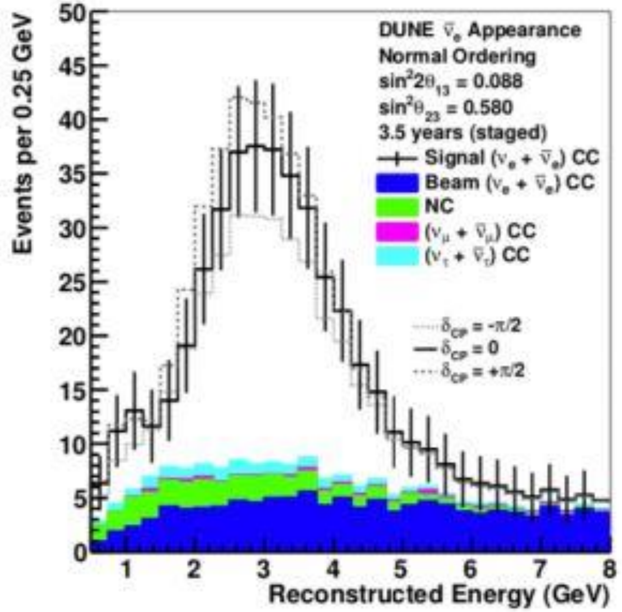

ND-LAr Event Rates

Ample statistics for FD constraint & rich physics program

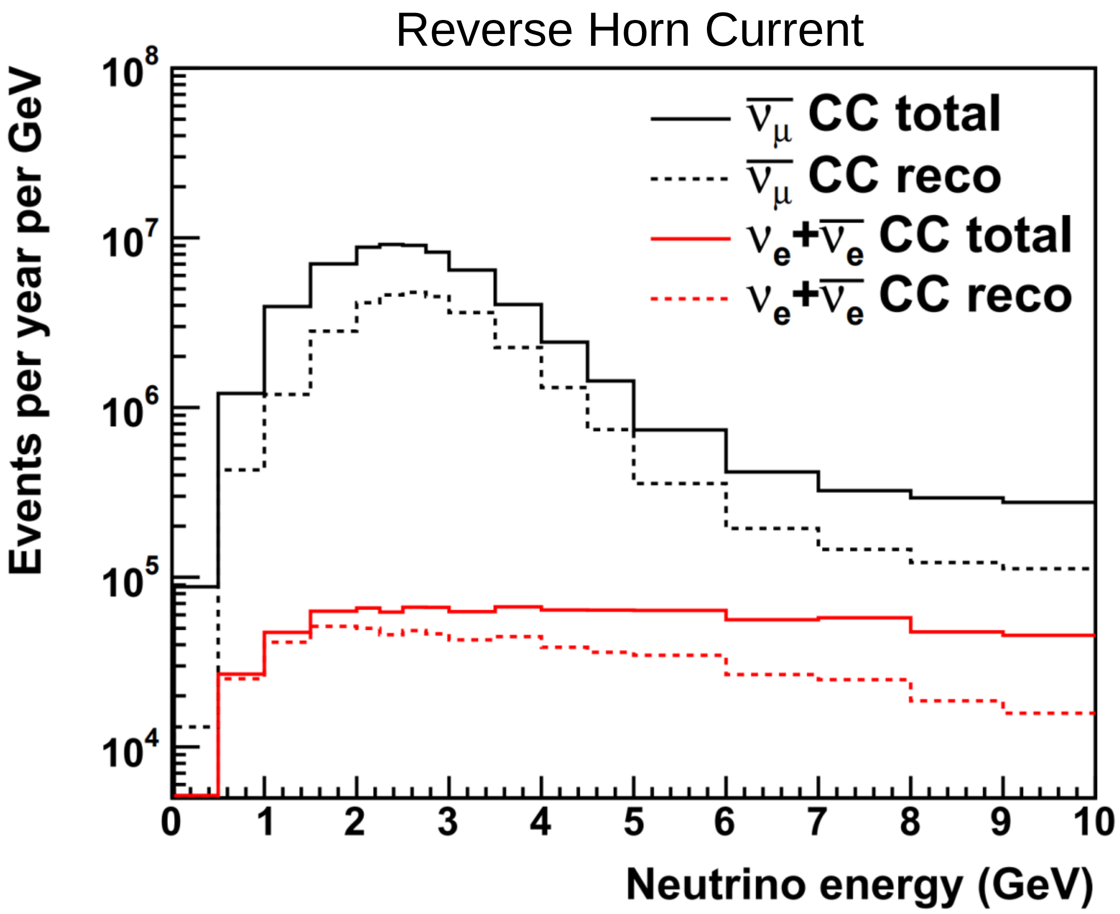

RHC mode	total	accepted	0.5 GeV to 4.0 GeV	accepted
CC $\bar{\nu}_\mu$	2.63e+07	1.23e+07	2.01e+07	9.67e+06
CC ν_μ	1.36e+07	3.51e+06	3.13e+06	1.28e+06
NC total	1.53e+07	9.33e+06	9.31e+06	7.21e+06
CC $\bar{\nu}_\mu + 0\,\pi$	1.17e+07	6.67e+06	1.01e+07	5.6e+06
CC $\bar{\nu}_\mu + 1\,\pi^\pm$	7.56e+06	3.5e+06	6.01e+06	2.73e+06
CC $\bar{\nu}_\mu + 1\,\pi^0$	2.39e+06	9.61e+05	1.86e+06	7.19e+05
CC $\bar{\nu}_\mu + 2\,\pi$	2.62e+06	8.14e+05	1.63e+06	4.99e+05
CC $\bar{\nu}_\mu + 3\,\pi$	8.3e+05	1.75e+05	3.02e+05	7.53e+04
CC $\bar{\nu}_\mu +$ other	1.16e+06	1.4e+05	1.96e+05	4.29e+04
CC $\nu_e + \bar{\nu}_e$	9.25e+05	4.01e+05	1.95e+05	1.5e+05
$\nu + e^-$	6.44e+03	5.75e+03	3.98e+03	3.42e+03

Far-field Induction

- Observe “lobing” charge preceding in time large electromagnetic showers
- Pixel response field of view is larger than anticipated (pixel pitch 4.43 mm)
- Simulated field response needs revisiting paired with optimization of pixel pad dimensions, etc.

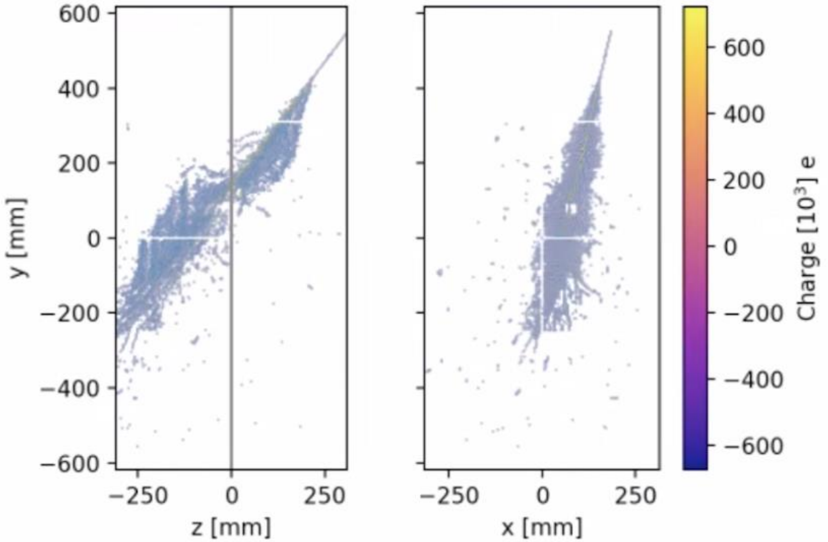

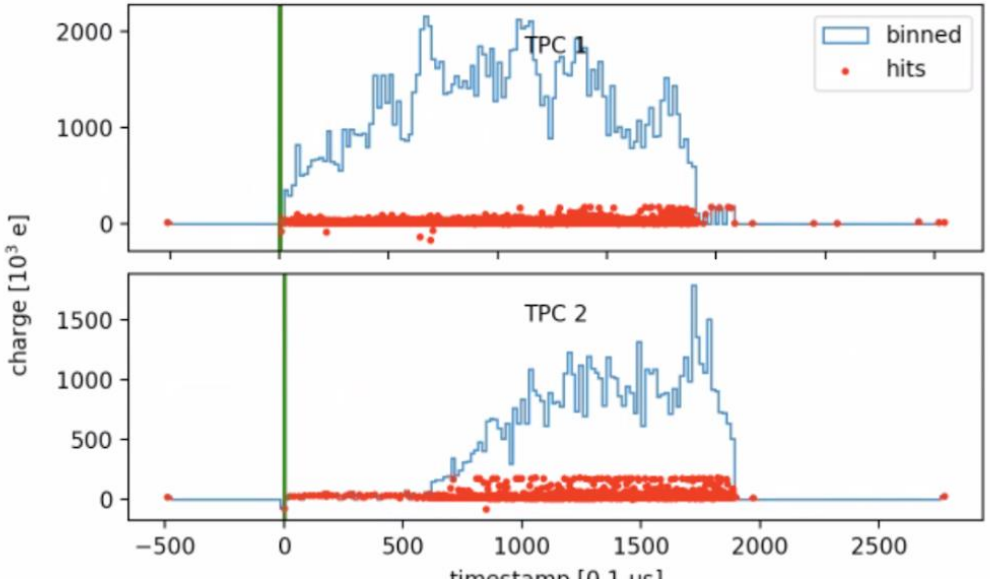

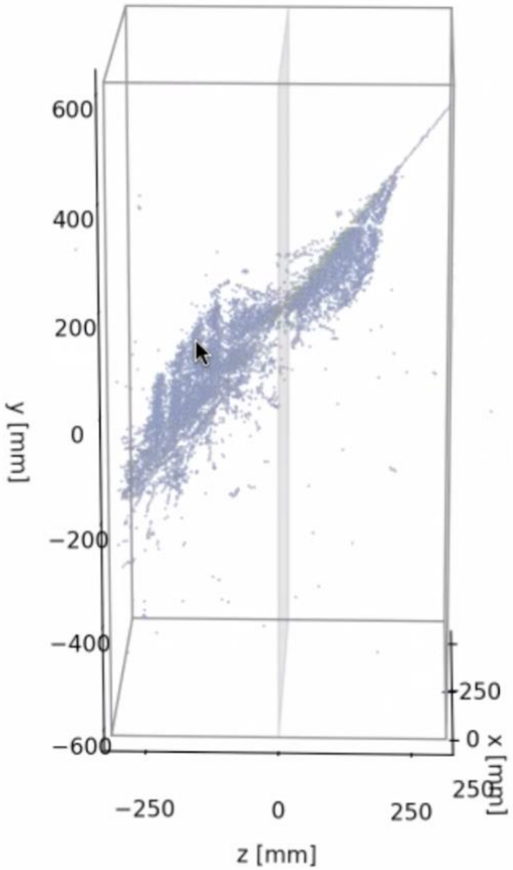

P. Madigan (UC Berkeley)

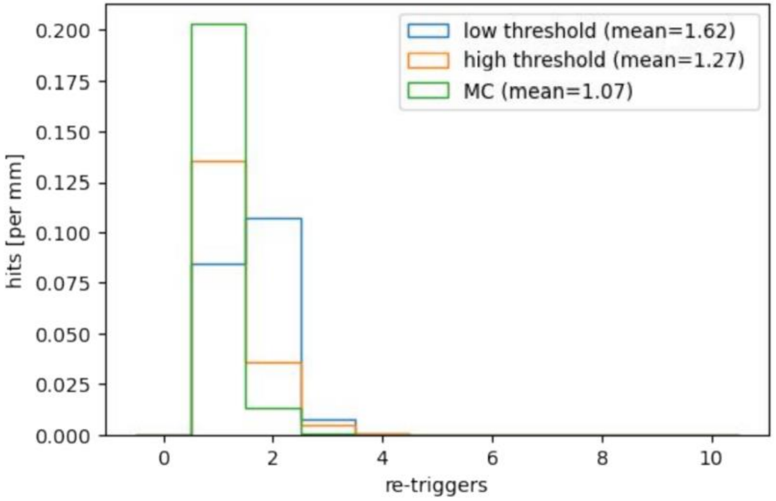

Simulated Pixel Field Response Model

- Induced signal from drifting point charge calculated at points across 3mm square pads at 4 mm pitch from D. Douglas (MSU)
- Field response calculated from ionization electron starting at 0.5 cm from anode
- Field response parameterization across pixel surface by S.R. Soleti (LBL)
- Induced current from neighboring pixel pad trajectories not yet incorporated into simulation, expected to be relatively minor correction

S.R. Soleti (LBL)

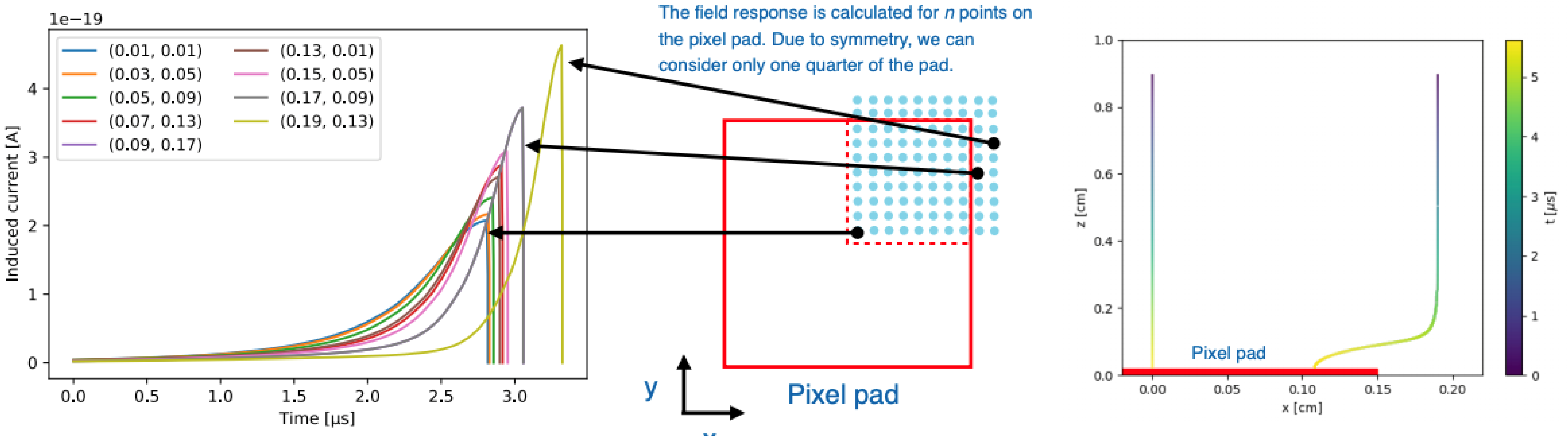

Field response for different points on the pixel pad. The coordinates (x, y) correspond to the distance in cm from the pixel pad center in the each direction.

Trajectories of two unit charges collected by the pixel pad and starting from two different points.

Whole-tile Triggering

- Significant fraction of channels on an anode tile trigger in a brief time period preceding in time large, spatially concentrated energy depositions
- Similar characteristics as instantiation of sync-correlated triggering and far-field induction
- Studying mechanism

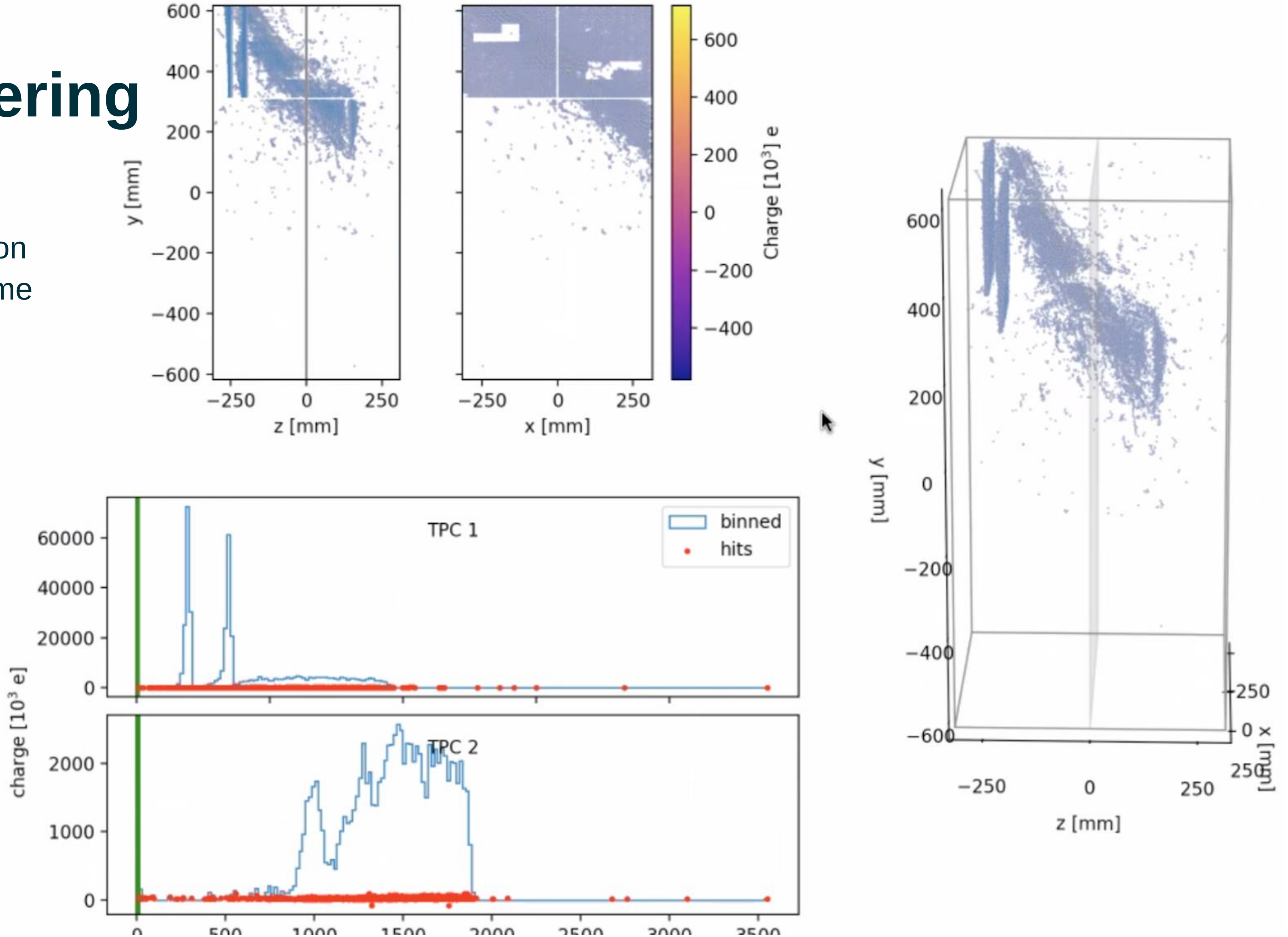

Channel, ASIC, & Tile Active Status

- 92.2% of 78,400 total channels active
- - 4.2% tile-tile edge pixel pedestal DC shift
- - 0.5% noise
- - 3.1% self-trigger stability

- No ASIC or tile failures at cold

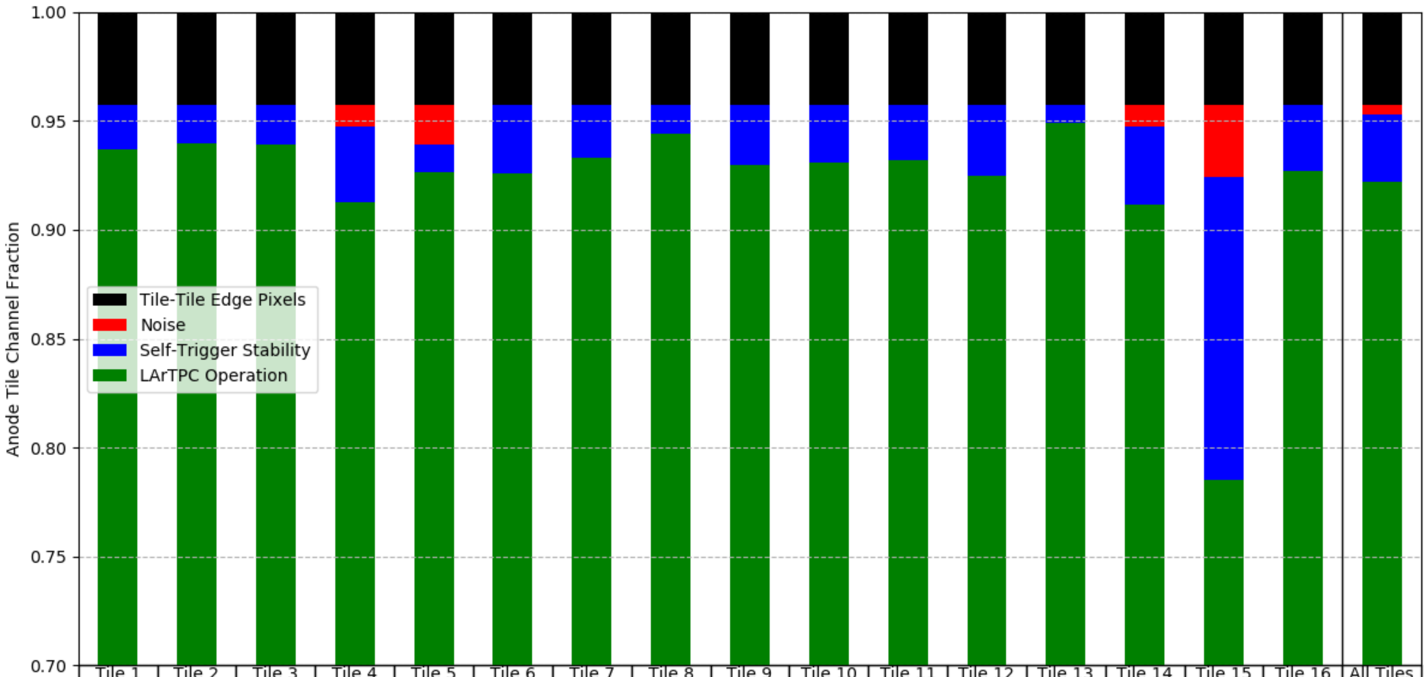

	Tile 1	Tile 2	Tile 3	Tile 4	Tile 5	Tile 6	Tile 7	Tile 8	Tile 9	Tile 10	Tile 11	Tile 12	Tile 13	Tile 14	Tile 15	Tile 16	All Tiles
Tile-Tile Edge Pixels	4692	4692	4692	4692	4692	4692	4692	4692	4692	4692	4692	4692	4692	4692	4692	4692	75072
Noise	4691	4692	4692	4643	4601	4692	4692	4692	4692	4692	4692	4691	4692	4643	4530	4692	74719
Self-Trigger Stability	4592	4606	4602	4471	4541	4537	4573	4627	4555	4561	4566	4533	4652	4468	3847	4543	72274

Specification	Requirement	Status
• Channel-level robustness	< 5% pixel channels inactive	7.8%
• Chip-level robustness	< 3% ASICs inactive	1.6%
• Tile-level robustness	< 0.1% tiles inactive	0%

Tile-Tile Edge Pixel Pedestal DC Shift

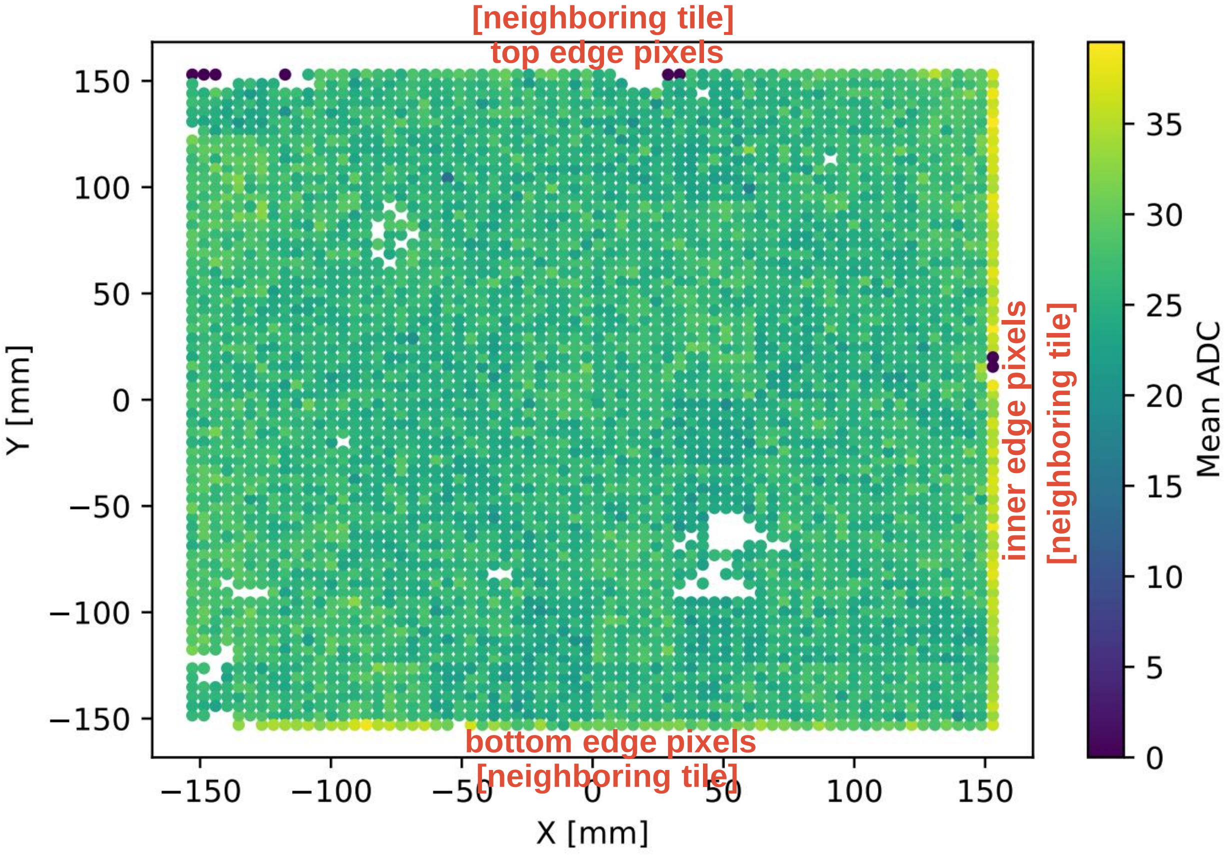

<u>Emerging feature</u>:
dedicated benchtop tests at LBL to reproduce this effect, characterize the mechanism, and make modifications to design if necessary

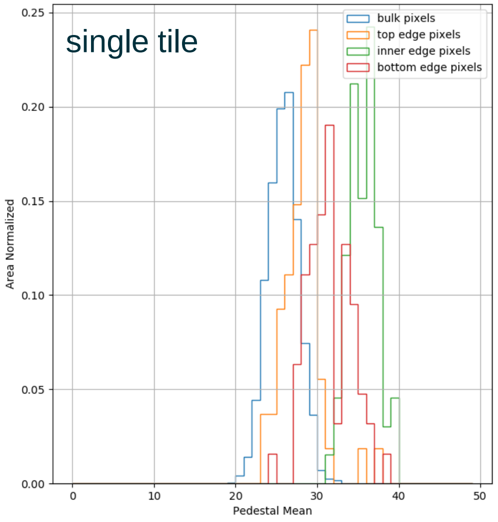

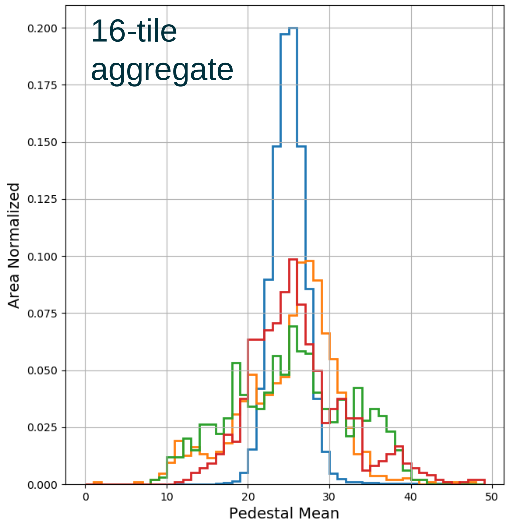

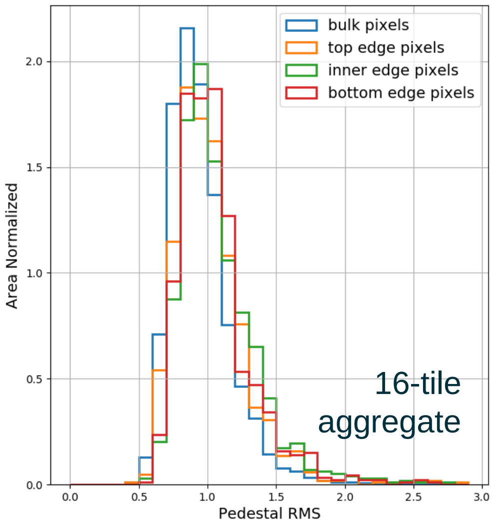

Neutrino Pile-up Mitigation with Optical Segmentation

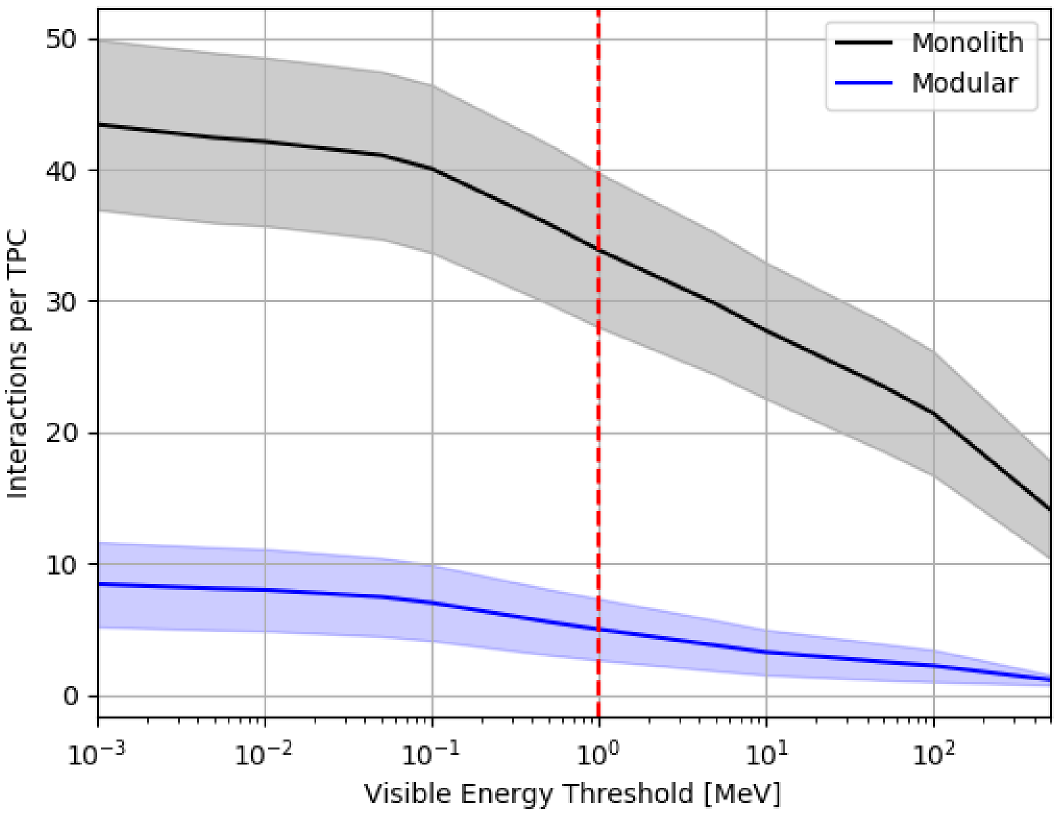

Optically segmenting the detector volume into 70 drift regions results in a mean of 5 scintillation signals per segment per spill.

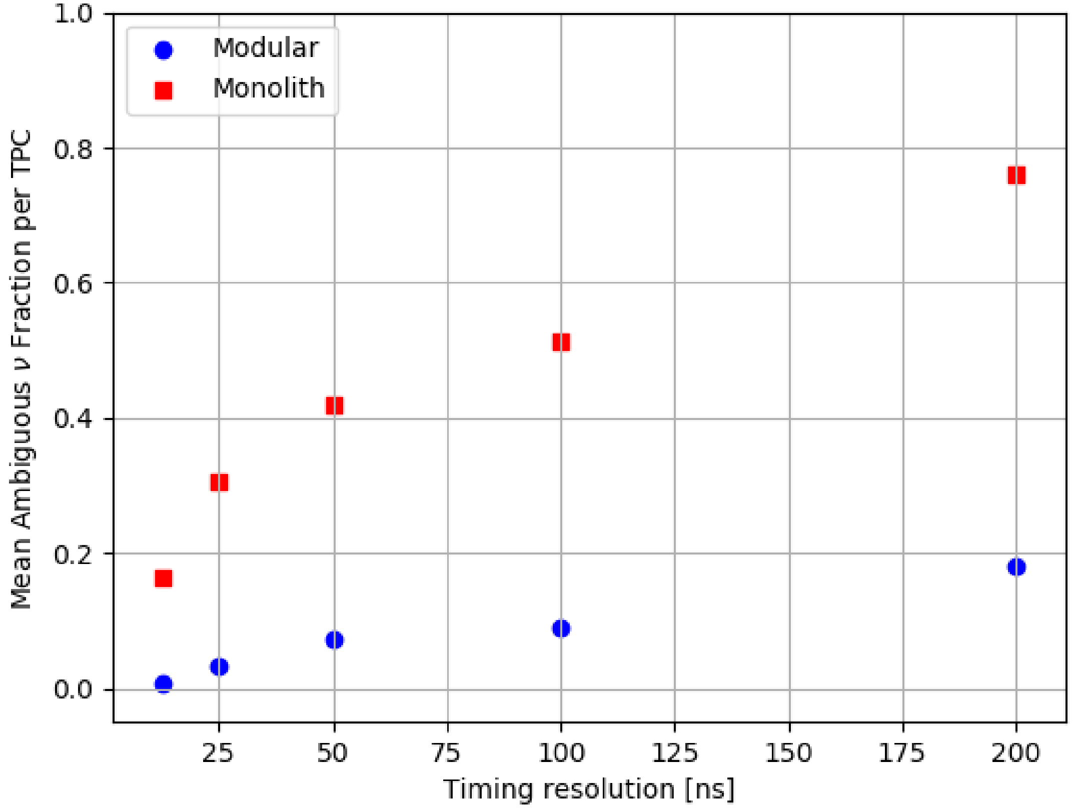

Assuming a scintillation time resolution of 25 ns, the rate of optical signal pile-up is 3% per TPC per spill, relative to 30% for a monolithic detector with two drift regions.

LArPix-v2 Bugs

All to be addressed in LArPix-v2b

Double Read FIFO Bug

- Depending on when the hit occurred relative to the CLX_TX phase a second read could happen
- Results in swallowed data
- *Mitigation*
  - Slow TX clock
  - Sacrificial channel 0
- *Fix*
  - Implement handshaking

512 FIFO Bug

- When the FIFO has significant data, the 512th data word can be delayed
- FIFO is implemented as four distinct, 512-word SRAM modules. When transferring over between modules, the next module would be selected before previous module deselected
- *Fix*
  - Implement handshaking

Hydra Bug

- When multiple chips are connected in a hydra network, programming failures can occur when CLK_TX is reduced from nominal (as is needed to mitigate double read FIFO bug)
- *Mitigation*
  - Reprogram chip (software reset)
- *Fix*
  - Implement handshaking

DUNE Near Detector: LArPix Charge Readout Architecture

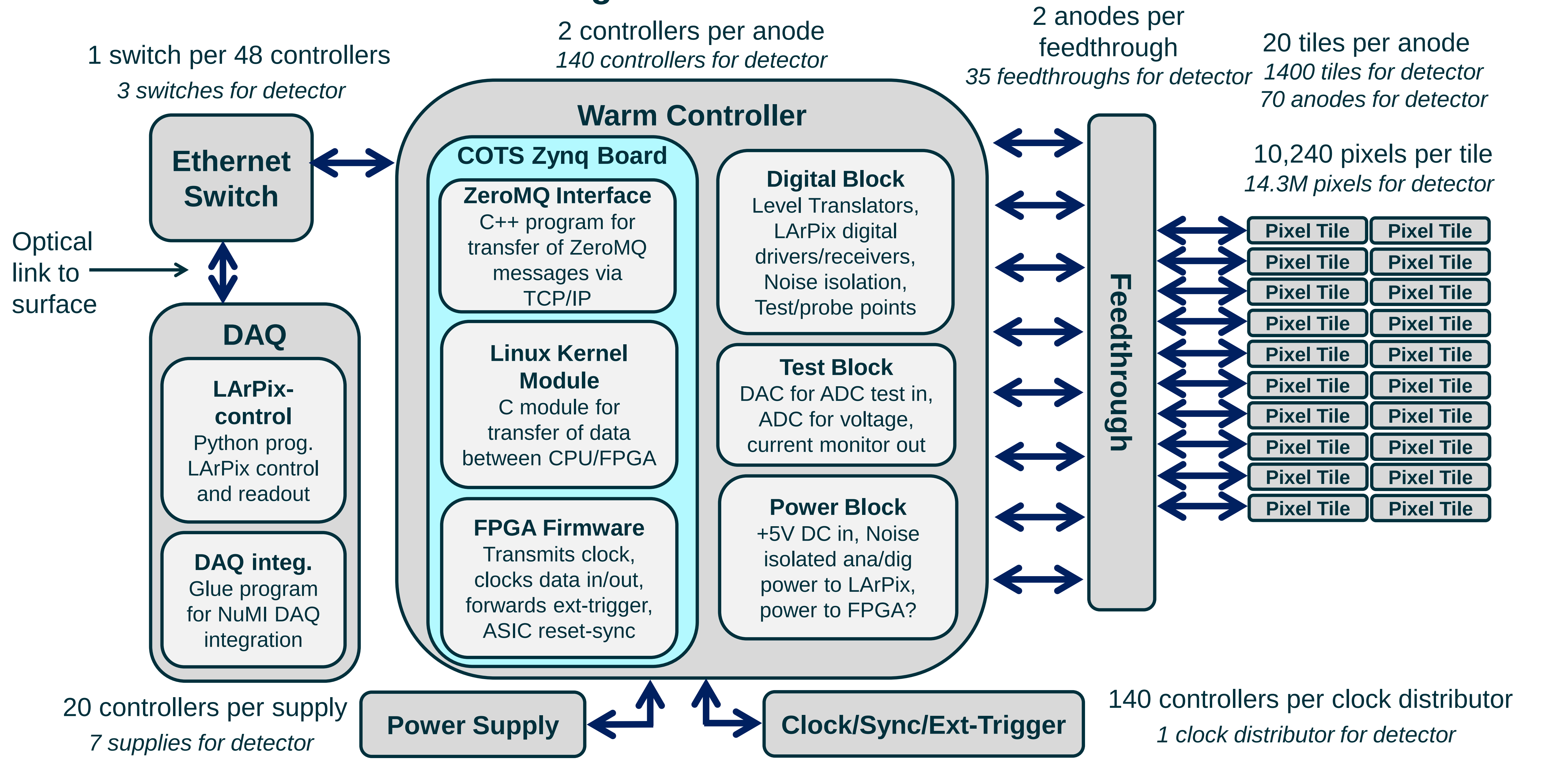

ProtoDUNE-ND particle momenta relative to DUNE

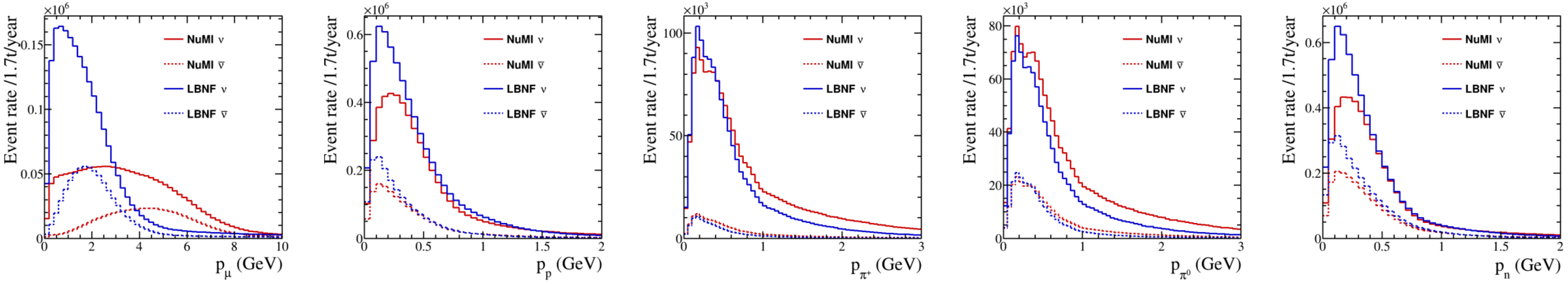

ProtoDUNE-ND track multiplicities relative to DUNE

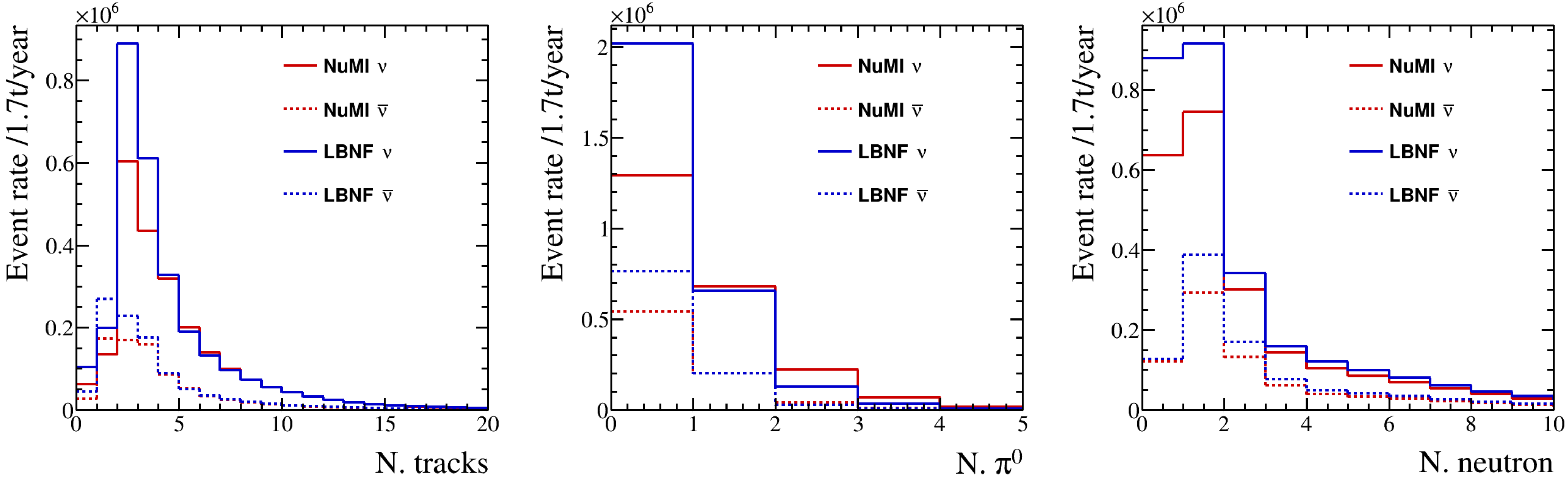

Is charge parity invariance (CP) violated in neutrino oscillations?

Ramifications for whether neutrinos are responsible for the matter-antimatter asymmetry in the universe

Look for an asymmetry between $P(\nu_\mu \rightarrow \nu_e)$ versus $P(\bar{\nu}_\mu \rightarrow \bar{\nu}_e)$ to study CP-violation

Investigated through **long-baseline** neutrino oscillation measurements

Figure credit: Symmetry magazine

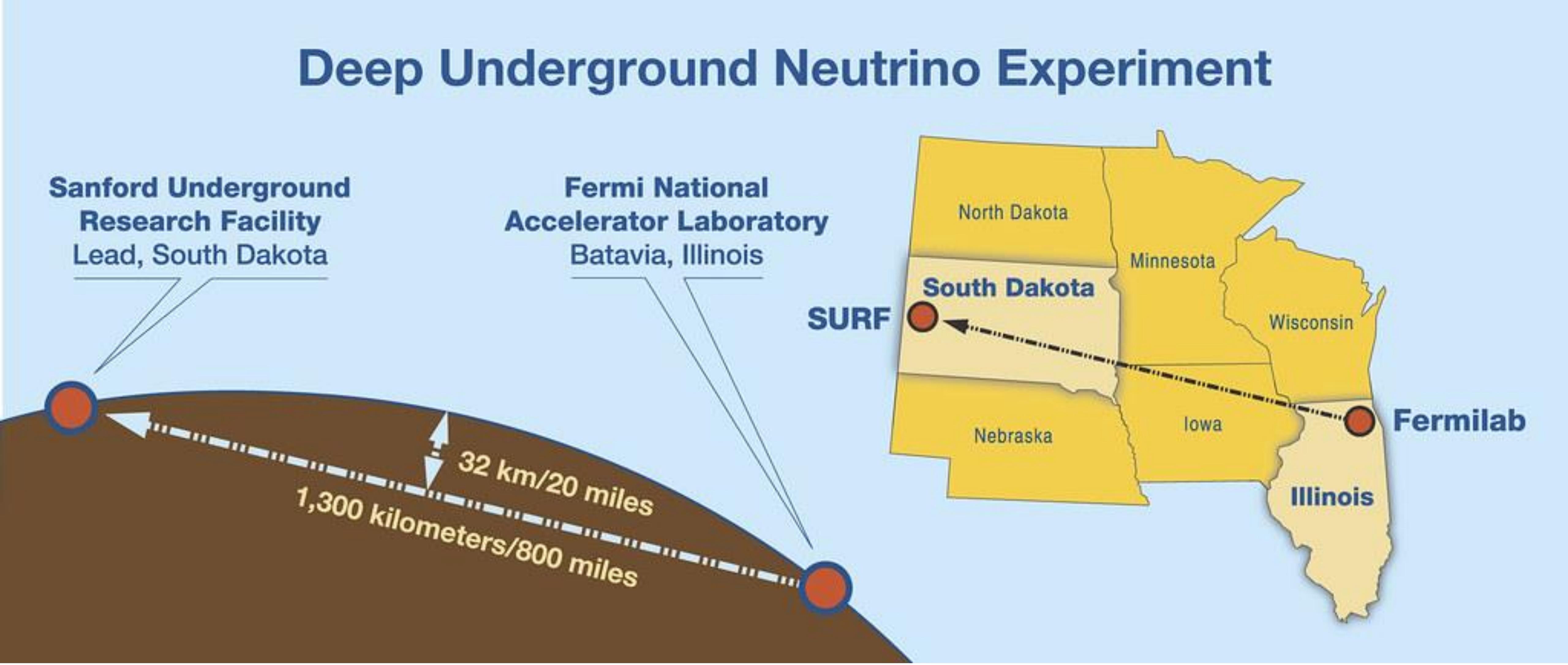

Leverage baseline and matter effects to search for CP violation

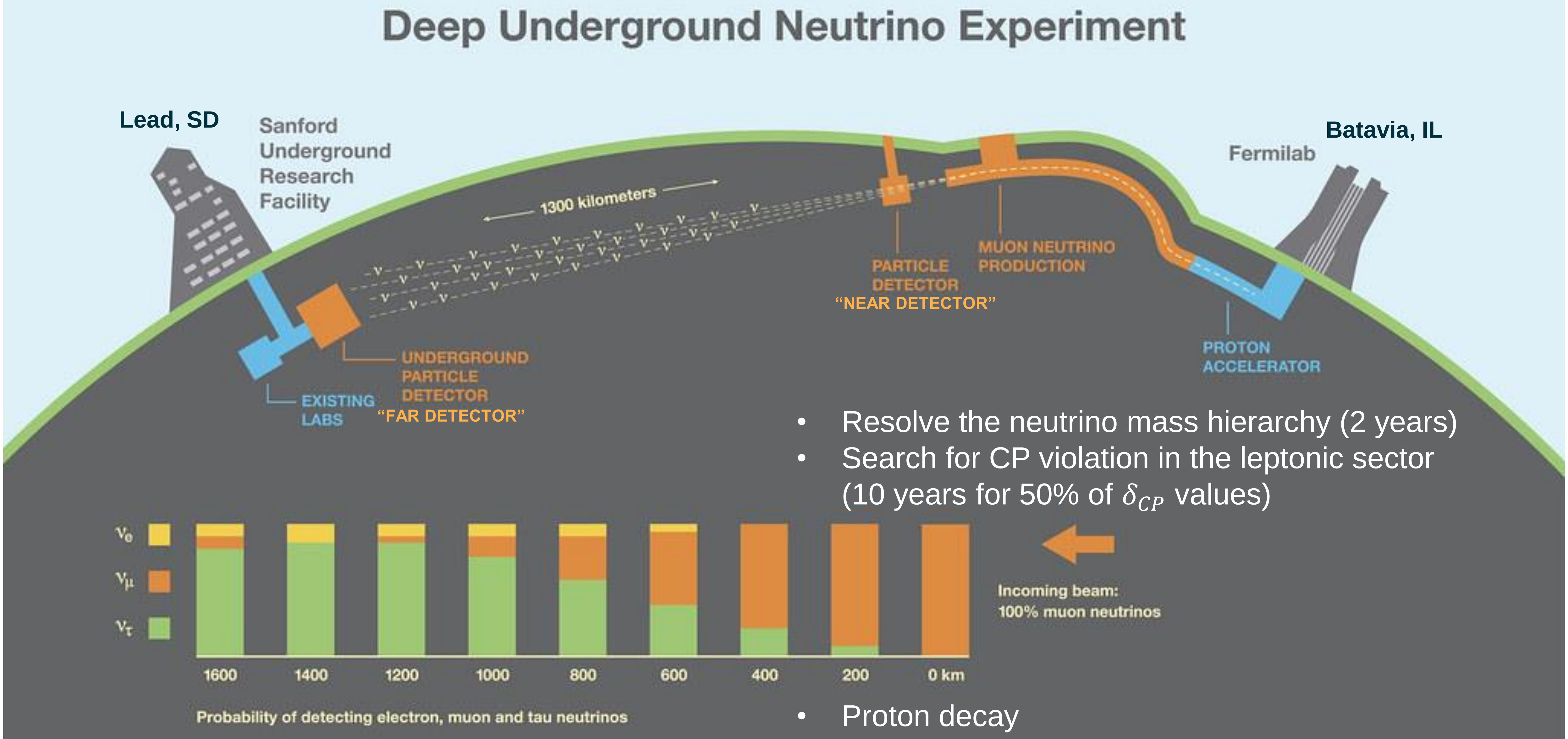

- Resolve the neutrino mass hierarchy (2 years)
- Search for CP violation in the leptonic sector (10 years for 50% of δ_{CP} values)

- Proton decay
- Neutron-antineutron oscillation
- Supernova neutrino bursts
- Beyond the Standard Model physics

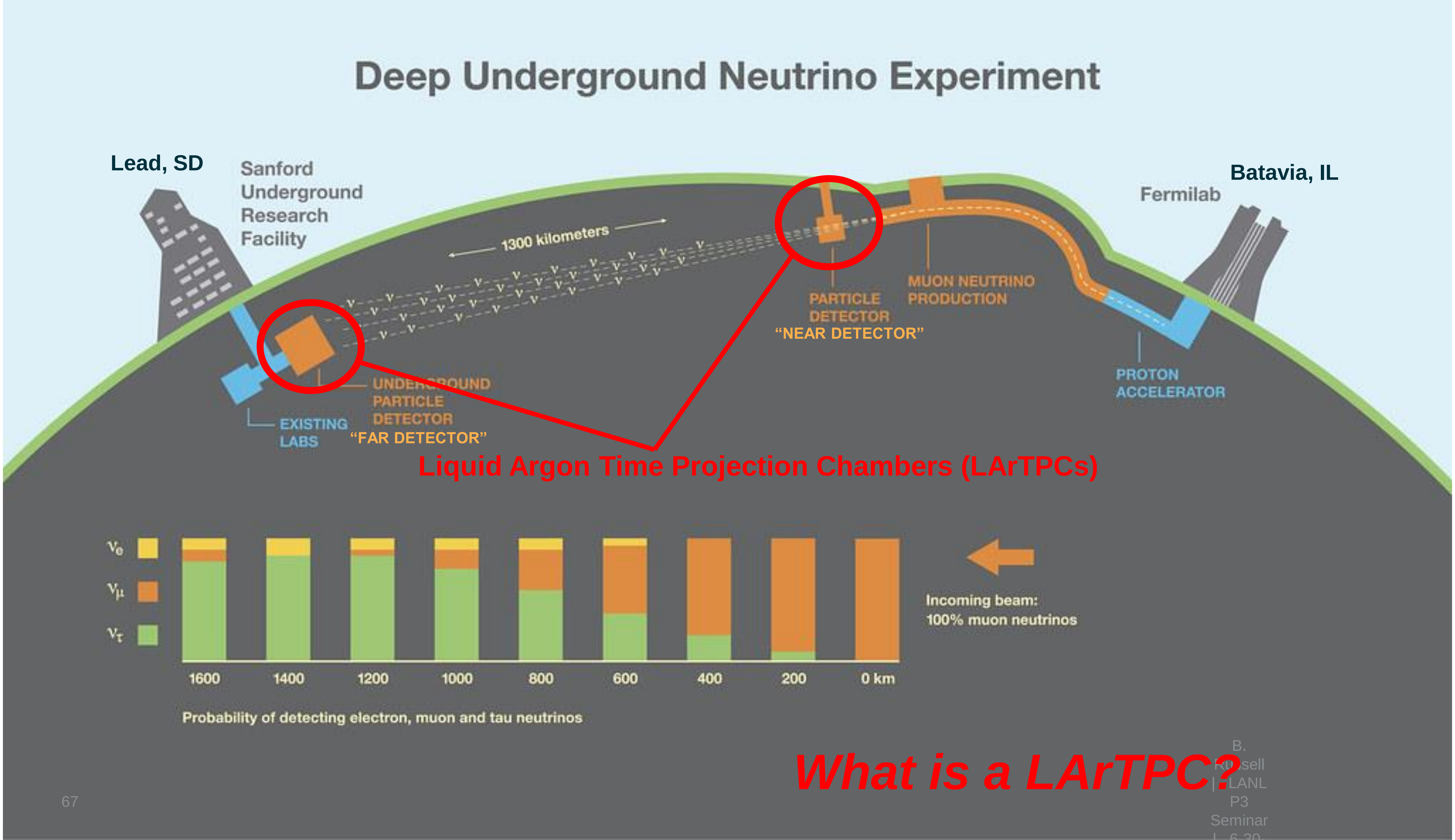

Liquid Argon Time Projection Chambers (LArTPCs)

What is a LArTPC?

LAr as total absorption calorimeter

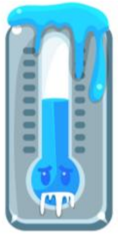

Liquid argon boiling point:
$-186℃ \quad (-303°F)$

1974

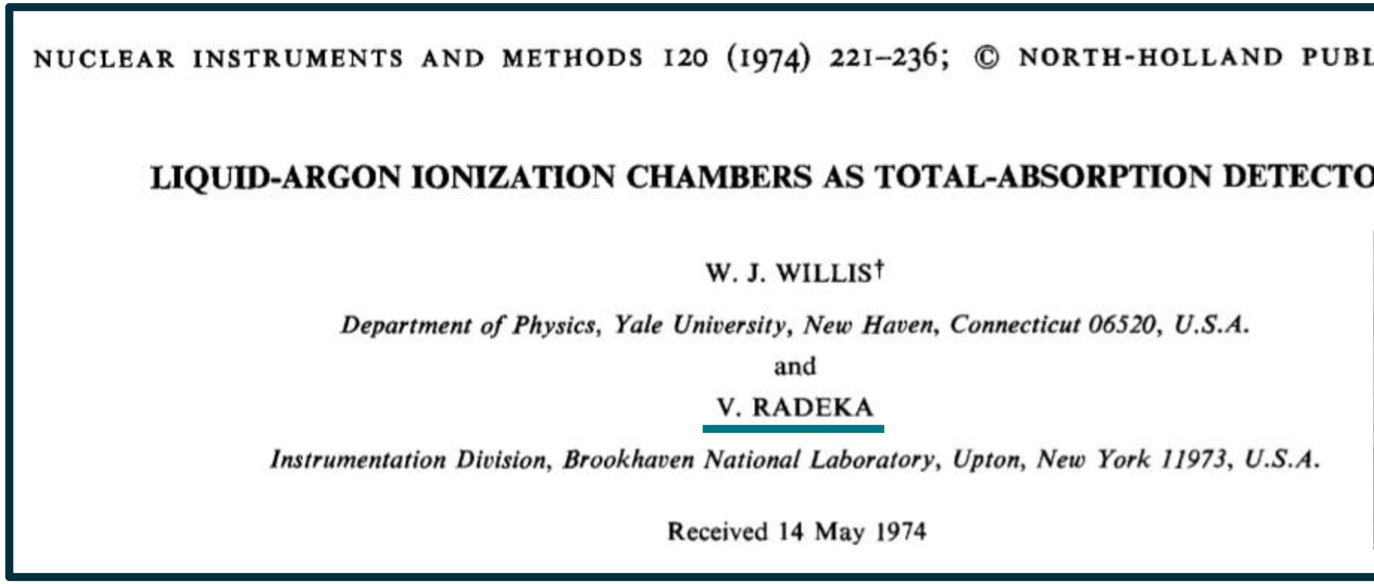

NUCLEAR INSTRUMENTS AND METHODS 120 (1974) 221–236; © NORTH-HOLLAND PUBLISHING CO.

LIQUID-ARGON IONIZATION CHAMBERS AS TOTAL-ABSORPTION DETECTORS*

W. J. WILLIS†
Department of Physics, Yale University, New Haven, Connecticut 06520, U.S.A.
and
V. RADEKA
Instrumentation Division, Brookhaven National Laboratory, Upton, New York 11973, U.S.A.

Received 14 May 1974

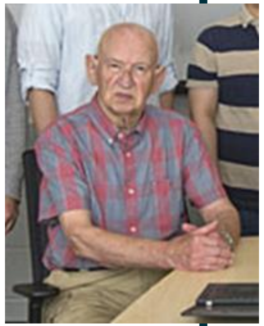

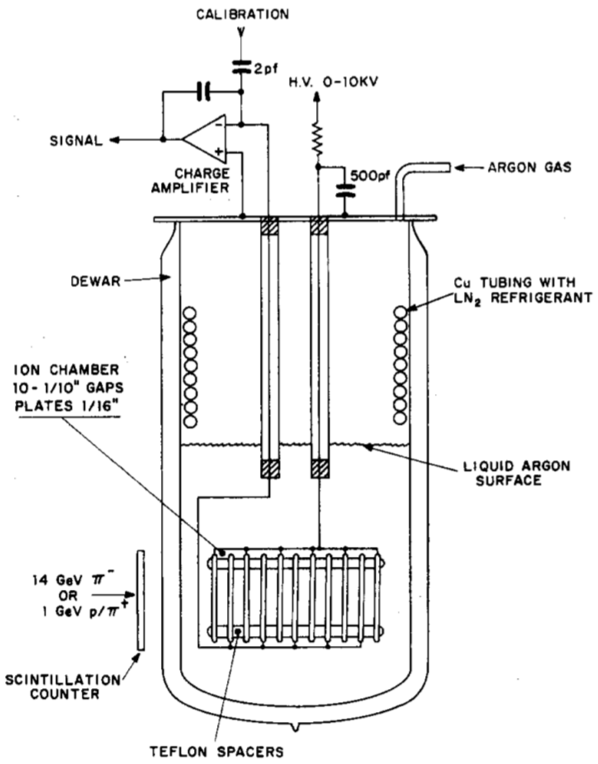

LAr is an attractive active target:

- Inert
- Many nucleons
- High electron mobility

TPC as 4π charged particle detector

1976

The Time-Projection Chamber
- A new 4π detector for charged particles

David R. Nygren

Lawrence Berkeley Laboratory
Berkeley, California 97420

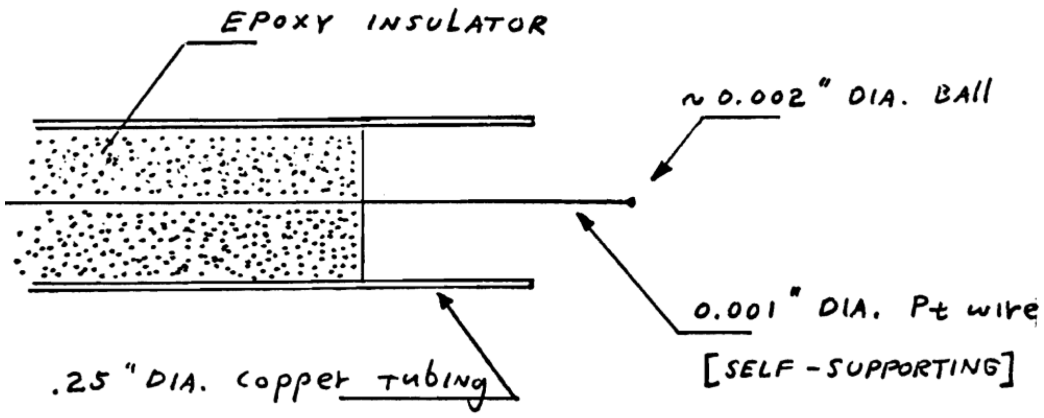

Ubiquitous application in modern experimental physics

- Neutrino-less double beta decay
- Dark matter direct detection
- Collider experiments
- Etc.

Liquid Argon Time Projection Chamber (LArTPC)

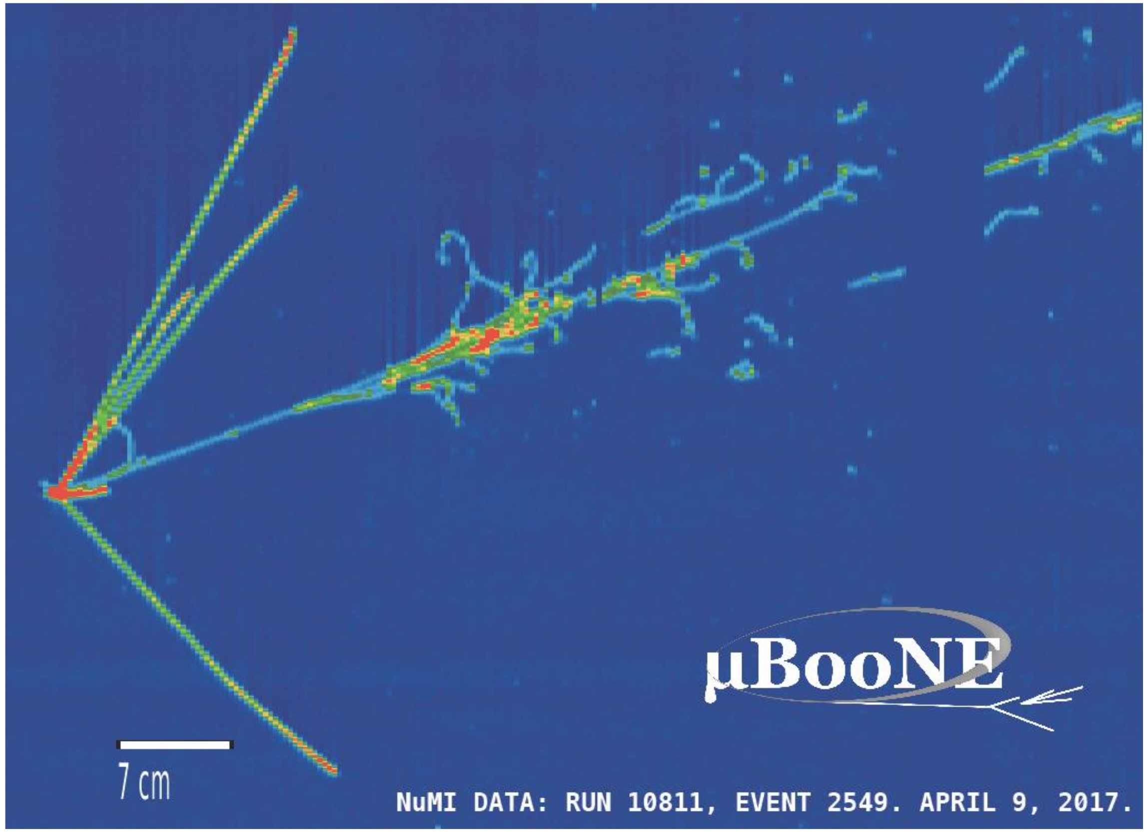

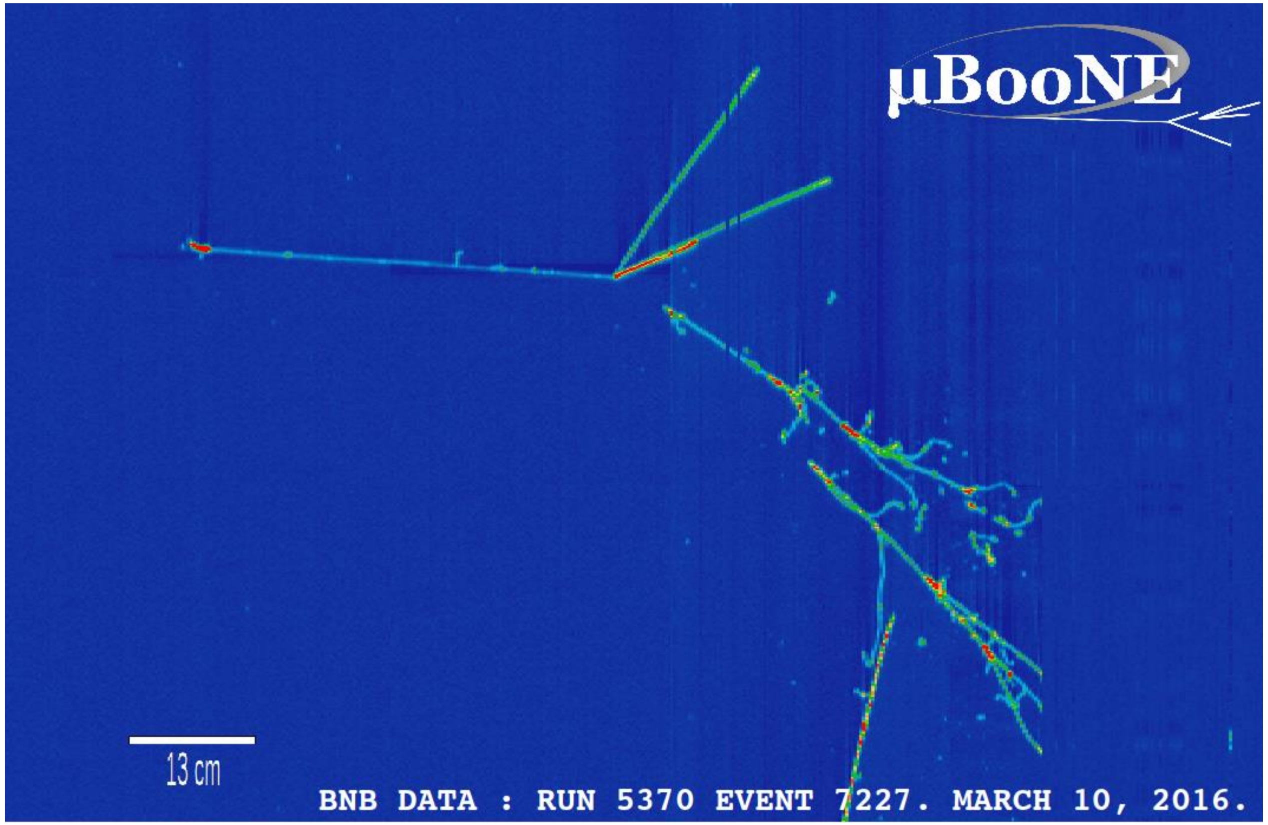

e^-/γ discrimination

critical for $P(\nu_\mu \rightarrow \nu_e)$ and $P(\bar{\nu}_\mu \rightarrow \bar{\nu}_e)$ measurements

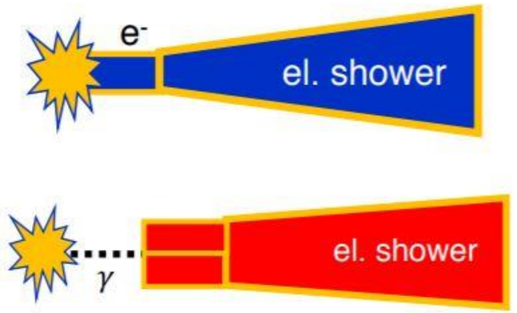

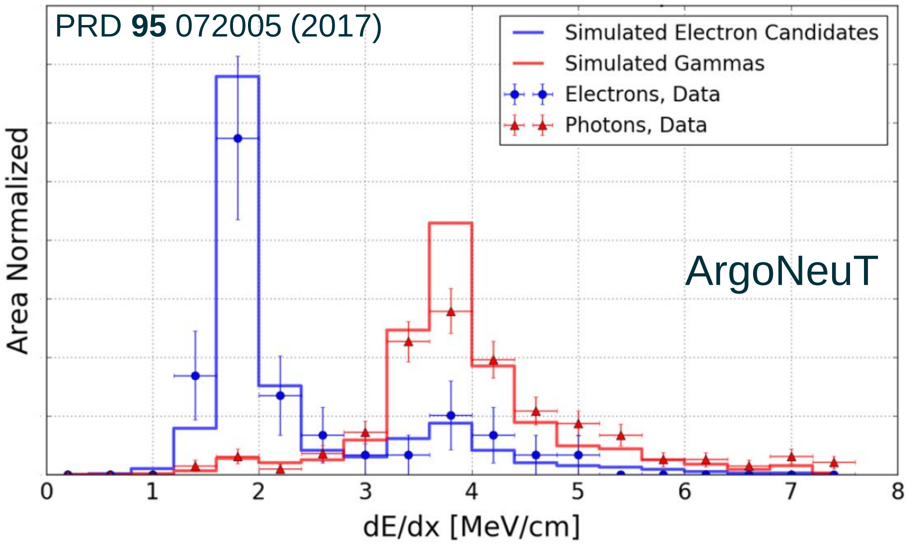

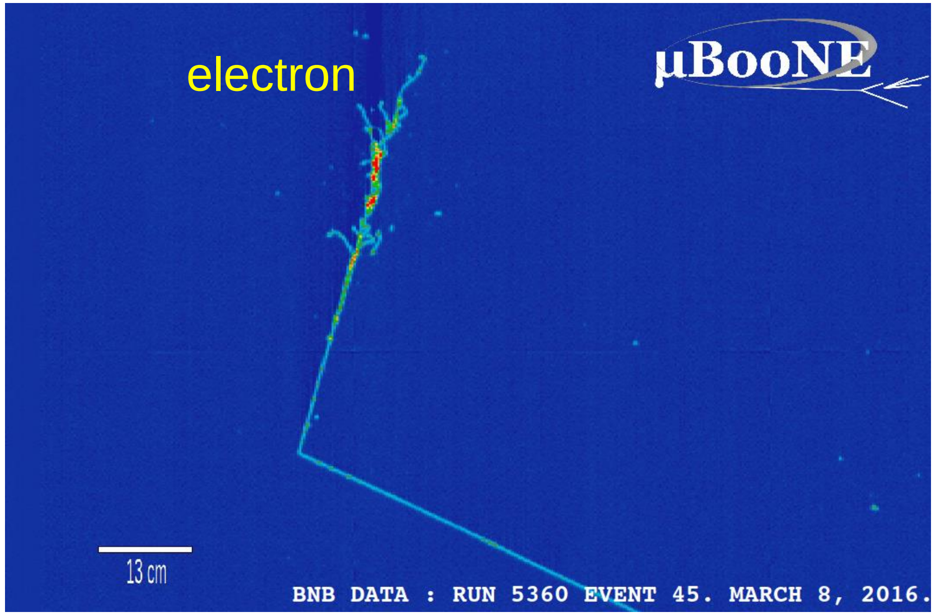

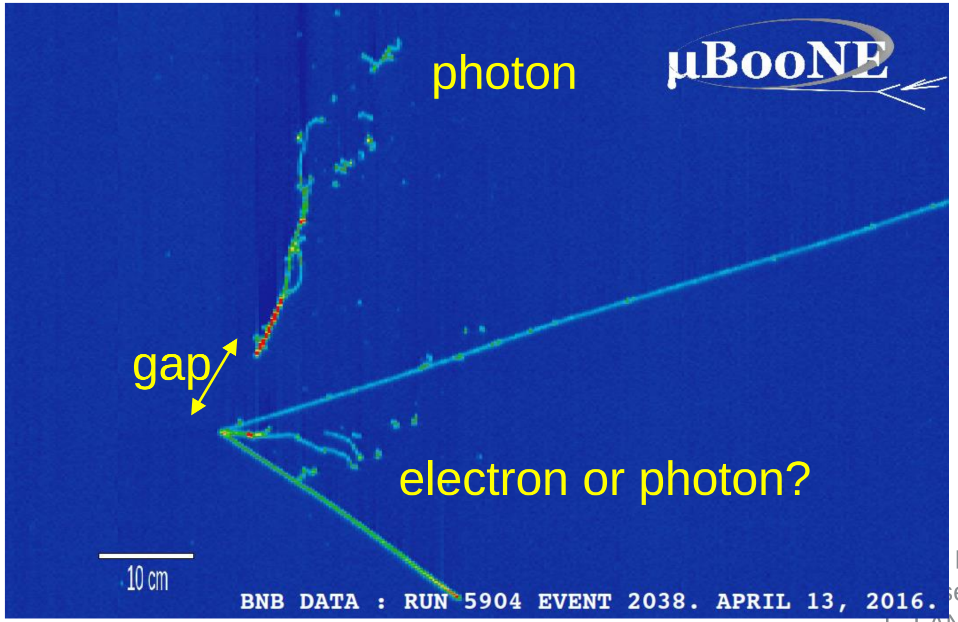

novel 3D pixelated charge readout

- Low noise, low power cryogenic operation
- **Unambiguous 3D charge readout**
- Highly scalable
- Mechanically robust

Game changer for LArTPC physics: self-triggering charge amplification and digitization

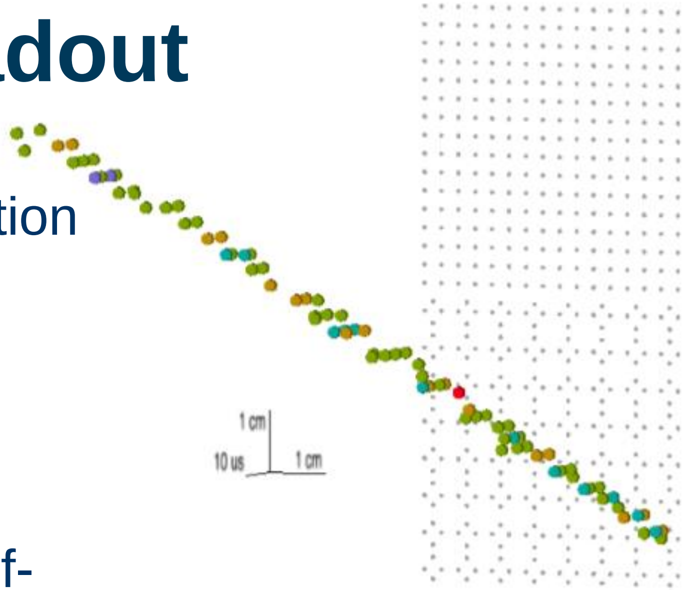

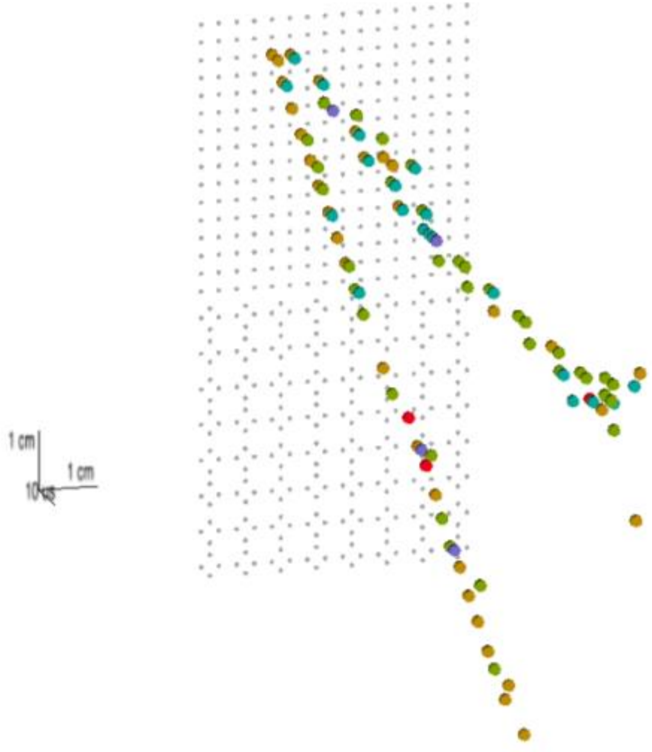

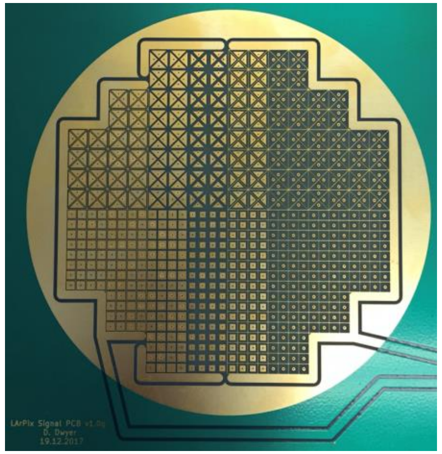

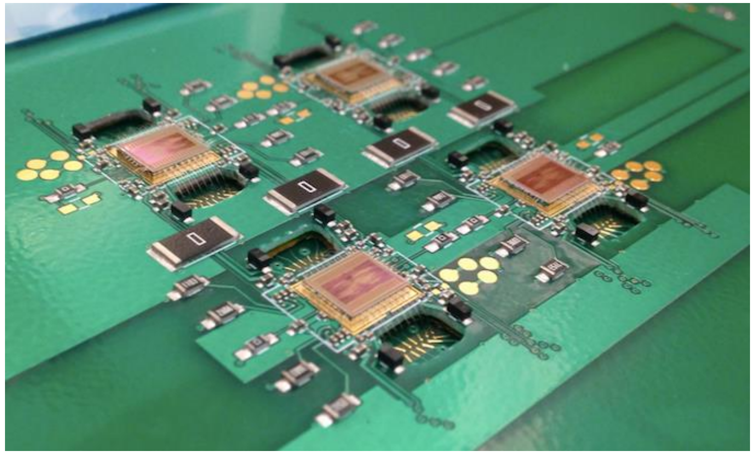

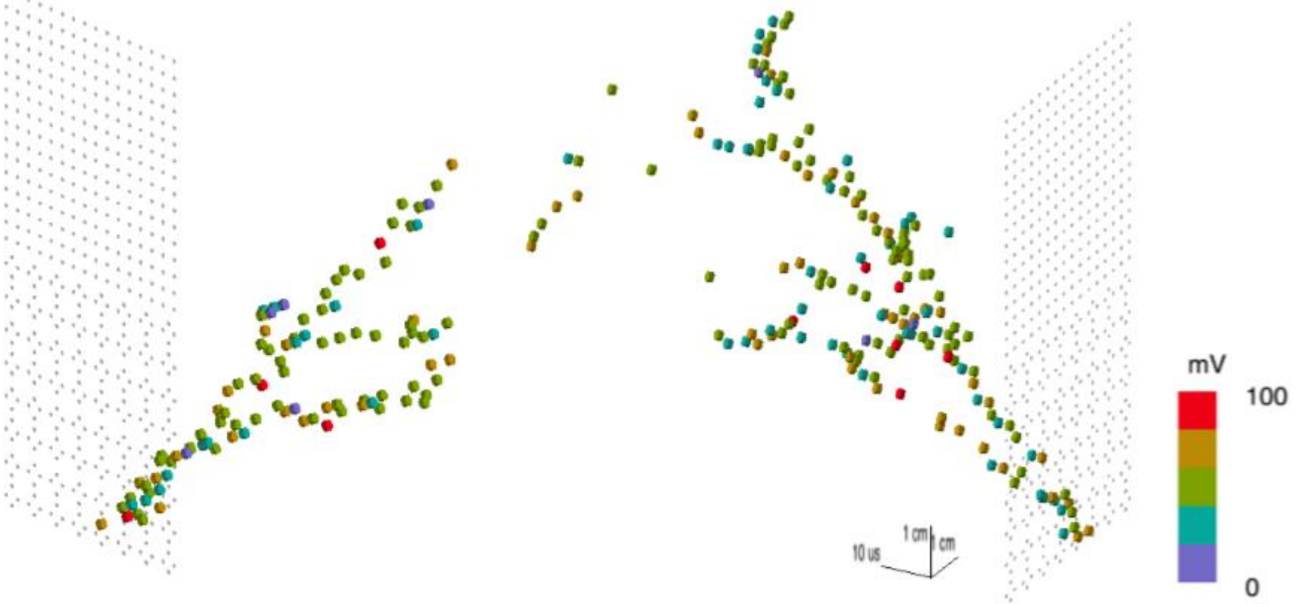

D. Dwyer *et al.* JINST 13 P10007 (2018)